TECHNISCHE UNIVERSITÄT DARMSTADT

Investigating the interplay of replication, transcription, and BER for the induction of DSBs after oxidative stress

Vom Fachbereich Biologie der Technischen Universität Darmstadt

zur Erlangung des Grades
Doctor rerum naturalium
(Dr. rer. nat.)

Dissertation
von Daniel Udo Pfeffel

Erstgutachter: Prof. Dr. Markus Löbrich

Zweitutachterin: Prof. Dr. M. Cristina Cardoso

Darmstadt 2022

Pfeffel, Daniel Udo: Investigating the interplay of replication, transcription, and BER for the induction of DSBs after oxidative stress
Darmstadt, Technische Universität Darmstadt
Jahr der Veröffentlichung der Dissertation auf TUprints: 2022
URN: urn:nbn:de:tuda-tuprints-223992
Tag der mündlichen Prüfung: 26.08.2022

Ehrenwörtliche Erklärung

Ich erkläre hiermit ehrenwörtlich, dass ich die vorliegende Arbeit entsprechend den Regeln guter wissenschaftlicher Praxis selbstständig und ohne unzulässige Hilfe Dritter angefertigt habe.

Sämtliche aus fremden Quellen direkt oder indirekt übernommenen Gedanken sowie sämtliche von Anderen direkt oder indirekt übernommenen Daten, Techniken und Materialien sind als solche kenntlich gemacht. Die Arbeit wurde bisher bei keiner anderen Hochschule zu Prüfungszwecken eingereicht. Die eingereichte elektronische Version stimmt mit der schriftlichen Version überein.

Darmstadt, den 13. Juni 2022

_____

Daniel Pfeffel

Table of contents

List of figures

Abbreviations

4-OHT	hydroxytamoxifen
53BP1	p53-binding protein 1
8-oxoG	8-oxoguanine
8-oxo-dG	8-oxo-2'-deoxyguanosine
8-oxo-dGTP	8-oxo-2'-deoxyguanosine-5'-triphosphate
A	adenine
AND-1	acidic nucleoplasmic DNA-binding protein
AP site	apurinic/apyrimidinic site
APE1	apurinic/apyrimidinic endonuclease 1
ATM	ataxia telangiectasia mutated
ATR	ataxia telangiectasia and Rad3-related
ATRIP	ATR interacting protein
a.u.	arbitrary units
BER	base excision repair
BIR	break-induced replication
BLM	blooms syndrome helicase
bp	base pair
BRCA1/2	breast cancer type 1/2 susceptibility protein
BrdU	5-bromo-2'-deoxyuridine
BSA	bovine serum albumine
C	cytosine
CDC45	cell division cycle 45
CDC6	cell division cycle 6
CDK	cyclin-dependent kinase
CMG	CDC45-MCM2-7-GINS complex
c-NHEJ	canonical-non-homologous end joining
ChIP	chromatin immunoprecipitation
ChIP-Seq	ChIP-Sequencing
CPT	camptothecin
CTD	C-terminal repeat domain
CTD1	chromatin licensing and DNA replication factor 1
CtIP	CtBP-interacting protein
DAPI	4',6-diamidino-2-phenylindole
DDK	Dbf4-dependent kinase
dHJ	double Holliday junction
D-loop	displacement loop
DMEM	Dulbecco's modified eagel's medium
DMSO	dimethyl sulfoxide
DNA	deoxyribonucleic acid
DNA2	DNA replication ATP-dependent helicase/nuclease 2
DNA-PK	DNA-dependent protein kinase
DRB	5,6-dichlorobenzimidazole 1-β-D-ribofuranoside
dsDNA	double-stranded DNA
DSB	double-strand break
DSIF	DRB sensitivity inducing factor

EDTA	ethylenediaminetetraacetic acid
EdU	5-ethynyl-2'-deoxyuridine
EGTA	egtazic acid
EXO1	exonuclease 1
FA	formaldehyde
FANCD2	Fanconi anemia group D2
FEN1	flap endonuclease 1
FCS	fetal calf serum
FPC	fork protection complex
G	guanine
G1 phase	gap 1 phase
G2 phase	gap 2 phase
GEN1	flap endonuclease GEN homolog 1
H2AX	H2A histone family member X
HEPES	4-(2-hydroxyethyl)-1-piperazineethanesulfonic acid
HR	homologous recombination
HT	high transcription
hTert	human telomerase reverse trancriptase
IF	immunofluorescence
LIG1/3/4	DNA ligase 1/3/4
LT	low transcription
M phase	mitosis phase
MCM2-7	minichromosome maintenance complex component 2 and 7
MDC1	mediator of DNA damage checkpoint protein 1
MEF	mouse embryonic fibroblast
MEM	minimal essential medium
MiDAS	mitotic DNA synthesis
MMS	methyl methanesulfonate
MRE11	double-strand break repair protein MRE11
MRN	MRE11-RAD50-NBS1 complex
MTH1	MutT homolog 1
MUTYH	MutY glycosylase homolog
NAC	N-acetylcysteine
NEAA	non-essential amino acid
NELF	negative elongation factor
NPC	nuclear pore complex
nt	nukleotide
OGG1	8-oxoguanine glycosylase
PARP1	poly (ADP-ribose) polymerase 1
PAXX	paralog of XRCC4 and XLF
PBS	phosphate buffered saline
PCNA	proliferating cell nuclear antigen
PLA	proximity ligation assay

PIKKs	phosphoinositol-3-kinase like kinases
PMSF	phenylmethylsulfonyl fluoride
Pol II	RNA polymerase II
Pol α/β/δ/ε/λ	DNA polymerase α/β/δ/ε/λ
PRIM1	DNA primase subunit 1
PRIMPOL	primase and DNA directed polymerase
P-TEFb	kinase positive transcription elongation factor
qPCR	quantitative real-time polymerase chain reaction
RAD51	DNA repair protein RAD51 homolog 1
RAD52	DNA repair protein RAD52 homolog
RECQL5	RecQ-like ATP-dependent DNA helicase Q5
RNA	ribonucleic acid
RNA-Seq	RNA-Sequencing
ROS	reactive oxygen species
RPA	replication protein A
S phase	synthesis phase
SDS	sodium dodecyl sulfate
SDSA	synthesis-dependent strand annealing
SOD	superoxide dismutase
SSB	single-strand break
ssDNA	single-stranded DNA
T	thymine
TFIIH	transcription factor II human
Top1	topoisomerase 1
Tris	tris(hydroxymethyl)aminomethane
WT	wild type
XLF	XRCC4-like factor
XRCC1/4	X-ray repair cross-complementing 1/4
γH2AX	H2AX phosphorylated on serine 139

1 Summary

Every day, a variety of different deoxyribonucleic acid (DNA) lesions occur in our genome, threatening the integrity and inheritance of genetic information. The lesions that occur are diverse and may have distinct consequences. The damage to DNA is thereby often caused by reactive oxygen species (ROS). These can be generated both endogenously and exogenously and can be responsible for the occurrence of various lesions. One of the most common DNA damage related to ROS is oxidative base modification. Several hundreds of these occur spontaneously in our genome every day and require efficient and correct repair via base excision repair (BER). However, several studies in recent years have demonstrated that the repair process of modified bases, and in particular the most abundant oxidative base modification 8-oxoguanine (8-oxoG), appears to be involved in the formation of the most dangerous lesion, the DNA double-strand break (DSB).

In this work, the DSB-inducing effect of oxidative stress was investigated by treatment with the established oxidative agent H_2O_2. A cell cycle-specific analysis was performed, which demonstrated the induction of DSBs mainly in the synthesis phase (S phase) of the cell cycle. These breaks were almost exclusively repaired via the homologous recombination (HR) repair pathway, and thus, the emergence of replication-associated one-ended DSBs was assumed. Inhibition of replication thereby led to a significant reduction of DSBs in S phase and confirmed their dependence on the replication process. In addition, a comparable reduction in induced DSBs was demonstrated by inhibition of transcription. Follow-up studies using the proximity ligation assay (PLA) confirmed the occurrence of replication-transcription conflicts after treatment with H_2O_2, thus identifying these events as the reason for the formation of DSBs.

Replication-transcription conflicts usually occur when obstacles in the DNA interfere with the progression of one or both of these two processes. H_2O_2 treatment induces, to a large extent, the oxidative base modification 8-oxoG which can be removed by the BER mechanism and replaced with a correct base via the formation of a single-strand break (SSB). This work demonstrates that the initiation of BER by the specific 8-oxoguanine glycosylase (OGG1) is required for DSB formation after H_2O_2 treatment. Inhibition of this initiation resulted in decreased DSB numbers, which in contrast greatly increased if the repair of SSBs was prevented. The removal of the damaged base and the resulting SSB are the reason for the occurence of conflicts between replication and transcription.

Due to the involvement of both replication and transcription in the formation of DSBs after H_2O_2 treatment, break induction should only be able to occur in regions with active

transcription. As confirmed by sequencing results in this work, the breaks induced by H_2O_2 occur more frequently in regions of elevated transcription. In addition, an increased density of genes and GC content could be detected for these regions. This shows that the breaks induced by H_2O_2 occur in gene-rich regions with strong transcription. Furthermore, it could be observed that this process of DSB induction also takes place without H_2O_2 treatment in unbertubed, proliferating cells. Thus, it is assumed that this process is significantly involved in the induction of endogenous breaks. A mechanism was elaborated specifically occuring in S phase, requiring the interplay of replication, transcription, as well as BER. This mechanism can explain the mutagenic effect of ROS, which plays an important role in the development of various diseases and clarifies the significance of simple base modifications for the fate of a cell.

Zusammenfassung

Tagtäglich entsteht in unserem Genom eine Vielzahl unterschiedlicher DNA-Schäden, welche die Integrität und eine korrekte Weitergabe der Erbinformation bedrohen. Die auftretenden Läsionen sind dabei vielfältig und besitzen unterschiedlich starke Auswirkungen. Die Ursache für die Schädigung der DNA ist dabei häufig auf reaktive Sauerstoffspezies zurückzuführen. Diese können sowohl endogen als auch exogen erzeugt werden und sind verantwortlich für das Auftreten verschiedener Läsionen in der DNA. Eine der am häufigsten auftretenden DNA-Schäden, in Verbindung mit reaktiven Sauerstoffspezies, ist dabei die oxidative Basenmodifikation. Diese tritt jeden Tag zu mehreren Hunderten spontan in unserem Genom auf und benötigt eine effiziente und korrekte Reparatur über die Basenexzisionsreparatur. Mehrere Studien konnten jedoch in den letzten Jahren nachweisen, dass der Reparaturprozess von modifizierten Basen und insbesondere der am häufigsten vorkommenden oxidative Basenmodifikation 8-oxoG an der Entstehung der weitaus gefährlicheren DNA-Doppelstrangbrüche beteiligt zu sein scheint.

In dieser Arbeit wurde die DSB-induzierende Wirkung von oxidativem Stress durch die Behandlung mit dem etablierten, oxidierenden Agens H_2O_2 untersucht. Mit Hilfe einer Zellzyklus-spezifische Analyse wurde eine Induktion von DSBs hauptsächlich in der S-Phase des Zellzyklus nachgewiesen. Diese Brüche wurden fast ausschließlich über den Reparaturweg der Homologen Rekombination repariert. Dies deutete darauf hin, dass es sich hierbei um Replikations-assoziierte ein-endige DSBs handelt. Die Abhängigkeit vom Replikationsprozess konnte durch eine signifikante Reduktion der DSBs in der S-Phase nach einer Inhibierung der Replikation bestätigt werden. Darüber hinaus konnte eine vergleichbare Reduktion der

induzierten DSBs durch eine Inhibierung der Transkription nachgewiesen werden. Nachfolgende Untersuchungen mit dem PLA bestätigten das Auftreten von Replikations-Transkriptions-Konflikten nach einer Behandlung mit H_2O_2 und identifizierten diesen Prozess als Ursache für die Ausbildung der DSBs.

Replikations-Transkriptions-Konflikte treten in der Regel auf, wenn Hindernisse in der DNA das Fortschreiten eines oder beider Prozesse behindern. Durch eine H_2O_2-Behandlung wird zu einem Großteil die oxidative Basenmodifikation 8-oxoG induziert. Diese kann im Zuge der BER entfernt und über die Ausbildung eines SSBs mit der korrekten Base ersetzt werden. Im Rahmen dieser Arbeit wurde festgestellt, dass eine Initiierung der BER durch die spezifische Glykosylase OGG1 für die Ausbildung der DSBs erforderlich ist. Während eine Inhibierung der Einleitung der BER zu einer verringerten DSB-Induktion führte, nahm diese stark zu, wenn eine Reparatur der SSBs unterbunden wurde. Die Entfernung der beschädigten Base und der daraus resultierende SSB ist die Ursache für das Auftreten von Konflikten zwischen der Replikation und der Transkription.

Die Beteiligung der Replikation sowie der Transkription in der Induktion von DSBs nach einer H_2O_2-Behandlung legen die Annahme nahe, dass die DSBs nur in Regionen der aktiven Transkription auftreten sollten. Wie die Sequenzierungsergebnisse in dieser Arbeit bestätigen, treten die durch H_2O_2 induzierten Brüche vermehrt in Regionen mit erhöhter Transkription auf. Zusätzlich konnte für diese Regionen eine erhöhte Gendichte und auch ein erhöhter GC-Gehalt nachgewiesen werden. Dies zeigt, dass die durch H_2O_2 induzierten Brüche in genreichen Regionen mit starker Transkription auftreten. Darüber hinaus konnte beobachtet werden, dass dieser Prozess der DSB-Induktion auch ohne H_2O_2-Behandlung in unbehandelten, proliferierenden Zellen auftritt. Es wird daher vermutet, dass dieser Prozess maßgeblich an der Induktion von endogenen Brüchen beteiligt ist. Es wurde damit ein Mechanismus der DSB-Induktion identifiziert, der spezifisch in der S-Phase auftritt und das Zusammenspiel von Replikation, Transkription sowie der BER erfordert. Dieser Prozess kann zur mutagenen Wirkung von reaktiven Sauerstoffspezies beitragen, welche bei der Entstehung verschiedener Krankheiten eine wichtige Rolle spielen, wodurch die Bedeutung einfacher Basenmodifikationen für das Schicksal einer Zelle verdeutlicht wird.

2 Introduction

The genetic information encoded in the DNA of each cell and organism is essential for its survival and reproduction. Therefore, maintenance of the genomic integrity is of utmost importance for all living beings. Nevertheless, DNA is exposed to a variety of endogenous and exogenous processes every day that cause damage to the DNA and compromise heredity (Lindahl, 1993). DNA damage from endogenous sources occurs frequently and includes replication errors, ROS, and enzymatic processes. Exogenous sources, although not as common, carry a high risk potential. Ionizing radiation, genotoxic drugs, or cigarette smoke are just some of the damaging agents that contribute to exogenously induced DNA damage. Considering that there are numerous sources, it is not surprising that there is a wide variety of potential DNA lesions. Estimations suggest that 70,000 DNA lesions are generated per day in each individual human cell (Lindahl and Barnes, 2000). These include frequently occurring chemical reactions on the nucleic acids of the DNA, such as oxidation or alkylation, which can lead to toxic as well as mutagenic base damage. In addition, mismatches, nucleotide dimers, and covalent bonds are amongst the most common damage that occurs to DNA. Far more dangerous, however, are SSBs and DSBs (Lindahl, 1993). In particular DSBs threaten the genomic integrity by leading to chromosomal rearrangements or disruptions of genetic information. To counteract the deleterious effects of DNA damage, the cell has evolved various mechanisms to repair these lesions and thus, maintain genomic integrity.

2.1 Oxidative stress

Oxidative stress is a metabolic state characterized by an imbalance between the production of ROS and the ability to detoxify or repair the resulting damage. This interplay is of great importance as ROS have the ability to damage all components of the cell and are linked to the development of a variety of diseases such as cancer, diabetes, metabolic disorders, atherosclerosis, and cardiovascular diseases (Pizzino et al., 2017; Rajendran et al., 2014).

ROS are the driving force of oxidative stress and are commonly defined as peroxides and free radicals such as hydrogen peroxide (H_2O_2), superoxide radical (O_2^{-}), hydroxyl radical ($^{\bullet}OH$), and singlet oxygen ($^1O_2$). These oxygen-derived species originate mainly as by-products of mitochondrial oxygen metabolism (Hansen et al., 2006). Here, the superoxide radical is formed instead of water when a premature and incomplete reduction of oxygen occurs on the electron transport chain (Li et al., 2013). The majority of superoxide radicals are, in turn, converted to hydrogen peroxide. H_2O_2 has no unpaired electrons and is therefore not a free

radical, but it can form the highly reactive hydroxyl radical through the Fenton or Haber-Weiss reaction (Genestra, 2007). Since these ROS are generated within the cell itself, they are referred to as endogenous ROS. Exogenous sources can also contribute to the ROS level. Cigarette smoke, alcohol, radiation, environmental pollutants, heavy metals, and special drugs (gentamycin and bleomycin) are all examples of exogenous ROS producers (Pizzino et al., 2017). If the normal redox state in cells is disturbed, it can lead to an increase in ROS levels and damage proteins, lipids, and DNA. While proteins and lipids are generally degraded and recycled, oxidative DNA damage must be removed to maintain genomic integrity. DNA damage caused by oxidative stress includes oxidized bases, oxidized sugar fragments, apurinic/apyrimidinic sites (AP sites), and SSBs, with oxidized bases being amongst the most common ones (Hegde et al., 2008).

To counteract the harmful effects of oxidative stress, cells have developed an antioxidant defense system based on enzymatic and non-enzymatic components (Birben et al., 2012). Superoxide dismutase (SOD), catalase, and glutathione peroxidase are the best studied enzymatic antioxidants. SOD is present in almost all aerobic cells and catalyzes the reaction of the superoxide radical to oxygen and H_2O_2 (Singh et al., 2017). The catalases then convert H_2O_2 into water and oxygen (Alfonso-Prieto et al., 2009). This reaction occurs in peroxisomes, where catalases are typically found. In contrast, peroxidases have multiple substrates, including H_2O_2, but also organic hydroperoxides. As the reaction of peroxidases is reversible, they are thought to play an important role in antioxidant metabolism by increasing or decreasing oxidation levels (Cardoso et al., 2017). However, in addition to enzymatic antioxidants, a whole range of radical scavengers have evolved that function without enzymatic activity. Glutathione, for example, because of its low redox potential, can accept an electron from a ROS, thereby neutralizing it (Amir Aslani and Ghobadi, 2016). In addition, there are also a number of essential antioxidants that must be consumed in the diet. The best known are ascorbic acid (vitamin C) and tocopherols/tocotrienols (vitamin E) (Buettner, 1993; Frei et al., 1989). The function is either that of a scavenger (tocopherol) or of an oxidation-reduction catalyst (ascorbic acid).

Further studies have since revealed a much more complex interplay between ROS production and detoxification. Thus, the potential of reactive oxygen species to damage cellular components is utilized and they can also exert positive effects on various processes. For example, the immune system uses ROS as a defense mechanism against pathogens. Phagocytes produce ROS such as superoxide, but also reactive nitrogen species such as nitric oxide ($^{\bullet}NO$) (Nathan and Shiloh, 2000). The lethal effect of these highly reactive compounds is used to attack pathogens that infect the host cells. The nonspecific damage induction of

these species also damages the host tissue, but it has the advantage of attacking all cellular compartments of the pathogens as well. It even prevents adaptation of the pathogen to the immune response by mutations of individual molecular targets (Vazquez-Torres et al., 2000). In addition, ROS can act as second messengers in redox-sensitive signaling pathways (Weyand et al., 2018). Redox signaling is involved in important processes like metabolism, cell growth, differentiation, and cell death. It is a highly regulated process that requires balanced production of oxygen species and antioxidant prevention to maintain cellular redox homeostasis. Studies have even shown that reducing ROS levels by vitamin E and A supplementation has negative effects (Bjelakovic et al., 2007). The short-term increase in ROS occurs, for example, after physical activity and is thought to have a positive effect on the correct folding of proteins. This behavior, called mitohormesis, states that a physiological amount of ROS is more beneficial than a completely diminished ROS level (Ristow and Zarse, 2010). Additional supplementation of antioxidants is nowadays increasingly questioned. However, this does not change the fact that a high amount of ROS is potentially harmful to different cellular compartments.

2.2 8-oxoG

Base modifications are one of the most common DNA lesions after oxidative stress. Since guanine has the lowest redox potential, guanine oxidation occurs more frequently than any other base oxidation (Burrows and Muller, 1998). The major product after the exposure to oxidative stress is the base modification 8-oxoG. Assumptions suggest that approximately 3,000 8-oxoG base modifications are present in a cell at any given time (Gedik and Collins, 2005). For this reason, 8-oxoG has been established as a marker for the assessment of oxidative stress (Dizdaroglu, 1985; Grollman and Moriya, 1993). Oxidation can occur either in the cellular nucleotide pool of ready-to-integrate bases, forming 8-oxo-2'-deoxyguanosine-5'-triphosphate (8-oxo-dGTP), or directly in the DNA duplex, forming 8-oxo-2'-deoxyguanosine (8-oxo-dG). The oxidation of guanine is the subject of many studies dealing with the aging process or the development of cancer (Barja, 2004; Xie et al., 2004). Its carcinogenic property is often associated with the ability of 8-oxoG to form a Hoogsteen base pair with adenine (Akiyama et al., 1989). This mispairing can lead to the formation of a G:C → T:A transversion during replication. If oxidized in the nucleotide pool, an 8-oxoG can be incorporated into the DNA opposite an adenine. The result is the potential reversed T:A → G:C transversion (Shibutani et al., 1991).

Because of its potential to cause point mutations, cells have developed a complex system to prevent damage from oxidized guanines (**Figure 2.1**). The term GO-system was established, to describe the interactions of a three-component enzymatic system dealing with 8-oxoG (also called GO lesion) (Michaels and Miller, 1992). To prevent incorporation from the nucleotide pool, the glycosylase MutT homolog 1 (MTH1) hydrolyzes the oxidized 8-oxo-dGTP to a monophosphate. Once the oxidized guanine is incorporated into DNA or by direct oxidation of guanine in the DNA, the 8-oxo-dG is recognized and removed by the 8-oxoguanine specific glycosylase OGG1 (Rosenquist et al., 1997). OGG1 is part of the BER repair mechanism that deals with modified bases and removes them from the DNA. However, the specificity of OGG1 is reduced once 8-oxoG is mispaired with an adenine. The glycosylase MutY glycosylase homolog (MUTYH), in contrast, is specific in recognizing a mismatched 8-oxoG:A and removes the incorrectly incorporated adenine (Williams and David, 1998). Afterwards a cytosine can be inserted and the OGG1-BER mechanism can function.

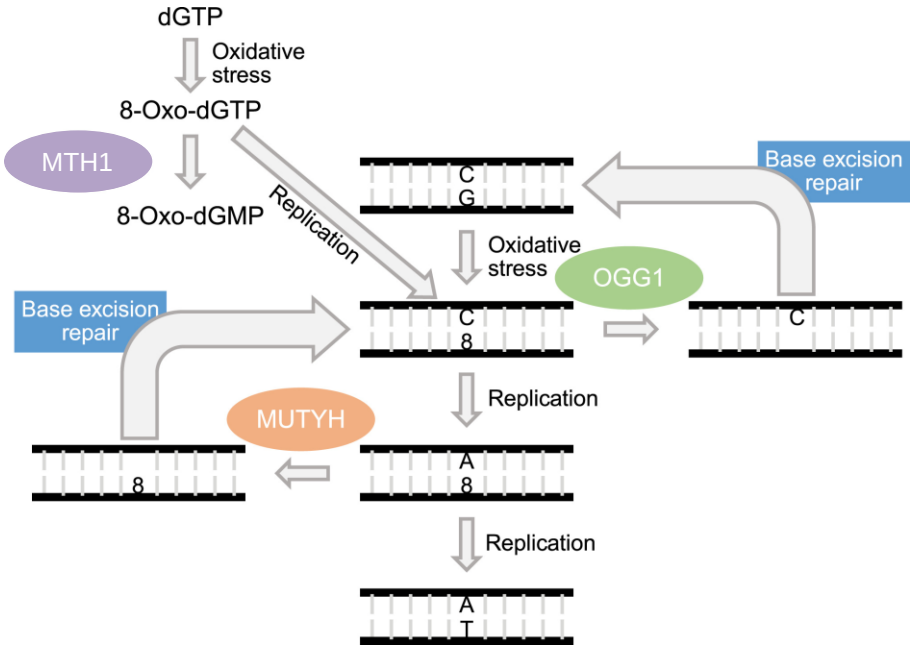

Figure 2.1 Repair system of the oxidized base modification 8-oxoG
If an 8-oxoG is incorporated into the DNA or an incorporated guanine is oxidized, this can result in a G:C → T:A transversion after two rounds of replication. To prevent incorporation, oxidized 8-oxo-dGTP is removed from the nucleotide pool by MTH1. Once an 8-oxoG is present in the DNA and pairs with cytosine, it can be recognized and removed by OGG1. The repair is thereby accomplished via the BER process. However, if there is a mismatch between an 8-oxoG and an adenine, the glycosylase MUTYH is required for detection and removal. MUTYH removes the mismatched adenine, also initializing repair by BER. If the incorporation of cytosine occurs, the OGG1-BER repair pathway can be performed. 8: 8-oxoG. Modified from van den Boogaard et al., 2021

The importance of these glycosylases was demonstrated in mice with double knockout of OGG1 and MUTYH. They showed a highly elevated risk of developing lung and small intestine cancer compared to control mice (Russo et al., 2004). The homologous 8-oxoG repair enzymes have been detected in a variety of bacteria, yeasts, mammals, and even plants. This underlines the importance of 8-oxoG and the corresponding repair mechanisms in most living organisms (Hirano, 2008).

2.3 Base excision repair

As pointed out before, the generation of oxidative products is an ongoing process that constantly threatens the genomic integrity. In this context, studies on healthy human volunteers revealed a steady-state number of about 3,000 oxidized base modifications of 8-oxoG per cell (Gedik and Collins, 2005). To prevent a long-term accumulation of DNA damage, cells have evolved an efficient mechanism to repair base modifications (**Figure 2.2**). BER is one of the most active repair mechanisms in our cells, and malfunctions in this process are embryonically lethal (Gu et al., 1994).

Initiation of BER occurs through specific glycosylases that recognize different types of base modifications in the DNA. Currently, eleven different glycosylases have been described (Jacobs and Schär, 2012). Some are specific for only one or two types of base modifications (OGG1, MUTYH), while others can recognize several different substrates (MPG, NEIL1). The glycosylases search the DNA for their target substrate and, once they have recognized it, remove it from the DNA. To do this, the glycosylase flips the base out of the double helix to allow for binding in the active site and cleaves the N-glycosidic bond, creating an AP site (Huffman et al., 2005). When the function is limited to the glycosylase activity, the glycosylases are called monofunctional. On the other hand, if the glycosylase also has AP lyase activity, such as OGG1, they are called bifunctional (Jacobs and Schär, 2012). These glycosylases cleave the DNA strand by β-elimination, leaving a 3'-α,β-unsaturated aldehyde next to a 5'-phosphate. In both cases, AP endonuclease 1 (APE1) must process the ends so that the gaps can be filled by the polymerase. For monofunctional glycosylases, APE1 cuts the DNA 5' from the AP site to create a 3'-OH end suitable for polymerases. For bifunctional glycosylases, a single-strand break is already induced by the AP lyase activity, but the 3'-α,β-unsaturated aldehyde must be removed by APE1 to generate the 3'-OH end. Both X-ray repair cross complementing 1 (XRCC1) and poly (ADP-ribose) polymerase 1 (PARP1) have been shown to bind at the AP site acting as mediators (D'Amours et al., 1999; Hanssen-Bauer et al., 2011).

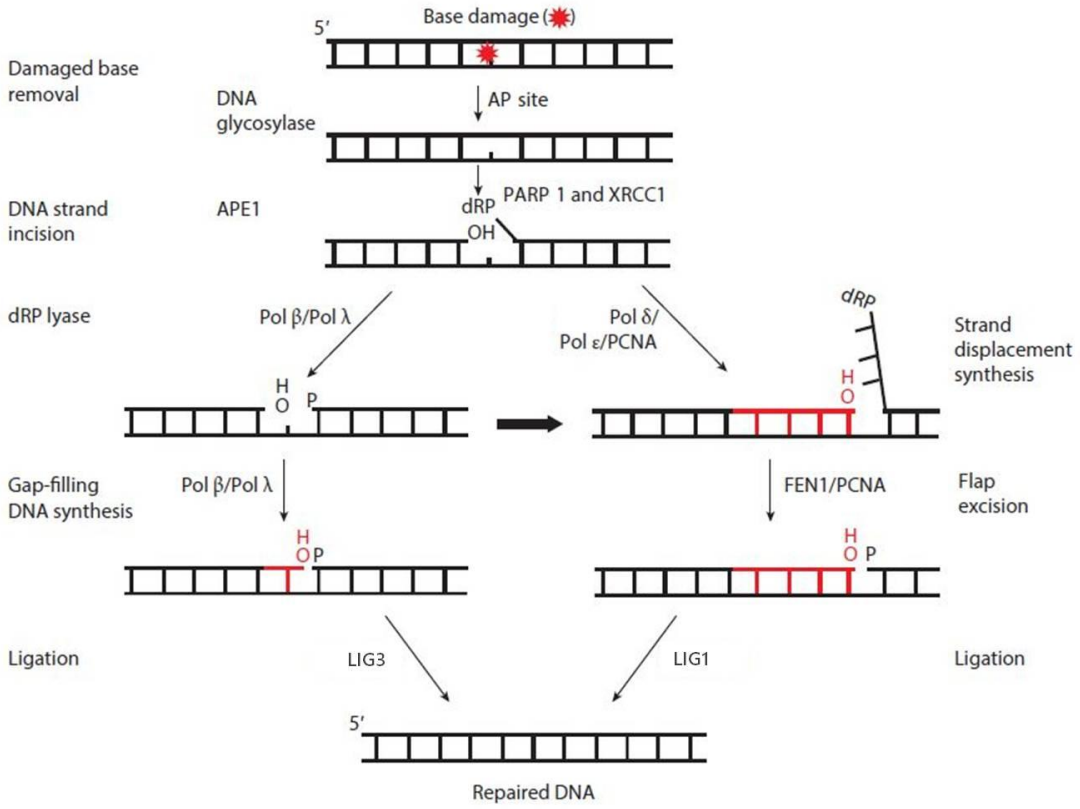

Figure 2.2 Schematic presentation of the base excision repair process
Modified bases are recognized by specific glycosylases and removed from the DNA backbone. The resulting AP site is processed by APE1 into a 3'-OH end to allow polymerase activity. PARP1 and XRCC1 act as mediators and enable further repair via two pathways. In short-patch repair (left), the gap is filled via Pol β/λ and the DNA backbone is ligated via LIG3. Long-patch repair (right) performs displacement synthesis mediated by Pol δ/ε and PCNA. The disassociated DNA flap is removed by FEN1 to allow ligation via LIG1. Modified from Beard et al., 2019

The next steps of base excision repair can be divided into two sub-pathways: the short-patch and long-patch repair. The short-patch repair is considered to be the dominant sub-pathway, and is active throughout the cell cycle. After the generation of an AP site and processing of the ends by the glycosylase and APE1, polymerase β (Pol β), and to a lesser extend polymerase λ (Pol λ), fills in the missing nucleotide using the information from the undamaged strand (Braithwaite et al., 2005). Once the gap is filled, DNA ligase 3 (LIG3) joins the 3' and 5' ends and completes the repair process (Hegde et al., 2008). Long patch repair only occurs in proliferating cells as several replication factors are involved in this process (Akbari et al., 2009). Gap filling is performed by polymerase δ (Pol δ) and ε (Pol ε) in cooperation with proliferating cell nuclear antigen (PCNA) and replication factor C. The term long patch arises from the displacing synthesis activity of the polymerases in this sub-pathway. Pol δ and ε displace a flap of 2-10 nucleotides that must be removed by flap endonuclease 1 (FEN1)

(Prasad et al., 2000). Ligation is performed by DNA ligase 1 (LIG1) to connect the DNA backbone. Since the repair of base modifications is accompanied by the formation of an abasic site and a related SSB, the repair of SSBs is regulated by a specific mechanism related to BER. The SSBs serve as a signal for the activation of PARP1 (Fisher et al., 2007). This recruits XRCC1/LIG3 together with other end-processing proteins to ligate the sugar-phosphate backbone (Caldecott, 2007).

2.4 DNA damage response and DSB repair

DSBs are the most severe DNA lesions, potentially leading to cell death and mutagenesis. Accordingly, it is important to recognize the break sites and initiate the DNA damage response. The DNA damage response is characterized by processes that trigger a diverse signaling cascade (Khanna and Jackson, 2001; van Gent et al., 2001). However, these cascades are bundled into three reaction pathways. If the induced DNA damage is too excessive and repair is no longer possible, the programmed cell death, apoptosis, can be initiated (Bernstein et al., 2002). In dividing cells, cell cycle control is activated to prevent transition into S phase or mitosis phase (M phase), in order to prevent the formation of highly carcinogenic chromosomal aberrations (Bartek and Lukas, 2001; Pearce and Humphrey, 2001). If repair of the induced damage is possible, DSB repair mechanisms are initiated to restore genomic integrity via two major repair pathways: canonical-non-homologous end joining (c-NHEJ) and homologous recombination (HR) (Cahill et al., 2006).

2.4.1 DSB recognition

The first response of a cell towards the induction of DSBs is the activation of the DNA damage response. Triggers of the DNA damage response are the so-called phosphoinositol-3-kinase like kinases (PIKKs). The conserved family of PIKKs possesses serine/threonine kinase activity and thus provides phosphorylation of many key proteins in the corresponding response pathways (Abraham, 2001; Durocher and Jackson, 2001). In mammals, the DNA damage response is mainly initiated by ataxia telangiectasia mutated (ATM), ataxia telangiectasia and Rad3-related (ATR), and DNA-dependent protein kinase (DNA-PK) (Abraham, 2001; Durocher and Jackson, 2001). It has been shown that ATM and DNA-PK respond mainly to DSBs, whereas ATR is activated by single-stranded DNA (ssDNA) arising, for example, at ultraviolet light damage and stalled replication forks.

The best studied process in this regard is the activation of ATM in response to the induction of DSBs. In undamaged cells, the ATM molecule is present as a dimer and thus inactive. Following DNA damage, ATM autophosphorylates itself at serine 1981 and the active monomer is formed (Bakkenist and Kastan, 2003). As a result, a rapid increase in the kinase activity is observed (Banin et al., 1998; Canman et al., 1998; Kozlov et al., 2003). This leads to the recruitment of ATM to the break ends which serves as a signal for further enzymatic reactions (Andegeko et al., 2001). Although no direct contact of ATM with damaged DNA can be observed, the signal of ATM activation leads to widespread chromatin modifications. One of these changes is the phosphorylation of H2A histone family member X (H2AX) (Rogakou et al., 1998). H2AX is a variant of histone H2A and represents approximately 10-20 % of H2A proteins in eukaryotic cells. Phosphorylation of the H2AX histone components at serine 139 leads to the formation of γH2AX (Burma et al., 2001). This phosphorylated variant serves as a platform for mediator of DNA damage checkpoint protein 1 (MDC1) which recruits the MRE11-RAD50-NBS1 complex (MRN) and additional ATM. These reactions create a positive feeback-loop spreading the phosphorylation of H2AX in an area of approximately 2 Mbp around the break site and is used as a signal for the presence of a DSB (van Attikum and Gasser, 2009).

In contrast to the activation of ATM, ATR is mainly functional in the presence of replication stress (Ward and Chen, 2001). Here, ssDNA bound with replication protein A (RPA) serves as a signal for ATR activation via the ATR interacting protein (ATRIP) (Shechter et al., 2004). These regions occur, for example, at arrested replication forks that, if not resolved, lead to break induction. ATR is able to phosphorylate the same target proteins as ATM and thus can induce the same downstream reactions, such as phosphorylation of H2AX. The function of the PIKKs is to some extent interchangeable and the loss of a kinase can thus be compensated (Cimprich and Cortez, 2008). In this way, DNA-PK, in addition to its essential role in DNA repair via c-NHEJ, can also initiate the recognition of DSBs and the following processes.

2.4.2 Canonical-non-homologous end joining

The histon modification γH2AX serves as a signal for the recruitment of DSB mediator proteins such as p53-binding protein 1 (53BP1) and MDC1 (Xie et al., 2007). The recruitment of these proteins induces a signaling cascade that leads to initiation of DSB repair mechanisms. One of the first targets is the Ku70/80 heterodimer, which binds to DSBs within seconds and prevents excessive DNA-end resection (Walker et al., 2001). Through Ku70/80, the catalytic subunit DNA-PKcs is recruited to the DSB and activated to form the functional

kinase DNA-PK. The active DNA-PKcs has a high affinity for Ku70/80 bound DNA and directs the repair of the DSB towards the c-NHEJ pathway (**Figure 2.3**) (Meek et al., 2008).
After binding to the DSB site, DNA-PKcs is autophosphorylated and recruitment of X-ray repair cross-complementing protein 4 (XRCC4) and DNA ligase 4 (LIG4) is promoted. XRCC4/LIG4 are responsible for the ligation of the two DNA ends if this is possible (Grawunder et al., 1997). If the two break ends cannot be easily ligated due to additional damage at the break ends such as nucleotide loss or base damage, additional processing is required. XRCC4-like factor (XLF) and paralog of XRCC4 and XLF (PAXX) promote c-NHEJ by stabilizing the ligase complex at such break ends. Studies suggest that the role of these two factors is to stabilize Ku70/80 together with other NHEJ proteins at break ends and allow for further processing (Ochi et al., 2015; Tsai et al., 2007). In such case, the Artemis endonuclease is recruited in complex with DNA-PKcs (Goodarzi et al., 2006). Autophosphorylation of DNA-PKcs in turn activates the nuclease activity of Artemis. 5'- and 3'-DNA overhangs are then removed by the Artemis/DNA-PKcs-complex to create DNA end structures that can be ligated by XRCC4/LIG4 (Ma et al., 2004). This process can result in deletions at the break ends, which is why c-NHEJ represents an error-prone repair pathway (Chang and Lieber, 2016). Since repair via the c-NHEJ is based on a simple ligation of the two break ends, this repair pathway is available in all cell cycle phases (Mladenov et al., 2016).

2.4.3 Homologous recombination

Repair via HR requires a sister chromatid that serves as a template for the damaged DNA strand (Kadyk and Hartwell, 1992). For this reason, HR is only available in S and G2 phase (**Figure 2.3**). DSBs repaired via HR are recognized and processed by MRN which exerts its role in stabilizing the two break ends and activating kinases such as ATM (de Jager et al., 2001). Furthermore, double-strand break repair protein MRE11 (MRE11) initiates the resection process, which is a key signature of the HR repair mechanism. In this process, MRE11 cleaves the DNA via its endonuclease activity and interacts with CtBP-interacting protein (CtIP) (Sartori et al., 2007). The resection occurs in both directions from the incision site. The exonucleases exonuclease 1 (EXO1), DNA replication ATP-dependent helicase/nuclease 2 (DNA2), and Blooms syndrome helicase (BLM) resect in the 5'-3' direction away from the break end while the exonuclease activity of MRE11 is responsible for 3'-5' resection towards the break end (Symington, 2014). The resection activity leads to the formation of a 3'-ssDNA overhang. The resulting 3'-ssDNA is covered by RPA to prevent degradation and formation of secondary structures of the resected ends (Chen et al., 2013).

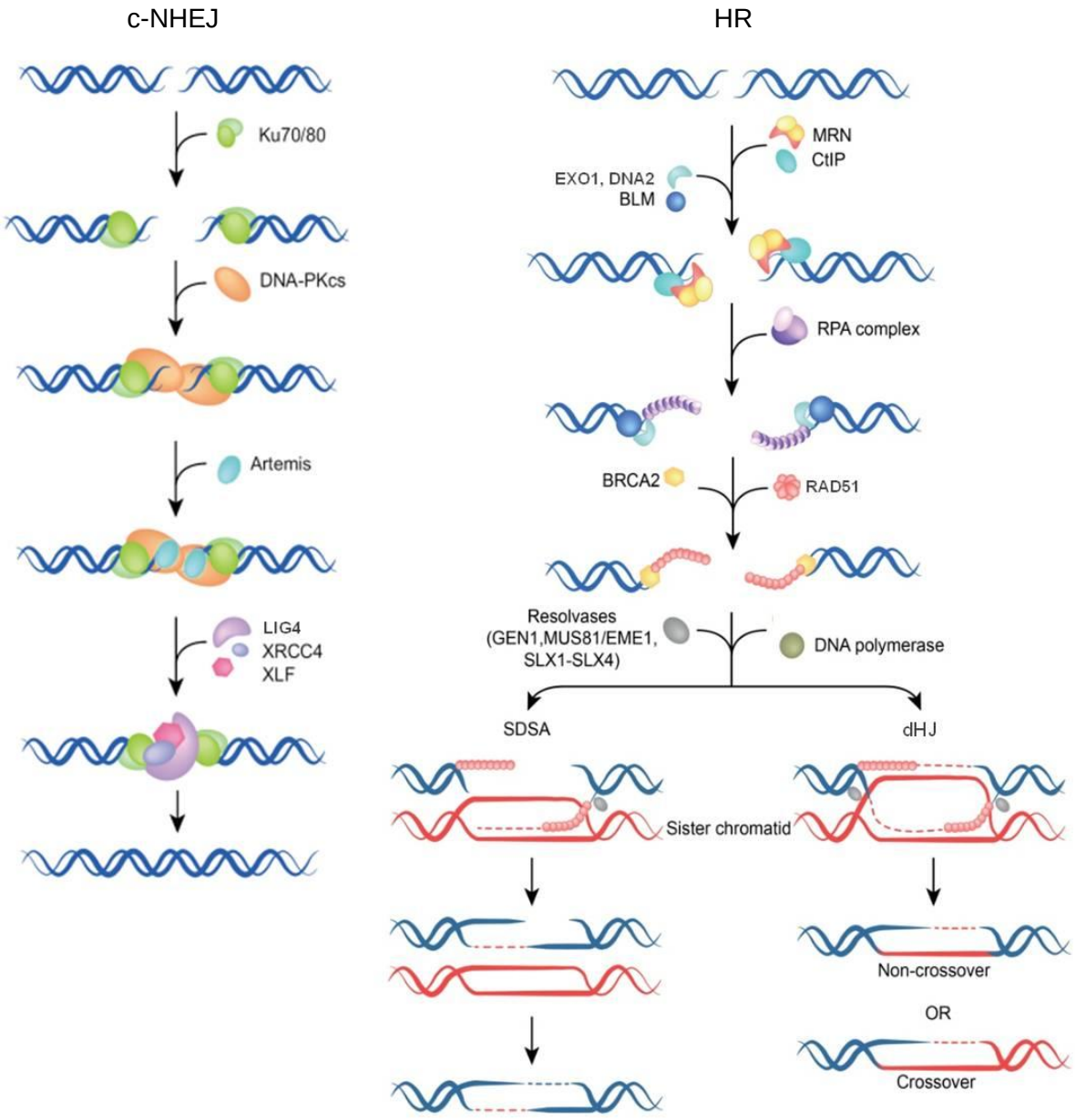

Figure 2.3 DSB repair processes: c-NHEJ and HR
c-NHEJ: After DSB induction, Ku70/80 is recruited to the break ends and promotes DNA-PKcs binding. By this, resection of the break ends is prevented and the functional kinase DNA-PK is formed. When processing of the break ends is needed, the autophosphorylation of DNA-PKcs can lead to the activation of the nuclease activity of Artemis. Factors XLF and PAXX (not shown graphically) stabilize XRCC4 and LIG4 at the break ends and ligation is performed.
HR: Repair is initiated by resection of the break ends. In this process, MRN acts as a damage sensor and initiator of resection. Recruitment of further nucleases such as CtIP, EXO1, DNA2, and BLM lead to the formation of 3'-ssDNA. To prevent degradation, the ssDNA is bound by RPA. Subsequently, BRCA2 mediates the replacement of RPA by RAD51. Loading of RAD51 forms the nucleoprotein filament, which performs strand invasion into the sister chromatid and thus homology search. A D-loop is formed and with the participation of a DNA polymerase, the strand is extended. HR can now be terminated via two sub-pathways. In SDSA, the newly synthesized strand attaches to the 3'-ssDNA overhang of the second break end and the remaining gaps are filled. The second pathway is initiated by a process called second-end capture. Here, the second break end anneals with the displaced strand creating a dHJ. After synthesis of the remaining gaps, the dHJ must be removed by enzymes, which leads to either crossover or non-crossover events. Modified from Dueva and Iliakis, 2013

Next, RPA is replaced by DNA repair protein RAD51 homolog 1 (RAD51), which is mediated by breast cancer type 2 susceptibility protein (BRCA2) (Liu et al., 2010). The loading of RAD51 forms a nucleoprotein filament which is important to allow strand invasion into the sister chromatid and thus homology search (Wyman et al., 2004). Once the homologous sequence is found a displacement loop (D-loop) is formed and the invading strand is extended by polymerase activity (Wright et al., 2018). The exact process of synthesis activity is not yet deciphered. However, it is assumed that PCNA, replication factor C complex, and Pol δ play an essential role (Sneeden et al., 2013).

Two main sub-pathways are available after DNA synthesis to complete repair: synthesis-dependent strand annealing (SDSA) and the double Holliday junction (dHJ) pathway. In SDSA, the D-loop is dissolved after a short stretch of repair synthesis took place. The newly synthesized 3' end can subsequently reattach to the 3' overhang at the break site in the damaged chromosome due to the homology created during DNA synthesis. SDSA is completed by filling the remaining single-stranded gaps and ligation of the DNA backbone (Wright et al., 2018). How these steps occur in mammalian cells has not been finally elucidated, but there are first candidates associated with displacement and annealing function (RECQ5, RECQ1, FANCJ) (Paliwal et al., 2014; Sommers et al., 2009). The dHJ pathway acts by the second end capture of the displaced strand of the D-loop by the 3' overhang that was not involved in strand invasion, forming a dHJ (Bzymek et al., 2010). After extended DNA synthesis and end ligation the dHJ needs to be processed. Two possible ways of processing are available to resolve this structure. Due to the cleavage activity of endonucleases such as flap endonuclease GEN homolog 1 (GEN1) or the SLX-MUS complex (SLX1-SLX4-MUS81-EME1), the processing of a dHJ can result in crossover or non-crossover events. This process is also referred to as resolution. In contrast, dissolution of a dHJ results exclusively in non-crossover events. In this case, branch migration and decatenation are performed via the BTR complex (BLM-TopIII-RMI1-RMI) (Sarbajna and West, 2014). In conclusion, HR provides a high-fidelity repair pathway by using sequence information from the sister chromatid to restore lost information at the break site.

2.5 Replication, replication stress and one-ended DSBs

To maintain genome stability and prevent oncogenic mutations, it is of particular importance for cells to replicate their DNA accurately and without errors. DNA replication usually occurs rapidly and only with occasional errors, using intrinsic (proofreading) and extrinsic (mismatch repair) error correction systems. All this has to be accomplished despite numerous DNA lesions caused by endogenous and exogenous factors.

2.5.1 Replication

Error-free duplication of the chromosome is essential for a successful cell cycle. Before a cell can enter M phase and divide into two daughter cells, it first prepares during interphase. In the two gap phases (G1 and G2 phase), mainly proteins and other cell components are synthesized, while in S phase the actual duplication of DNA takes place. Already during G1 phase, the replication origins are bound by the pre-replication complex. Therefore, the origin recognition complex binds to the replication origins and initiates the recruitment of cell division cycle 6 (CDC6) and chromatin licensing and DNA replication factor 1 (CTD1) (Tanaka and Araki, 2013). This leads to the binding of two inactive minichromosome maintenance complex component 2 and 7 (MCM2-7) proteins loaded as a head-to-head double hexamer to allow for bidirectional fork movement. When this process is completed, the replication origins are also referred to as licensed (Ticau et al., 2015). Once cells enter S phase, cyclin-dependent kinase (CDK) and Dbf4-dependent kinase (DDK) phosphorylation events lead to the recruitment of cell division cycle 45 (CDC45) and the GINS complex (Heller et al., 2011). The resulting complex of CDC45, MCM2-7, and GINS (CMG) forms the active CMG dependent helicase, which unwinds the DNA (Moyer et al., 2006). This process is continued by the recruitment of numerous additional replication factors and includes, among others, the association of DNA polymerases (Sengupta et al., 2013). An active replisome forms and the so-called pre-initiation complex is established (**Figure 2.4**).

Elongation is initiated by DNA polymerase α (Pol α), which forms a complex with RNA primase. The primase synthesizes a short 10 nucleotide long ribonucleic acid (RNA) segment, the so-called RNA primer (Núñez-Ramírez et al., 2011). These primers are needed as an attachment site for the polymerases, since they require a free 3'-OH end to incorporate nucleotides. Pol α can start synthesizing the DNA strand after primers are attached to it. However, Pol α is not able to continue DNA replication and after the synthesis of approximately 20 nucleotides is replaced with the actual replication polymerases (Bullock et

al., 1991). As the activity of the CMG helicase results in two differently processed ssDNA strands, the leading and lagging strand, two mechanistically distinct ways of replication have been established. On the leading strand, replication can occur continuously, and on the lagging strand, replication occurs discontinuously (McCulloch and Kunkel, 2008). As the polymerases can only synthesize in the 5'-3' direction, and due to the double-helical structure of DNA, the lagging strand is oriented in the opposite direction of replication fork movement. For this purpose, the replisome forms a loop that allows the polymerase to process both strands with the same orientation promoted by acidic nucleoplasmic DNA-binding protein (AND-1) (Simon et al., 2014). Replication on the leading strand is performed by Pol ε and on the lagging strand by Pol δ (McCulloch and Kunkel, 2008). The clamp protein PCNA is required for the effective exchange of polymerases and their functionality. This is strengthening the interaction between the polymerase and the template DNA and enhances the polymerase processivity up to 1,000-fold (Chilkova et al., 2007).

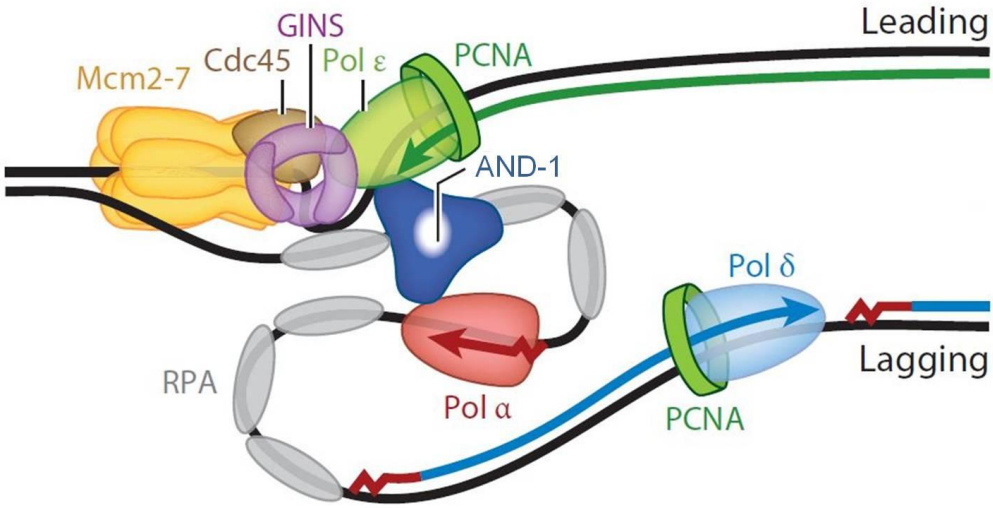

Figure 2.4 Structure of the replication fork
MCM2-7, together with CDC45 and the GINS complex, forms the active CMG helicase. The activity of Pol α together with RNA primase initiates elongation and synthesizes short DNA fragments. Subsequently, Pol ε/δ are recruited and longer segments are synthesized with the participation of PCNA. Due to the double-helical structure of DNA, a loop of the lagging strand is formed by AND-1, as polymerases only synthesize in 5'-3' direction. Synthesis at the leading strand is continuous. On the lagging strand synthesis is discontinuous, whereby ssDNA regions are formed which are bound by RPA for protection. Modified from Burgers and Kunkel, 2017

Different polymerases are needed for the lagging strand, due to his discontinuous replication, where RNA primers have to be placed repetitively. These can be removed by Pol δ using its strand displacement activity, which Pol ε is lacking. The resulting RNA-DNA single strand flap

is cut by FEN1 and ligated by LIG1 (Garg et al., 2004). The discontinuous DNA regions that arise on the lagging strand are also known as Okazaki fragments (Okazaki et al., 1968). Since longer regions of ssDNA are formed during the synthesis on the lagging strand, RPA binds to this regions to achieve a stabilization of the DNA by preventing secondary structures (Wobbe et al., 1987). Replication is complete as soon as two replication forks meet or the end of the chromosome is reached.

2.5.2 Replication stress

Some structures that occur in the DNA double helix have the potential to interfere with the unhindered progression of the replisome. These obstacles can become a threat to genomic integrity, as they can slow down replication or cause complete arrest at hard-to-replicate sites. This replication stress is generated, for example, at G-rich sequences, the G-quadruplexes, at common fragile sites, or hairpin structures (Barlow et al., 2013; Bochman et al., 2012; Kaushal and Freudenreich, 2019; Spiegel et al., 2020). In many cases, however, DNA damage, such as base modifications, base losses, SSBs or DSBs, and protein-DNA cross-links, also lead to replication stress (Gómez-González and Aguilera, 2019). When the replisome encounters a structure that impedes progression, various mechanisms have evolved to re-start and continue replication of the genome (**Figure 2.5**).

The first step in responding to replication stress is to stabilize the replisome at stalled forks via the fork protection complex (FPC), thereby preventing fork collapse (Tye et al., 2021). Defects in replication fork protection often lead to toxic lesions that can induce apoptosis. A stabilized replication fork provides longer time to remove the blocking lesion and an adjacent replisome can then in turn lead to a replication restart (Yekezare et al., 2013). Furthermore, replicative DNA polymerases can be replaced by more nonspecific polymerases. These polymerases, such as DNA Polymerases β, κ, η, τ, and ζ, also insert a nucleotide opposite a DNA lesion. This process is called translesion synthesis and is highly error-prone due to the non-specificity of the polymerases and is associated with mutation formation (Ma et al., 2020). Alternatively, the cell can perform the process of template switching, in which the strand of the blocked polymerase switches to the sister chromatid. There, synthesis can continue for a few nucleotides and the newly synthesized strand can bind again behind the lesion. This bypass of the blocking structure allows for the replication to continue. However, the lesion remains until it is removed by a specific repair mechanism. Another process that reinitiates replication but does not remove the lesion is repriming (Quinet et al., 2021). Here, replication-associated proteins are recruited behind the lesion and re-initiate the replication process. This creates a

gap in the DNA strand that can only be filled once the lesion has been removed. Crucially, primase and DNA directed polymerase (PRIMPOL) and DNA primase subunit 1 (PRIM1) are involved in mediating replication rebinding downstream of the lesion (Mourón et al., 2013).

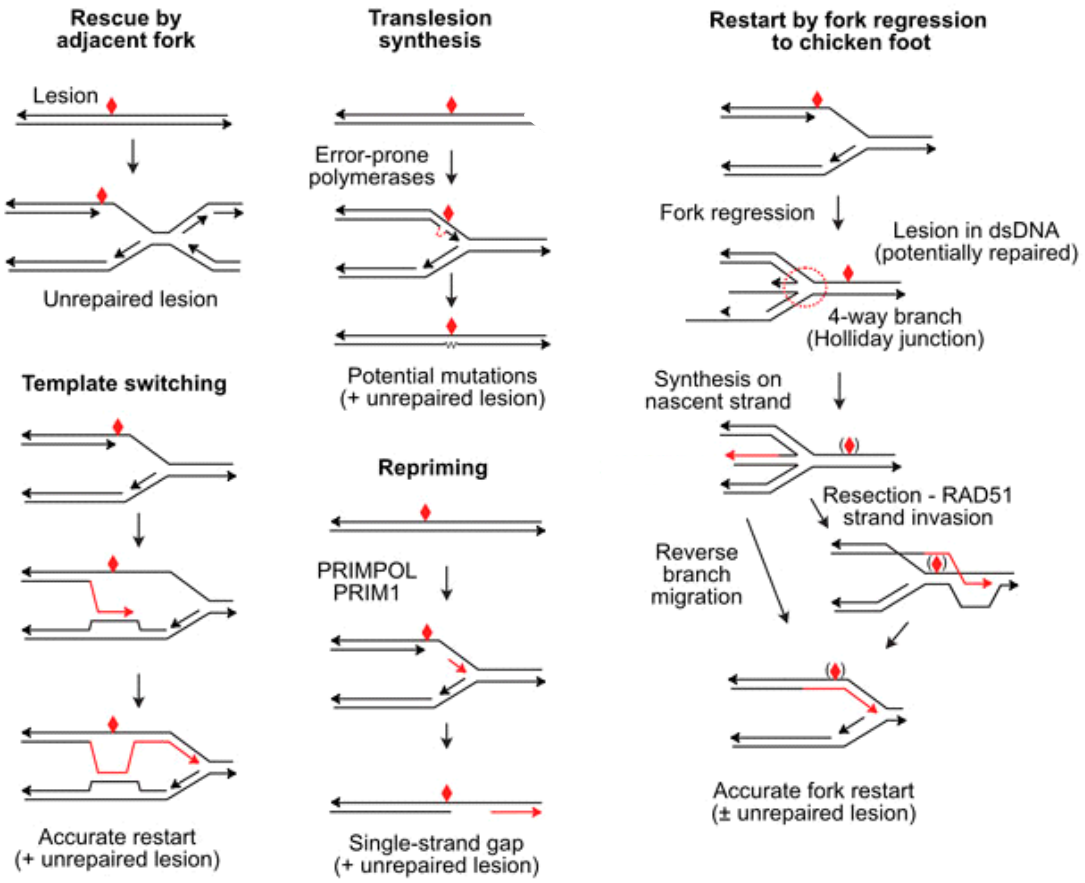

Figure 2.5 Mechanisms to overcome replication stress
There are several ways to respond to DNA damage that leads to replication stress. An arrested and stabilized replication fork provides the time to repair the lesion and for a replication re-start by an adjacent fork. Replacement with an error-prone polymerase allows progression of replication via translesion synthesis, a process that is associated with the formation of mutations. Template switching allows the lesion to be skipped and replication to continue. In addition, replication can be re-initiated downstream of the lesion and the so-called repriming can take place. This involves PRIMPOL and PRIM1 to reassemble replication factors behind the lesion. Additional ssDNA areas are formed, which are susceptible to further damage. However, in all these processes, the lesion remains in the DNA and must subsequently be removed via specific repair processes. The formation of a chicken-foot structure is an alternative scenario to occur. In this case, fork regression takes place and the newly synthesized DNA strands dissociate from the parental strands and anneal to form a Holliday junction. Gaps can be filled and branch migration or strand invasion mediated by RAD51 can occur to generate a new replication fork. Replication can then be restarted and the lesion can be repaired subsequently or during processing. However, the formation of a chicken-foot structure involves the generation of a dsDNA-end, which can be the target of chromosomal rearrangements. Modified from Nickoloff et al., 2021

A further process that can lead to a restart of replication, but involves the formation of a structure with a double-stranded DNA-end (dsDNA), is the restart via fork regression (Zellweger et al., 2015). In this case, the replication fork shifts in the opposite direction to the direction of replication. The newly synthesized DNA strands dissociate from the parental DNA and form a Holliday junction with the characteristic shape of a chicken foot (Heyer et al., 2010). After annealing of the newly synthesized DNA strands, a blunt dsDNA-end can be generated by filling in the missing sequence information. This has no complementary end and can be incorrectly ligated by end-joining processes, causing genome rearrangements. Despite the potential risk of generating a dsDNA-end, the synthesis on the nascent DNA strands allows for bypassing of the lesion. The restart of replication can be initiated by reversed branch migration via association of the newly synthesized DNA strands back to the parental DNA. In addition, fork regression with the formation of a chicken foot structure represents a stable construct that allows enough time for the removal of the DNA lesion. Different HR components like RAD51, BRCA1, and Fanconi anemia group D2 (FANCD2) are involved in the stabilization of the regressed fork (Rickman et al., 2020; Schlacher et al., 2012). The exact mechanisms in vertebrates have not yet been deciphered, but RAD51 is thought to be essential for the formation of a chicken foot structure by having a stabilizing effect, preventing the degradation of nascent DNA strands by nucleases. This process is of critical importance, as fork cleavage by nucleases results in the formation of DSBs. Although reversed forks were initially thought to be rare in eukaryotes, recent studies show otherwise. It has been described that after the induction of replication stress, up to 25 % of replication forks exhibit a chicken foot structure (Zellweger et al., 2015). This indicates that the process of fork regression has a greater impact on replication fork protection than initially thought.

2.5.3 Fork collapse and break-induced replication

When a replication fork collapses, this leads to the formation of a so-called one-ended DSB that lacks the second break end. These break ends are prone to chromosomal aberrations, as ligation via end-joining processes can lead to the linkage of mismatched ends. To prevent this, a mechanism has evolved to resume replication via a sub-pathway of HR called break-induced replication (BIR) (Costantino et al., 2014). Identical to other HR pathways, BIR proceeds by extensive resection of the 5'- to 3'-end (**Figure 2.6**). The 3'-ssDNA end is bound by RPA, followed by the formation of the RAD51 nucleoprotein filament. The nucleoprotein filament is responsible for the subsequent homology search, strand invasion, and formation of the D-loop. Accordingly, the first steps of the BIR require the same proteins involved in the repair

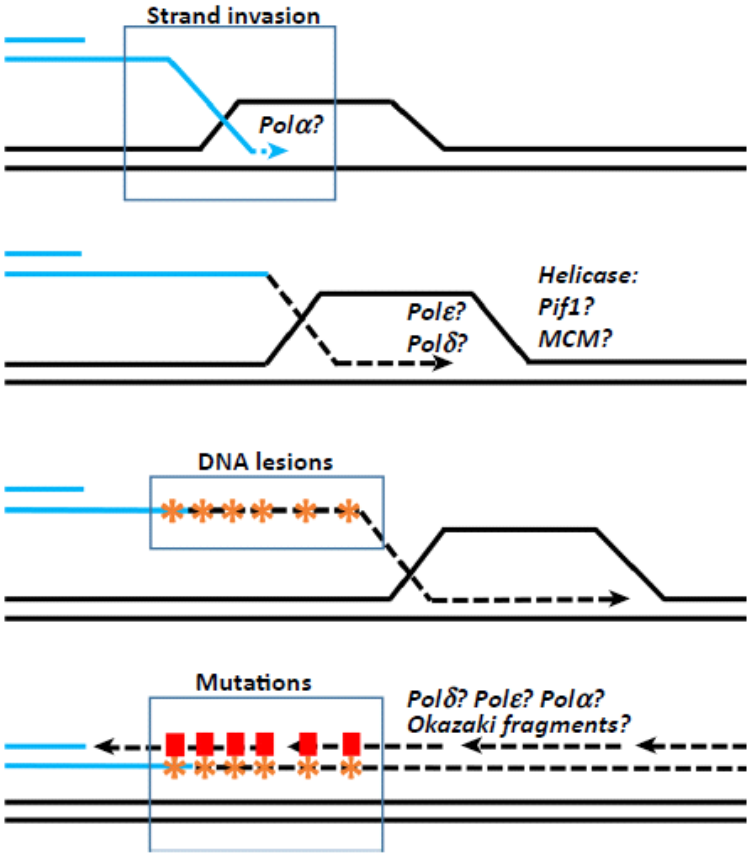

Figure 2.6 The break-induced replication process
After resection of the break end, the RAD51 nucleoprotein filament is formed and strand invasion occurs with the formation of a D-loop. With the participation of Pol α, the synthesis of new DNA is initiated. Helicases such as Pif1 or MCM2-7 unwind the DNA, and replication polymerases Pol ε/δ continue the synthesis. This can continue until the end of the chromosome or until merging with a replication fork (not shown graphically). Asynchronous synthesis results in a long ssDNA segment that is susceptible to damage induction and serves as a template for the synthesis of the second strand. If not repaired, this leads to increased genomic instability emanating from BIR. Modified from Kramara et al., 2018

of two-ended DSBs by HR (Davis and Symington, 2004; Ruff et al., 2016). DNA synthesis, on the other hand, is carried out differently and is dependend on replication-associated proteins (Lydeard et al., 2010). Interestingly, unlike S-phase DNA replication, BIR synthesis occurs asynchronously. This means that the invaded strand is continuously extended at the 3'-OH end and persists as a long strand of ssDNA while the D-loop migrates (Kramara et al., 2018; Saini et al., 2013). However, the exact role of each component has not yet been deciphered. For example, MCM2-7 was initially thought to be the main helicase involved in BIR progression (Lydeard et al., 2010). In contrast, more recent results are contradictory considering Pif1 helicase to be an essential component of BIR (Wilson et al., 2013). All three

replication polymerases (Pol ε, Pol α, and Pol δ) are involved in BIR, although it is not clear how each of these is utilized. Pol δ is thought to be the main polymerase performing strand synthesis. The Pol α primase complex is considered to be involved in the synthesis of the lagging strand (Lydeard et al., 2007). The lagging strand uses the leading strand as a template to complete the repair, resulting in a conservative duplication of the DNA strand (Saini et al., 2013). This process is needed as the second end capture cannot take place and the formation of a dHJ is not possible due to the missing second end (Petermann et al., 2010). Once synthesis begins, it often proceeds to the end of the template chromosome, or until another replication fork is encountered.

BIR is generally associated with an increased risk of genetic instability (Smith et al., 2007). This is mostly attributed to the frequent dissociations of Pol δ from the DNA strand, reduced efficiency of mismatch repair and a generally, compared to its activity during S phase, lower efficiency of the polymerase. In addition, the formation of a long ssDNA strand is thought to increase the susceptibility of DNA for further DNA lesions to occur during BIR. The BIR process plays a crucial role in, for example, the overexpression of oncogenes such as cyclin E. Oncogene overexpression leads to a massive breakdown of replication forks and the formation of one-ended DSBs, which are repaired by BIR (Halazonetis et al., 2008). Furthermore, BIR has been detected in cancer cells that possess deregulated origin licensing, leading to replication stress (Galanos et al., 2016). In addition, BIR is associated with alternative telomere lengthening, a mechanism of telomere maintenance that lengthens telomeres in the absence of telomerase. This process is used by up to 15 % of all human tumors to preserve their telomeres (Conomos et al., 2013). Another aspect of BIR involves mitotic DNA synthesis (MiDAS). This describes the repair of under-replicated regions often found in common fragile sites that are fixed by a BIR process during mitosis (Minocherhomji et al., 2015). Although the process of BIR is important in many ways, there are still several questions that remain unanswered. For example, it was recently shown that a RAD51-independent BIR pathway also exists in mammalian cells (Sotiriou et al., 2016). This was first demonstrated in yeast and requires the function of DNA repair protein RAD52 homolog (RAD52). Further studies are needed to decipher the exact processes of BIR in mammalian cells.

2.6 Transcription and conflict potential

As described earlier, there are numerous obstacles for the replisome on its way replicating the genetic information. This often involves unnatural changes in the structure of the DNA. Moreover, a transcription complex competing for the same DNA template can also interfere

with unhindered replication and represent a special case of replication stress. When replication and transcription collide, it can lead to genomic instability by chromosomal recombination, DNA damage, tumor formation, or cell death (Helmrich et al., 2011; Prado and Aguilera, 2005; Trautinger et al., 2005). To prevent these replication-transcription conflicts both processes need to be spatially and temporally organized.

2.6.1 Transcription

Along with translation, transcription is the central component of gene expression and is crucial for the transfer of genomic information in the form of DNA into RNA, which is required for protein biosynthesis. Transcription is divided into three phases: initiation, elongation, and termination.

During the initiation phase, the promoter region is recognized, the DNA helix structure is opened, and synthesis of a short RNA oligomer is initiated. This initiation process is mainly dependent on general transcription factors. These associate at the promoter DNA together with the RNA polymerase II (Pol II) to form the pre-initiation complex (Buratowski et al., 1989; Matsui et al., 1980). Transcription initiation is thereby also regulated by gene-specific transcription factors. These bind the promoter regions and ensure the formation of the pre-initiation complex. It has been shown that gene-specific transcription factors do not interact directly with the pre-initiation complex but on cofactors that regulate transcription. One of the best known and studied cofactors is the multiprotein complex Mediator (Malik and Roeder, 2000; Ryu and Tjian, 1999). The role of Mediator is to link gene-specific transcription factors to the Pol II pre-initiation complex. The transcription factor II human (TFIIH) has helicase and protein kinase activity, which unwinds DNA and makes it accessible to the active site of the polymerase. Furthermore, the kinase activity of TFIIH leads to phosphorylation of the C-terminal repeat domain (CTD), which causes dissolution of the pre-initiation complex and synthesis of the first RNA nucleotides (Grünberg et al., 2012).

The elongation phase is characterized by the successive growth of the RNA chain. In this step, the polymerase uses the DNA template to transcribe the DNA into RNA. Initially, however, the Pol II elongation complex pauses at the transcription start site (Rougvie and Lis, 1988). The paused Poll II is stabilized by the two elongation factors DRB sensitivity inducing factor (DSIF) and negative elongation factor (NELF) and, is sent into active elongation due to the activity of the kinase positive transcription elongation factor (P-TEFb) (Marshall and Price, 1995; Yamaguchi et al., 1999). P-TEFb phosphorylates Pol II at the CTD domain, as well as DSIF and NELF (Komarnitsky et al., 2000). This leads to the recruitment of elongation factors

that stimulate Pol II progression and initiate elongation. During this process, factors for 5' capping and splicing of pre-messenger RNA and 3' processing are recruited, as well as enzymes that modify histones. This ensures that transcription proceeds smoothly.
The transcription is completed at the terminator region. The DNA and RNA are released, and the polymerase can be removed. To do this, Pol II must pass through the polyadenylation site at the end of the transcribed region. This leads to cleavage of the nascent RNA transcript and maturation of the messenger RNA. However, Pol II often does not recognize the end of the transcribed region and continues synthesizing. The excess RNA is degraded by an exonuclease (Rat1) faster than Pol II can synthesize it. When the nuclease and polymerase encounter each other, Pol II is released from the DNA, triggering the end of transcription (Kim et al., 2004; West et al., 2004).

2.6.2 Replication-transcription conflicts

To avoid conflicts between replication and transcription prokaryotes have evolved a unique method. A large proportion of genes found in prokaryotes are aligned with the direction of replication, minimizing the potential collision of replication and transcription (Brewer, 1988; Kunst et al., 1997; Srivatsan et al., 2010). Prokaryotes benefit from the fact that they have only one origin of replication. Therefore, adaptation to the direction of replication is easily accomplished. In eukaryotes, however, there are multiple origins of replication, which requires a much more sophisticated adaptation. Different strategies have evolved to prevent replication-transcription conflicts or to resolve them. One way is to separate replication and transcription in time and space. For example, for the gene encoding cyclin B1, replication has been shown to occur in the early S phase, whereas transcription is restricted to the late S phase (Helmrich et al., 2011). Another way replication and transcription are separated is by natural competition for the DNA template. It is known that active transcription facilitates the accumulation of replication initiation complexes due to the open chromatin structure (Cadoret et al., 2008; Danis et al., 2004). In contrast, various studies have demonstrated that in the case of highly expressed genes, the dense accumulation of transcription factors can avoid the assembly of the replication initiation factors (Letessier et al., 2011; Martin et al., 2011). Vice versa, replication can cause the transcription bubble to be dislodged and re-initiated after replication is complete (Helmrich et al., 2011; Pomerantz and O'Donnell, 2008).

Since replication and transcription occur at relatively the same rate in eukaryotes (17-50 nt/s), it has been long assumed that replication-transcription conflicts are unlikely to occur (Singh and Padgett, 2009). Nevertheless, many studies have now confirmed the occurrence of replication-transcription conflicts and their damaging effects. In this regard, these damaging effects are associated with two processes. First, the torsional stress that builds up during both ongoing replication and transcription. Pol II can wrap around the DNA during transcription and prevent the formation of supercoiled DNA. However, during transcription, the interaction of transcription start and end sites can create a loop of transcribed DNA. Continuous processing of nascent RNA creates a connection to the nuclear pore complex (NPC) that connects the DNA to the nuclear membrane, preventing its rotation (Bermejo et al., 2012). If the replisome encounters a region that cannot rotate, torsional stress increases and, if not removed, can lead to the induction of DNA damage (Bermejo et al., 2011; Prado and Aguilera, 2005). Normally, topoisomerases work hand in hand with replication and transcription to avoid torsional stress. When the function of topoisomerases is impaired, replication-transcription conflicts occur more frequently and lead to an increase in genomic damage (Bermejo et al., 2009; Tuduri et al., 2009). Second, is the formation of non-B structure DNA. If the DNA double helix is not in its conventional conformation, it can form structures that impede replication or transcription. One of these structures is the formation of a DNA:RNA hybrid, a so-called R-loop (Huertas and Aguilera, 2003). DNA:RNA hybrids are natural intermediates of the transcription bubble and support their normal progression. However, the nascent RNA strand can invade the dsDNA outside the transcription bubble and connect to the transcribed strand to form an R-loop (Reaban et al., 1994). Typically, these R-loops are short and do not interfere with the transcription or the replication (Nudler, 2012). In the case of paused or stalled Pol II, R-loops can increase in both number and length and form stable barriers to the replication machinery, resulting in DNA damage (Domínguez-Sánchez et al., 2011; Skourti-Stathaki et al., 2011). Another well studied structure is the G-quadruplex. G-quadruplexes consist of four repeats of at least three guanines that form an interaction. G-quadruplexes occur at the lagging-strand of replication or during transcription in the displaced DNA strand (Audry et al., 2015). These structures can influence ongoing transcription and replication and lead to genomic instability.

The orientation of the replication machinery and transcription process is equally important for the formation of a conflict (**Figure 2.7**). A head-on collision occurs when a gene is transcribed in the lagging strand of replication orientation. In contrast, when a gene is transcribed in the leading strand of replication orientation, it is called co-directional. Previously, the head-on orientation was considered to be more harmful than the co-directional. Head-on collisions are

known to cause fork pausing (Srivatsan et al., 2010). This is thought to be due to the fact that positive supercoiling occurs ahead of both transcription and replication polymerases. The torsional stress subsequently leads to a blocking of both processes. Damage-free resolution of this blockage is usually achieved by displacing Pol II (Pomerantz and O'Donnell, 2008). Co-directional collisions do not affect fork progression unless Pol II is stably stalled (Pol II backtracking) (Nudler, 2012). When Pol II backtracks, it relies on RNA-cleavage stimulatory factors to remove the nascent RNA. As long as Pol II remains stalled, it possesses an increased risk for the occurrence of a replication-transcription conflict. More recent studies have shown that collisions in the co-directional orientation can lead to DNA damage and often include the formation of secondary structures such as G-quadruplexes and R-loops at stalled Pol II (Dutta et al., 2011).

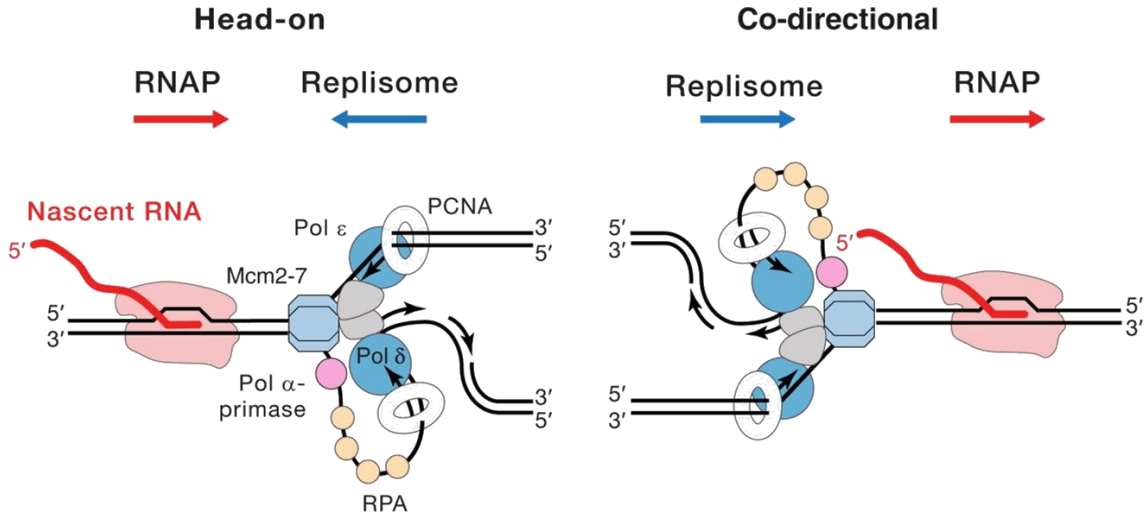

Figure 2.7 Different orientations of replication-transcription conflicts
Two orientations of replication-transcription conflicts can occur. If the transcription takes place in the lagging strand, it leads to the head-on orientation. In this case, transcription and replication run towards each other and have a blocking potential. If transcription occurs in the leading strand, it results in a co-directional orientation. Due to blocked Pol II the replisome encounters with the transcription machinery and interference occurs, leading to the formation of a conflict. RNAP: Pol II. Modified from Hamperl and Cimprich, 2016

Although many studies focus on these proceses, there are still many unresolved questions regarding replication-transcription conflicts. For example, it is not yet clear whether the RNA and DNA polymerases come into direct physical contact or whether changes in chromatin and DNA structure occur before the two polymerases meet. Furthermore, new insights into how replication-transcription conflicts can be prevented are emerging. The RecQ-like

ATP-dependent DNA helicase Q5 (RECQL5) has been shown to interact directly with Pol II in human cells, leading to a reduced elongation rate. Cells lacking RECQL5 show an increased occurrence of transcriptional pauses, arrest, and backtracking (Saponaro et al., 2014). In this context, RECQL5 is assumed to play a role in the transcription process by preventing uncontrolled elongation progression. Moreover, endogenous DSBs have been shown to occur in RECQL5-depleted cells in the context of replication and transcription (Hu et al., 2007). As mentioned previously, overexpression of oncogenes, such as the gene encoding cyclin E, can increase replication initiation rates. The resulting replication stress is mainly associated with conflicts between replication and transcription (Jones et al., 2013). In addition, replication fork progression is frequently disrupted at common fragile sites. Results suggest that replication-transcription conflicts are also the cause of damage induction in this case (Helmrich et al., 2011).

2.7 Aim

The occurrence of oxidative stress is associated with the development of various diseases. The thereby generated ROS are a constant threat to the genomic integrity and are an important indicator of health, as well as the aging process. ROS possess a damaging effect that is reflected, for example, in the generation of DNA lesions. From the lesions generated, oxidative base modifications are one of the most common, especially the oxidation of guanine to 8-oxoG. The impact that a single base modification can have on the genomic integrity has already been demonstrated in a previous study by this research group (Ensminger et al., 2014). Here, the potential for methylated base modifications to form DSBs was investigated. Crucial for the formation of a DSB is the repair of the modified base via BER and concurrent replication during S phase. Thus, it was shown that removal of the modified base by the specific glycosylase and the resulting SSB is essential for DSB formation. If a replication fork encounters exactly this BER intermediate of a SSB, the replication process cannot continue due to the existing gap. The result is the formation of an S-phase specific one-ended DSB.

For this reason, studies on the risks arising from oxidative base modifications are of particular importance. The aim of the present work was to determine the impact of oxidative base modifications, more specifically 8-oxoG, on the formation of replication-associated DSBs. Moreover, the involvement of BER in this process should be investigated. New findings such as the occurrence of replication-transcription conflicts were taken into account and should allow a more sophisticated understanding of the process involved in break induction. Due to the natural occurrence of ROS as a by-product of metabolism, untreated cells are also exposed to the reactivity of ROS. For this reason, the effect of ROS on the induction of endogenous DSBs should additionally be examined. This should provide a more accurate assessment of the involvement of oxidative stress in the formation of DSBs and the associated development of various diseases.

3 Materials and Methods

3.1 Materials

3.1.1 Laboratory consumables

Consumable	*Vendor*
Cell culture dishes	VWR
Cell culture flasks	TPP
Centrifuge tubes	Greiner
Cover slips	Roth
Dynabeads Protein G	Invitrogen
FastStart Universal SYBR Green Master (Rox)	Sigma-Aldrich
Immersion oil	Zeiss
Kim wipes	NeoLab
Micro tubes	Roth
Microscope slides superfrost	Roth
Parafilm	Bemis
Pasteur pipettes, glass	Roth
Pasteur pipettes, plastic	Roth
Pipette tips	Sarstedt
Pipette tips, filtered	Roth
Plastic pipettes	Sarstedt
qPCR 96-well plates	Applied Biosystems

3.1.2 Instruments and Devices

Instrument/Device	*Model*	*Vendor*
Agarose gel electrophoresis set	Horizon 58/Horizon 11-14	Life Technologies
Cell counting chamber	Neubauer	Marienfeld Superior
Centrifuge	5415 R/5804 R	Eppendorf
Centrifuge	Biofuge pico	Heraeus
Chemiluminescence detection	Fusion FX	VilberLourmat
Fluorometer	Qubit 4	Invitrogen
Microscope (cell culture)	Eclipse TS 100	Nikon
Microscope (fluorescence)	Imager.Z2/Imager.M2	Zeiss
Nanophotometer	P-Class	Implen
pH meter	pMX2000	WTW
Real Time PCR system	StepOnePlus	Applied Biosystems
Scale	ADB 200-4/PCB 1000-2	Kern
Sonicator	Sonopuls BM70	Bandelin
Thermoblock	mb-102	Bioer
Thermoblock	Thermomixer comfort	Eppendorf
Vortex	Vortex genie2	Scientific Industries
Water bath	1083	GFL

3.1.3 Software

Software	*Vendor*
FusionCaptAdvance FX7	VilberLourmat
ImageJ	Open source
Metafer4	MetaSystems
MS Office	Microsoft
Prism	GraphPad
StepOne and StepOnePlus Software v2.3	Applied Biosystems

3.1.4 Software Bioinformatics

Software	*Version*	*Reference*
Bowtie2	2.3.4.3	http://bowtie-bio.sourceforge.net/bowtie2/index.shtml
deepTools	3.1.0	https://deeptools.readthedocs.io/en/develop/
FastQC	0.11.8	https://www.bioinformatics.babraham.ac.uk/projects/fastqc/
FastQScreen	0.13	https://www.bioinformatics.babraham.ac.uk/projects/fastq_screen/
Galaxy	21.05	https://usegalaxy.org/
IGV Browser	2.9.0	https://software.broadinstitute.org/software/igv/home
MultiQC	1.9	https://multiqc.info/
Picard	2.20.3	https://broadinstitute.github.io/picard/
Samtools	1.10	http://www.htslib.org/
STAR	2.7.3a	https://github.com/alexdobin/STAR
Subread	1.6.5	http://subread.sourceforge.net/

R Package	*Version*	*Reference*
BSgenome.Hsapiens.UCSC.hg38	1.50.0	https://bioconductor.org/packages/release/data/annotation/html/BSgenome.Hsapiens.UCSC.hg38.html
DESeq2	1.22.2	https://bioconductor.org/packages/release/bioc/html/DESeq2.html
GenomicAlignments	1.18.1	https://bioconductor.org/packages/release/bioc/html/GenomicAlignments.html
GenomicRanges	1.34.0	https://bioconductor.org/packages/release/bioc/html/GenomicRanges.html
GenomicTools	0.2.8	https://cran.r-project.org/web/packages/GenomicTools/index.html
R	3.5	https://cran.r-project.org/
rtracklayer	1.42.2	https://bioconductor.org/packages/release/bioc/html/rtracklayer.html

3.1.5 Chemicals and Reagents

Chemical	*Vendor*
10 % FA (formaldehyde)	Roth
4-OHT (hydroxytamoxifen)	Sigma-Aldrich
Agarose	Roth
BrdU (1 mM)	BD Bioscience
BSA	AppliChem
$CaCl_2$	Roth
DAPI	Sigma-Aldrich
DMSO	Sigma-Aldrich
EDTA	Roth
EdU (10 mM)	Invitrogen
EGTA	Roth
Ethanol	Roth
FCS	Biochrom
Glycerol	Roth
Glycine	Roth
H_2O_2	Roth
HCl	Roth
Isopropanol	Roth
KCl	Roth
KH_2PO_4	Roth
LiCl	Roth
MEM	Sigma-Aldrich
Methanol	Roth
$MgCl_2$	Roth
Mounting medium Vectashield	Axxora Alexis
N-acetylcysteine (NAC)	Sigma-Aldrich
NaCl	Roth
$NaHCO_3$	Roth
Na_2HPO_4	Roth
NaOH	Roth
NEAA (non-essential amino acids)	Biochrom
NP-40 (alternative)	Merck
Paraformaldehyde	Roth
PhosStop 10x	Roche
PMSF	Roth
Protease inhibitor 25x Complete	Roche
Proteinase K	Lucigen
SDS	Roth
Sodiumdeoxycholate	Sigma-Aldrich
Tris	Roth
Triton X-100	Roth
Trypsin	Roth
Tween 20	Roth

3.1.6 Kits

Kit	*Vendor*
Duolink In Situ PLA Kit	Sigma-Aldrich
EdU Click-IT Kit	Baseclick
QIAquick PCR Purification Kit	Qiagen
Qubit 1X dsDNA HS Assay Kit	Invitrogen

3.1.7 Inhibitors

Inhibitor	*ID*	*Vendor*	*Concentration*
Aphidicolin	178273	Merck	1 μM
CPT	C9911	Sigma-Aldrich	20 nM
DNA-PK (NU7441)	S2638	Selleckchem	50 μM
DRB	D1916	Sigma-Aldrich	100 μM
O8	SML1697	Sigma-Aldrich	50 μM
Olaparib (AZD2281)	S1060	Selleckchem	1 μM
RAD51 (B02)	553525	Merck	60 μM
Triptolide (PG490)	S3604	Selleckchem	1 μM

3.1.8 Solutions, buffers and media

Cell culture	*Vendor/Composition*	
Dulbecco's Modified Eagle's Medium (DMEM)	Sigma-Aldrich	
Fetal calf serum (FCS)	Biochrom	
Minimum Essential Medium Eagle (MEM)	Sigma-Aldrich	
Non-essential amino acids (NEAA)	Sigma-Aldrich	
Penicilin/Streptomycin	Sigma-Aldrich	
Trypsin/EDTA	2.5 % (v/v) Trypsin	
	0.5 M EDTA	pH 8 in PBS

Buffer	*Composition*	
PBS	137 mM NaCl	
	2.7 mM KCl	
	8 mM Na_2HPO_4	
	1.5 mM KH_2PO_4	pH 7.4

Chromatin Immunoprecipitation	*Composition*	
Lysis Buffer 1	50 mM HEPES	
	140 mM NaCl	
	1 mM EDTA	
	10 % Glycerol	
	0.5 % NP-40	
	0.25 % Triton X-100	pH 8

Lysis Buffer 2	10 mM Tris-HCl	pH 8
	200 mM NaCl	
	1 mM EDTA	
Shearing Buffer	50 mM Tris-HCl	
	5 mM EDTA	
	0.2 % SDS	pH 8
Dilution Buffer	20 mM Tris-HCl	
	100 mM NaCl	
	2 mM EDTA	
	0.5 % Triton X-100	pH 8
Wash Buffer 1	20 mM Tris-HCl	
	150 mM NaCl	
	2 mM EDTA	
	0.1 % SDS	
	1 % Triton X-100	pH 8
Wash Buffer 2	20 mM Tris-HCl	
	500 mM NaCl	
	2 mM EDTA	pH 8
	1 % Triton X-100	
Wash Buffer 3	10 mM TrisHCl	
	250 mM LiCl	
	1 mM EDTA	
	1 % NP-40	
	1 % Sodiumdeoxcholate	pH 8
TE Buffer	10 mM Tris-HCl	
	1 mM EDTA	pH 8
Elution Buffer	100 mM $NaHCO_3$	
	1 % SDS	
	Proteinase K	

Immunofluorescence	*Composition*	
Wash 1	0.1 % Tween	in PBS
Fixation	2 % FA	in PBS
Permeabilization	0.2 % Triton X-100	in PBS/1% FCS
Wash 2	1 % FCS	in PBS
Blocking	5 % BSA	in PBS/1% FCS
Wash 3	3 % BSA	in PBS/1% FCS
DAPI	0.4 μg/ml	in PBS

EdU/BrdU double labeling	*Composition*	
Crosslink	2.5 % FA	in PBS
Denaturation	2.5 M HCl	in ddH_2O

Proximity Ligation Assay	*Composition*	
Pre-extraction	10 mM Tris	
	2.5 mM $MgCl_2$	
	0.5 % NP-40	
	1 mM PMSF	pH 7.5
Fixation	4 % FA	in PBS
Blocking	2 % BSA	in PBS
Wash Buffer A	10 mM Tris	
	150 mM NaCl	
	0.05 % Tween	pH 7.4
Wash Buffer B	200 mM Tris	
	100 mM NaCl	pH 7.5

3.1.9 Antibodies

Primary antibodies	*ID*	*Vendor*	*Application*	*Dilution*
Rabbit-anti-γH2AX	ab2893	Abcam	ChIP	1 μg
Rabbit-anti-IgG	sc-2027	Santa Cruz	ChIP	1 μg
Mouse-anti-γH2AX	05-636	Merck	IF	1:2000
Rabbit-anti-γH2AX	ab81299	Abcam	IF	1:2000
Mouse-anti-BrdU	555627	BD Biosciences	IF	1:500
Rabbit-anti-PCNA	sc-7907	Santa Cruz	IF/PLA	1:1000
Mouse-anti-Pol II	sc-56767	Santa Cruz	PLA	1:1000

Secondary antibodies	*ID*	*Vendor*	*Application*	*Dilution*
Goat-anti-mouse AlexaFluor 488	A11001	Molecular Probes	IF	1:1000/ 1:500
Goat-anti-mouse AlexaFluor 594	A11005	Molecular Probes	IF	1:1000
Goat-anti-rabbit AlexaFluor 594	A11012	Molecular Probes	IF	1:1000

3.1.10 Primers

Target	*Primer fwd 5'->3'*	*Primer rev 5'->3'*	*Vendor*
DSB 12	CGAGAGGCCACCAGACTAAA	TTCACGAAGCGATGTGTAGG	Eurofins
DSB II	CCCTGGTGAGGGGAGAATC	GCTGTCCGGGCTGTATTCTA	Eurofins
NC A	AGTTGGAAAGTGGCAGTCGT	GCTTGTCTGGATTCCCGAGT	Eurofins
NC B	GTGACACAGCATCACTAAGG	ACAGCACCGTGTTGGCGT	Eurofins
HT 1	GTCTCTGCCCACACCTCACAC	ACGTCCCCCATCCTCTCTGAA	Eurofins
HT 2	GGCAAGACTCTGGCACCTTT	CCACTCTCCCACTGAGGATG	Eurofins
HT 3	GAGGACACAGACTAGCAGGAAG	TTACCCCACATCCCTCCTCAG	Eurofins
LT 1	GCTTTCACTCCGGATTTCGC	CCCTTGCTGCATTTCGCATT	Eurofins
LT 2	CCTTTATGCCAGGAGTAGTGC	AAGCCCCTGCTGTCATTAGC	Eurofins
LT 3	CAAACAGGGGCCATTCACAAG	CTGGGCTTTCTCCCTCCTATC	Eurofins

3.1.11 Cell lines

82-6 hTert — Human skin fibroblast cell line. Immortalized by expression of the human telomerase. Cells were cultivated in MEM supplemented with 20 % FCS, 1 % NEAA and 1 % Penicillin/Streptomycin. Kind gift from Penny Jeggo.

HeLa-S3 — Human epithelial cancer cell line. Derived from adenocarcinoma of the cervix isolated from Henrietta Lacks. Cells were cultivated in DMEM supplemented with 10 % FCS, 1 % NEAA and 1 % Penicillin/Streptomycin. Source: ATCC.

DIvA — A*si*SI–ER-U2OS cells. Human epithelial cancer cell line. Derived from osteosarcoma and stably expressing the A*si*SI ER fusion protein. Cells were cultivated in DMEM supplemented with 10 % FCS and 1 % NEAA. Kind gift from Gaelle Legube.

MEF — Mouse embryonic fibroblast cell line. MEF OGG1$^{-/-}$ derived from knock-out mice. Cells were cultivated in DMEM supplemented with 10 % FCS and 1 % Penicillin/Streptomycin. Kind gift of Bernd Kaina.

3.2 Methods

3.2.1 Cell culture

Only sterile media, buffers, reagents, and consumables were used for cell culturing. Cells were cultivated at 37 °C with 5 % atmospheric CO_2 in an incubator and routinely tested for mycoplasma by PCR to check for contamination.

Thawing of cells

To obtain fresh cells, the respective cryotube was removed from the liquid nitrogen tank and defrosted in a 37 °C water bath for approximately 2 min. The cell suspension was mixed with 6 ml of prewarmed medium and centrifuged at 300 x g for 8 min. The supernatant was discarded and the pelleted cells were resuspended in 6 ml of medium and seeded in a 25 cm^2 cell culture flask. The next day, the medium was changed or the cells were passaged into a 75 cm^2 cell culture flask, depending on the confluence of the cells.

Cell passaging

Cells were passaged once a confluency of 80-90 % was achieved. For this purpose, the medium was aspirated, and the cells were washed once with 5 ml of PBS. To detach the adherent cells from the flasks, the PBS was removed, and 1 ml of a Trypsin/EDTA solution was added, followed by incubation at 37 °C until the cells began to detach. To quench the reaction, cells were resuspended in medium and added to a new 75 cm^2 cell culture flask at a ratio of 1:5 to 1:10.

Seeding of cells

Depending on the requirements of the experiment, cells were seeded on sterile glass coverslips in 60x20 mm dishes or directly in 150x20 mm dishes. The cell number was determined using a Neubauer counting chamber and an adequate number of cells were seeded according to the culture vessel and the cell type.

3.2.2 Cell cycle-specific analysis and inhibitor treatment

Treatment with thymidine analog

For cell cycle-specific analysis, cells were treated with the thymidine analog 5-ethynyl-2'-deoxyuridine (EdU). EdU is incorporated into DNA by replicating cells during

S phase and can be specifically stained with a Click-IT reaction. An additional non-specific staining of the DNA by 4',6-diamidino-2-phenylindole (DAPI) allows for the detection of G1 and G2 phase cells. Accordingly, EdU-positive cells are identified as S phase, while EdU-negative cells can be determined as G1 or G2 phase, based on their DNA content. Generally, EdU treatment was performed for 30 min before damage induction with a final concentration of 10 μM unless stated otherwise. This allowed for the identification of S-phase cells during damage induction.

Inhibitor treatments

Inhibitor treatment was always carried out in medium, with incubation periods at 37 °C in the incubator. In case of repair times after damage induction, cells were incubated in medium with the appropriate concentration of inhibitors until fixation. Dimethyl sulfoxide (DMSO) was used as a control treatment.

For treatment with aphidicolin, cells were first treated with EdU for 30 min to allow for incorporation into DNA. Subsequently, aphidicolin was added at a final concentration of 1 μM. The incubation period was 30 min before further treatments followed.

5,6-dichlorobenzimidazole 1-β-D-ribofuranoside (DRB) treatment was performed for a total time of 3 h before damage induction. EdU was added in the last 30 min of the incubation period to allow for cell cycle-specific analysis. The applied concentration of DRB was 100 μM.

The treatment with the inhibitors of DNA-PKi (50 μM), RAD51i (60 μM), O8 (50 μM), olaparib (1 μM), triptolide (1 μM), and N-acetylcysteine (NAC) (10 mM) was carried out for 1 h. If indicated, EdU was added for the final 30 min of the incubation period to allow for cell cycle-specific analysis.

3.2.3 DNA damage induction

H_2O_2 treatment was performed immediately after EdU and/or inhibitor treatment. For this purpose, the medium was removed and a 4 °C H_2O_2 solution in PBS was added to the cells. Cold PBS alone was used as a control. After incubation at 4 °C for 30 min, the H_2O_2 was aspirated and the cells were washed twice with PBS to remove residual H_2O_2. After the last washing step, the medium was added back. If inhibitors were used previously, medium plus the corresponding inhibitors were added to the cells until fixation.

Camptothecin (CPT) treatment was performed different to H_2O_2 treatment. Briefly, CPT was added with warm medium instead of cold PBS and cells were incubated at 37 °C for 1 h. After

the incubation time, the media was removed, and the cells were washed twice with PBS before adding medium with or without inhibitors.
Specific damage induction of DIvA cells was performed using hydroxytamoxifen (4-OHT) treatment. For this purpose, cells were treated with 300 nM 4-OHT for 2 h in medium.

3.2.4 Immunofluorescence

For immunofluorescence (IF) experiments, cells were seeded in a 60x20 mm dish with sterile glass coverslips. After 2 days, when approx. 60-70 % confluency was reached, cells were treated with the corresponding inhibitors and/or treated with EdU and H_2O_2/CPT as indicated in section 3.2.2 and 3.2.3.
After the incubation time, the medium was removed and the cells were washed once with PBS/0.1 % Tween, followed by fixation with 2 % FA for 15 min at room temperature. After fixation, cells were washed 3 x with PBS/0.1 % Tween and permeabilized with 0.2 % TritonX-100/PBS/1 % FCS for 5 min at 4 °C. After washing three times with PBS/1 % FCS, cells were blocked with a 5 % BSA/PBS/1 % FCS solution for 30 min at room temperature.
Primary antibodies were added at the dilution indicated in section 3.1.9 in blocking buffer overnight at 4 °C in a humidity chamber. After washing with PBS/1 % FCS, EdU was labeled with the EdU Click-IT kit according to the manufactures instructions and then washed three times with 3 % BSA/PBS. Secondary antibodies were added in blocking solution for 1 h at room temperature with the indicated concentrations from section 3.1.9. After washing once with 3 % BSA/PBS, DNA was stained with 0.4 μg/ml DAPI for 5 min. The coverslips were embedded on microscope slides with 2 μl of mounting medium and sealed with nail polish.
A semi-automated approach was used to analyze the IF experiments. Using a Zeiss microscope and Metafer software, cells were analyzed for their DAPI and EdU intensity for cell cycle-specific evaluation. Accordingly, cell cycle phases were determined, and for each experiment, at least 40 cells were analyzed and foci were counted manually.

3.2.5 EdU/BrdU double labeling

The EdU/BrdU double labeling was established in the group of Prof. Löbrich and described recently (Llorens-Agost et al., 2021). The aim of this staining method is to allow for a more precise differentiation of S-phase cells. For this purpose, cells were seeded as described in section 3.2.4.

On the day of the experiment, S-phase cells were pulse-labeled with 10 μM EdU for 1 h before the medium containing EdU was removed and washed with PBS twice. This was followed by a 2 h treatment with 10 mM 5-bromo-2'-deoxyuridine (BrdU). BrdU, like EdU, is a thymidine analog and is incorporated into the DNA of replicating cells. After washing off the BrdU-medium solution, cells were treated with H_2O_2 for 30 min for damage induction or with cold PBS for control. For the combination of the EdU/BrdU double labeling together with inhibitor treatments the corresponding inhibitors were added directly into the EdU and/or BrdU-medium solutions. For DRB the treatment was performed during the whole EdU and BrdU treatment, respectively. O8, olaparib, and NAC were added in the last 1 h of the incubation time with BrdU. Following the H_2O_2 treatment, cells were kept under inhibitor treatment until cells' harvest. Fixation, permeabilization, and primary antibody treatment were performed as described in section 3.2.4.

After antibody treatment, cells were washed twice with PBS/1 % FCS before primary antibodies were cross-linked with 2.5 % FA for 20 minutes at room temperature. Following 3 x washing with PBS/0.1 % Tween, DNA was denatured by treatment with 2.5 M HCl for 20 min at room temperature. To wash out the excess HCl, washing with PBS was performed for at least 4 h before adding the primary antibody against BrdU in blocking buffer over night at room temperature (concentration see 3.1.9). After BrdU antibody treatment, cells were washed 3 x with PBS/1 % FCS and the EdU Click-IT staining was performed according to the manufactures instructions. Followed by a washing step with 3 % BSA/PBS for 3 times, cells were treated with secondary antibodies for 1 h at room temperature (concentrations see 3.1.9). DAPI staining and mounting of the cells was carried out as described before in section 3.2.4.

Analysis of the experiment was carried out with the same approach as described under section 3.2.4. However, in addition to DAPI and EdU intensity, BrdU intensity was measured as well. This resulted in three distinctive S-phase populations: cells positive for BrdU but not EdU, cells positive for BrdU and EdU, and cells only positive for EdU. Differentiation of G1 and G2 phase could be determined based on DAPI intensity. Cells positive for BrdU but not EdU were selected and analyzed. A minimum of 40 cells was evaluated.

3.2.6 Proximity ligation assay

For the PLA, cells were seeded and treated as described previously in section 3.2.4. Cells were washed once with PBS before pre-extraction with 0.5 % NP-40 for 4 min at 4 °C. After pre-extraction, cells were washed once briefly with PBS and then immediately fixed with 4 %

FA for 10 minutes. Following a 3 x washing step with PBS, the cells were blocked with 2 % BSA/PBS for 1 h at room temperature. Next, the cells were incubated with primary antibodies in blocking solution overnight at 4 °C (concentrations see 3.1.9). After treatment with the primary antibodies, the Duolink In Situ PLA kit was used according to the manufactures instructions, except for the PLUS and MINUS PLA probes, which were used at a 1:10 dilution instead. In addition, before the final wash step, EdU Click-IT staining was performed as previously described (3.2.4). Coverslips were mounted with Duolink In Situ mounting medium containing DAPI on microscope slides and sealed with nail polish. Analysis was performed in a semi-automated approach as described before (3.2.4).

3.2.7 RNA-Sequencing

Exponentialy growing cells were harvested and snap frozen in liquid nitrogen. Total RNA isolation and RNA-Sequencing (RNA-Seq) were performed at BGI Genomics. DNBSeq technology was used with paired-end sequencing and 100 bp read length, resulting in 30 million reads per sample. FastQC and MultiQC were used for quality control of sequenced reads. The presence of contaminated RNAs was verified using FastQ Screen. Alignment with the human reference genome hg38 (GENCODE Release 37 canonical gene annotation) was performed using STAR. For visualization of RNA-seq tracks, normalized coverage tracks were generated using the bamCoverage function of deepTools and normalized using the counts per million mapped reads method. The mapped reads were assigned to annotated features such as genes, exons, and promoters using the Subread tool featureCounts. Normalization and differential expression analysis between the replicates were performed using the R/Bioconductor package DESeq2.

3.2.8 Chromatin immunoprecipitation and quantitative polymerase chain reaction

For chromatin immunoprecipitation (ChIP), two days before the experiment, cells were seated in a 150x20 mm dish to reach 70-80 % confluence on the day of the experiment. Cells were treated with H_2O_2 or 4-OHT (see 3.2.3) to induce DSBs. Treatment with inhibitors was performed as described before without EdU (3.2.2).

First, the cells were washed 2 x with PBS and then fixed with 1 % FA at room temperature for 10 min. To quench the reaction, 0.5 ml of 2.5 M glycine was added for 5 min. After removal of the fixative, the cells were washed 2 x with 4 °C cold PBS, scraped off, and collected in a 15 ml centrifuge tube. Cells were pelleted at 400 x g at 4 °C for 5 min and resuspended in

5 ml of cell lysis buffer 1. After incubation at 4 °C for 15 min, the cells were pelleted at 1,500 x g at 4 °C for 10 min and resuspended in 5 ml of nuclear lysis buffer 2. Followed by another centrifugation at 1,500 x g at 4 °C for 10 min, the pelleted cells were resuspended in 100 μl shearing buffer per 1 million cells.

Next, chromatin sonication was performed using the Sonopuls BM70 sonicator. The sonication was carried out at a setting of 40 % power and 0.5 cycle for 20-30 min with 30 s on/off to achieve optimal sonication of the chromatin at 200 to 500 bps. The lysate was centrifuged at 13,000 x g at 4 °C for 10 min to remove cell debris. Approximately 2 million cells were used to perform one IP reaction. The lysate was replenished with three times the amount of dilution buffer and pre-clearing with 30 μl Dynabeads Protein G for 40 min at 4 °C under rotation was performed. After removal of the beads, 5 % of the supernatant was used as an input sample. 1 μg of γH2AX or IgG antibody was added per reaction and incubated overnight at 4 °C under rotation.

The next day, 30 μl of Dynabeads Protein G were added per reaction and incubated for 3 h at 4 °C under rotation. Subsequently, the samples were washed 2 x with each of the three wash buffers and TE buffer (see 3.1.8) and incubated for 10 min at 4 °C under rotation. Elution was performed by adding 100 μl of elution buffer to the beads and incubating for 1 h at 55 °C followed by overnight incubation at 65 °C in a thermoblock with gentle mixing to avoid settling of the beads. The next day, DNA was purified using the Qiagen QIAquick PCR Purification Kit according to the manufactures instructions. The purified DNA was stored at 4 °C for short-term or at -20 °C for long-term storage.

DNA concentration was measured using a Qubit Fluorometer and the 1x dsDNA high sensitivity kit according to the manufactures instructions. For quantitative polymerase chain reaction (qPCR), the purified DNA was used in combination with the FastStart Universal SYBR Green Master Mix according to the manufactures instructions. The primers used for qPCR are listed in section 3.1.10. qPCR was run with an initial 95 °C step for 10 minutes followed by 40 cycles with 60 °C for 1 min and 95 °C for 15 sec. Additionally, a melt curve was performed to allow for primer specificity check-up. Samples were run at least in duplicate (technical replicates) for each reaction. The percent input method was used for evaluation. Depending on the experimental outcome a minimum of 10 ng of purified DNA was sent to the IMB core Facility in Mainz after quality control. Bioanalyzer analysis and sequencing were performed at the IMB.

3.2.9 ChIP-Sequencing and downstream analysis

The Illumina NextSeq 500 platform was used for ChIP-Sequencing (ChIP-Seq) to obtain paired-end sequences of 40 bp length. An average of 27 million reads was obtained, and quality control was performed using FastQC and MultiQC. Reads were aligned to the human hg38 reference genome (GENCODE Release 37 canonical gene annotation) using Bowtie2, sorted using SAMtools, and converted directly into binary files. PCR-duplicated reads were marked and removed with Picard.

Downstream analysis was performed using R version 3.5 and the packages listed in section 3.1.4. The reference genome was divided into 0.5 Mbp windows. The number of reads for each window was then annotated. The number of reads was normalized to the library size (total number of reads in sample) using the reads per kilobase per million mapped reads method. The normalized number of reads in the input sample was subtracted and then log-transformed. Each window was sorted according to the expression determined from RNA-Seq results. The correlation of the RNA-Seq and ChIP-Seq reads was plotted, and windows were grouped by the number of RNA reads for better visualization.

Information on GC content and gene density was obtained from the UCSC Genomics Institute public databases.

3.2.10 Statistical analysis

For the statistical analysis of the independent biological replicates, the standard error of the mean (SEM) between the means of the independent experiments was calculated. For each experiment, at least 40 cells were evaluated for this purpose. A Student's t-test was used to calculate P values (* = $P<0.05$, ** = $P<0.01$, *** = $P<0.001$, ns = not significant).

4 Results

A previous study in the group of Prof. Löbrich showed that the repair of methylated bases by BER is involved in the formation of S-phase specific DSBs (Ensminger et al., 2014). Treatment of cells with the alkylating agent methyl methanesulfonate (MMS) leads to the induction of base modifications but no direct DSBs. However, treatment during S phase resulted in a specific increase in DSB formation in this cell cycle phase. Further investigations revealed that SSBs generated by BER are substantial for the induction of these DSBs, since they are converted into one-ended DSBs during S phase by the replication process. This study shows the danger that even a simple base modification can have for the genomic integrity. Since base modifications are one of the most common DNA lesions, it is of great importance to gain further insight into the potential risk of this process.

4.1 Formation of DSBs by H_2O_2 treatment

The damaging effect of methylated base modifications is used, for example, in cancer therapy. There, alkylating agents were the first anti-cancer drugs applied and are still the most commonly used agents in chemotherapy (Lehmann and Wennerberg, 2021). Naturally, however, oxidative base modifications induced by ROS occur more frequently (Lindahl, 1993; Marnett, 2000). ROS can be produced endogenously by the cellular metabolism and thus pose a constant threat to induce DNA damage. For this reason, investigations using oxidative base modifications represent a physiologically more relevant condition. Therefore, the potential DSB-inducing effect of oxidative base modifications should be investigated.

Highly reactive O_2 derivatives, such as peroxides or hydroxyl radicals, however, can react with a variety of cellular compartments and cause damage to the DNA, cell membrane, or proteins. DNA damage, in turn, is not limited to oxidative base modifications either. At higher concentrations, ROS can lead to the direct formation of DSBs (Hegde et al., 2008). Since the contribution of oxidative base modifications to the formation of DSBs was to be studied for this work, it was crucial to keep the induction of these direct DSBs as low as possible. For the induction of oxidative base modifications, the well-studied H_2O_2 was chosen. It is the simplest peroxide and consists of an oxygen single bond with high reactivity. Many studies regarding oxidative stress have been performed using H_2O_2, and therefore good knowledge about the effects of H_2O_2 already exists.

4.1.1 Cell-cycle specific analysis of γH2AX foci formation after H_2O_2 treatment

The DSB-inducing effect of H_2O_2 has already been demonstrated in several studies, but without considering the cell cycle phases (Li et al., 2006; Ye et al., 2016). Yet, it was the cell cycle phase status of a cell that was critical for the occurrence of MMS-induced DSBs according to *Ensminger et al. 2014*. To investigate DSB induction by H_2O_2, the γH2AX foci assay was performed. This sensitive method allows a cell-cycle specific analysis of the formation and repair of DSBs (Löbrich et al., 2010). To this aim, fluorescent labeling of a DSB damage marker (γH2AX) is combined with a labeling of S-phase cells with EdU and unspecific staining for DNA. A microscopic scanning approach subsequently allows for the specific differentiation of cells into the cell cycle phases G1, S, and G2 and is represented by a typical horseshoe pattern (**Figure 4.1 A** and **B**). For the experiment, exponentially growing cells were treated with different concentrations of H_2O_2. To avoid degradation of H_2O_2 by SOD, cells were treated with H_2O_2 at 4 °C for 30 min. Prior pulse treatment with EdU for 30 min allowed for the identification of S-phase cells during H_2O_2 treatment. After removal of H_2O_2, medium was added, and cells were fixed after 15 min or 4 h. Additional staining with DAPI allowed for the identification of all cell cycle phases using Metafer software.

Treatment with H_2O_2 induced γH2AX foci mainly in the S phase of the cell cycle (**Figure 4.1 C** to **F**). This observation was made in three different cell lines. For the cancer cell lines used, HeLa and DIvA, a higher number of γH2AX foci were detected in the S phase compared to 82-6 hTert fibroblast cells. The γH2AX foci induction generally occurred in a dose-dependent manner, resulting in increasing foci numbers with elevated H_2O_2 concentrations. In both G1 and G2 phases, an increase in the formation of γH2AX foci is observed only after higher H_2O_2 concentrations, reflecting the increasing induction of direct DSBs. However, the γH2AX foci induced in S phase are several times higher than in G1 or G2. This suggests that additional DSBs are generated in S phase that do not result from direct induction. Interestingly, comparing the detected foci numbers 15 min and 4 h after H_2O_2 treatment, a strong decrease was observed in G1 and G2 phases whereas foci numbers increased in S phase (**Figure 4.1 C** and **D**). This indicates that additional breaks are formed in S phase after H_2O_2 was removed. The reduced foci numbers in G1 and G2, in contrast, are indicative of a fast repair of the induced DSBs.

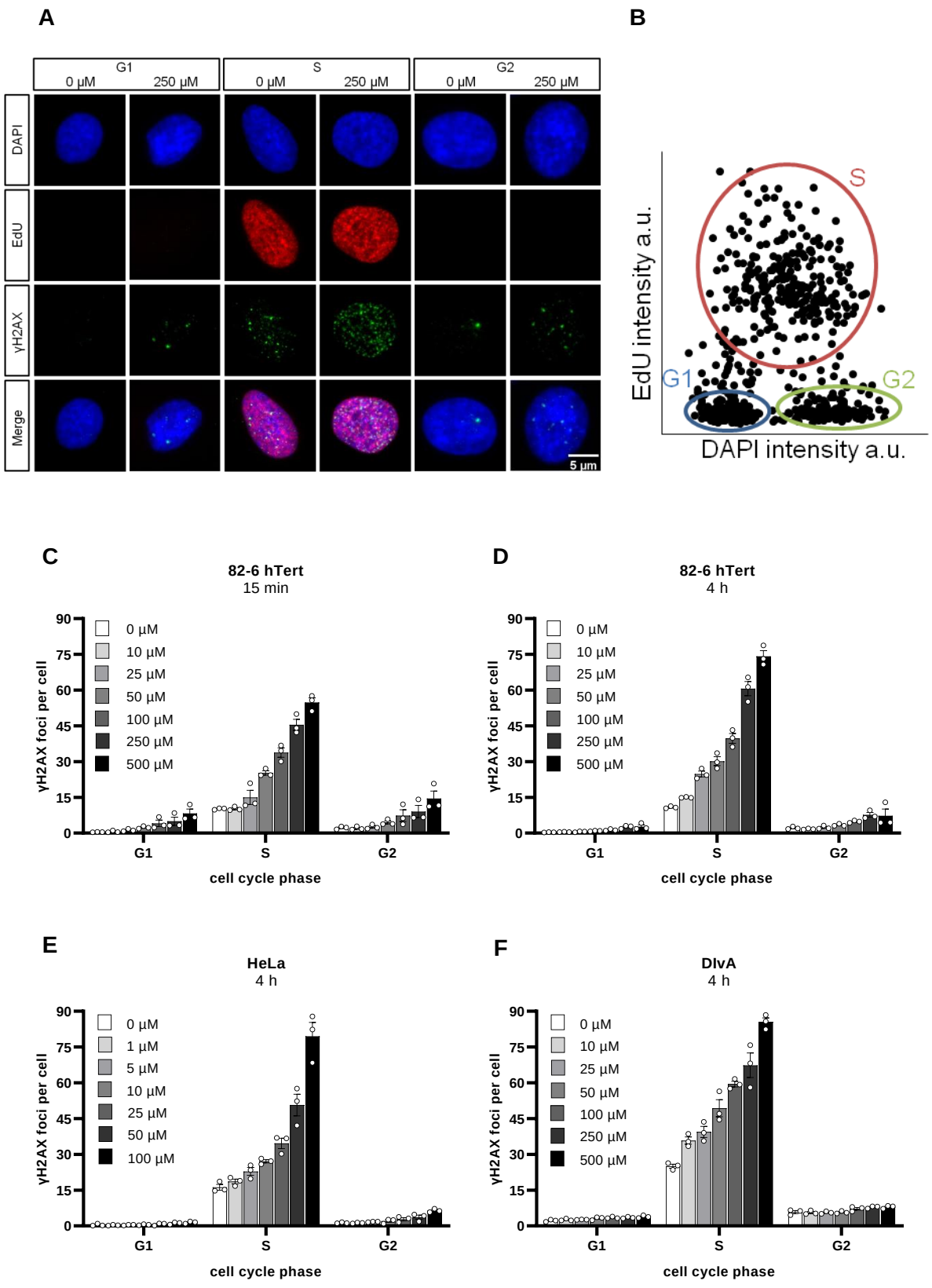
A
G1
S
G2
0 µM
250 µM
DAPI
EdU
γH2AX
Merge
5 µm
B
EdU intensity a.u.
DAPI intensity a.u.
S
G1
G2
C
82-6 hTert
15 min
γH2AX foci per cell
0 µM
10 µM
25 µM
50 µM
100 µM
250 µM
500 µM
G1
S
G2
cell cycle phase
D
82-6 hTert
4 h
E
HeLa
4 h
1 µM
5 µM
F
DlvA
4 h

Figure 4.1 Cell cycle-specific γH2AX foci formation after H_2O_2 treatment
82-6 hTert, HeLa, and DIvA cells were treated with EdU for 30 min to identify S-phase cells. Afterwards, damage induction was performed using H_2O_2 for 30 min. After washing out H_2O_2 and adding fresh medium, cells were fixed after 15 min or 4 h. Staining with anti-γH2AX antibodies, DAPI, and EdU followed. The samples were subsequently scanned using Metafer software. (**A**) Representative images of 82-6 hTert cells 4 h after treatment with 0 μM or 250 μM H_2O_2 in the different cell cycle phases. (**B**) Representative scan-plot of the EdU and DAPI intensity of the analyzed cells. Intensities were plotted in a graph, showing a horseshoe pattern, and labeling of G1 (blue), S (red), and G2 (green) phases. (**C**) Obtained γH2AX values after evaluation of all cell cycle phases 15 min after H_2O_2 treatment in 82-6 hTert cells. (**D**) As in (**C**), only 4 h after H_2O_2 treatment. (**E-F**) As in (**D**), only HeLa or DIvA cells were used. For each individual experiment, 40 cells per cell cycle phase were evaluated. Data points show individual experiments. Mean ± SEM (n=3).

4.1.2 Repair kinetics and contribution of the different repair mechanisms after H_2O_2 treatment

The observations obtained above indicate that DSBs are formed in S phase even hours after H_2O_2 was removed. This suggests that these DSBs are not directly generated by H_2O_2. Here, so-called secondary DSBs could arise when replication forks interfere with SSBs formed either directly by H_2O_2 or during BER-mediated repair of H_2O_2-induced oxidized bases. Studies demonstrated that these secondary DSBs are one-ended and can only be repaired by HR processes (Ensminger et al., 2014; Nikolova et al., 2010). The repair pathway choice can therefore already provide first indications of the origin of the breaks.

To determine the repair pathways involved in the repair of H_2O_2-induced DSBs in the different cell cycle phases, the repair of these breaks was investigated up to 16 hours after damage induction. As previously described, 82-6 hTert cells were pulse labeled with EdU for detection of S-phase cells followed by treatment with H_2O_2. In addition, inhibitors against the two important repair factors DNA-PK (c-NHEJ) and RAD51 (HR) were used to determine which repair pathway is used. In G1 phase, only the c-NHEJ and the related subpathways are available for repair. In G2 phase, HR is available in addition to c-NHEJ after DNA has been replicated. S phase represents a special scenario since at the beginning the required sister chromatid for HR is not available. In the course of replication, however, the sister chromatid is formed, and HR becomes available.

In G1 phase, the number of γH2AX foci in control cells decreased rapidly in the first 4 h after H_2O_2 treatment (**Figure 4.2 A**). In contrast, inhibition of DNA-PK resulted in almost complete abrogation of the decrease in γH2AX foci numbers. Inhibition of RAD51 had no such effect on the amount of γH2AX foci compared to control cells. Double depletion showed similar behavior to DNA-PK inhibition alone and no additive effect, confirming that c-NHEJ is the major repair pathway for breaks induced in G1.

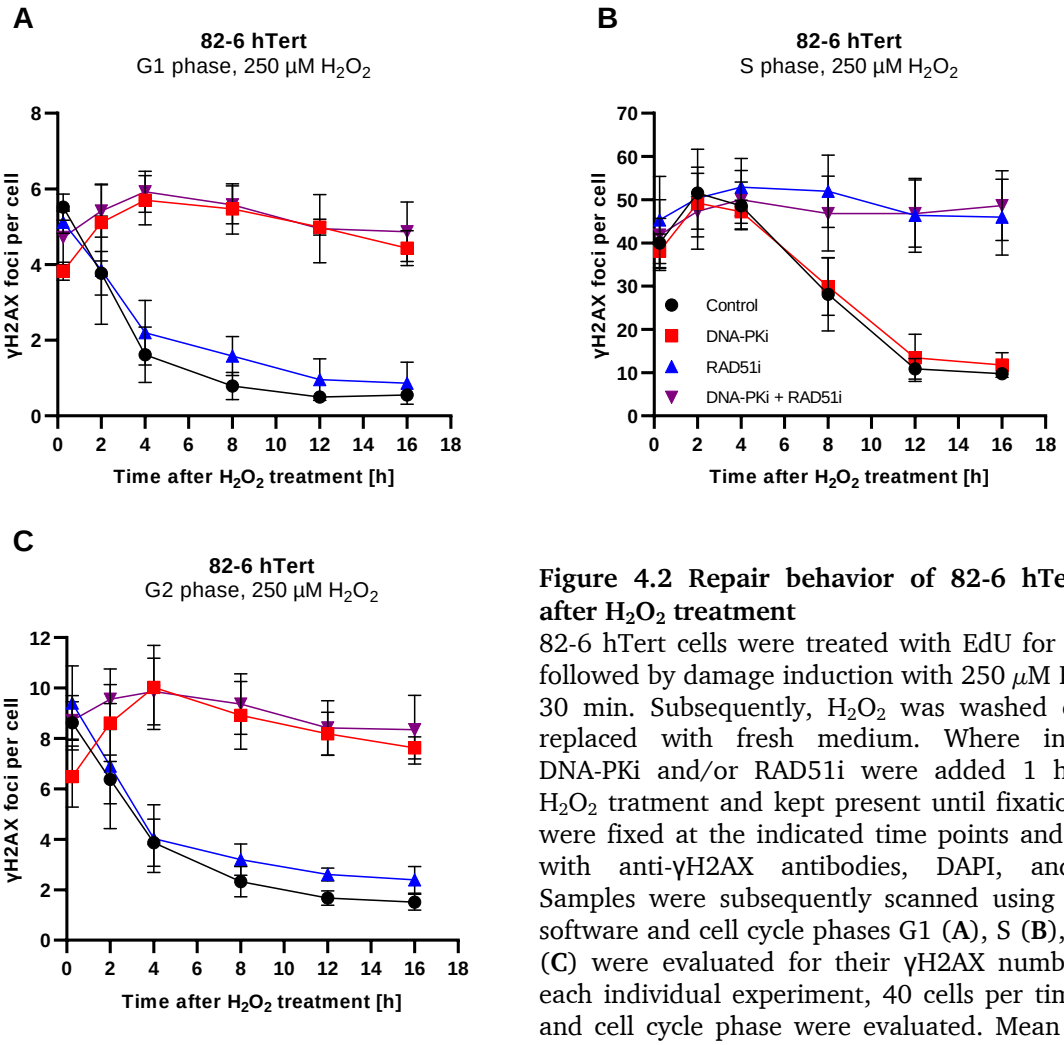

Figure 4.2 Repair behavior of 82-6 hTert cells after H_2O_2 treatment
82-6 hTert cells were treated with EdU for 30 min, followed by damage induction with 250 μM H_2O_2 for 30 min. Subsequently, H_2O_2 was washed out and replaced with fresh medium. Where indicated, DNA-PKi and/or RAD51i were added 1 h before H_2O_2 tratment and kept present until fixation. Cells were fixed at the indicated time points and stained with anti-γH2AX antibodies, DAPI, and EdU. Samples were subsequently scanned using Metafer software and cell cycle phases G1 (**A**), S (**B**), and G2 (**C**) were evaluated for their γH2AX numbers. For each individual experiment, 40 cells per time point and cell cycle phase were evaluated. Mean ± SEM (n=3).

Repair in S phase differed from that in G1. After H_2O_2 removal, the number of γH2AX foci in control cells increased for the first hours (**Figure 4.2 B**). This result confirms that additional DSBs are created during S phase and is consistent with the previous results obtained (**Figure 4.1 C** and **D**). The number of γH2AX foci started to decrease after 4 hours and did not reach the background level until 12 to 16 hours. Looking at the repair kinetics with DNA-PK and RAD51 inhibitors, the behavior was opposite to that described in G1. Inhibition of DNA-PK had no effect on the decrease of γH2AX foci compared to the control, whereas inhibition of RAD51 showed no considerable reduction of γH2AX foci in S phase. This demonstrates that the majority of breaks induced in S phase are repaired by HR. Dual depletion of DNA-PK and RAD51 had no additive effect, confirming that HR is the major repair pathway for the breaks in S phase.

G2 phase showed a similar behavior to that already observed in G1 phase (**Figure 4.2 C**). Reduction of γH2AX foci numbers occured within the first 8 h to background levels in control cells. Inhibition of DNA-PK resulted in persistence of γH2AX foci numbers, whereas inhibition of RAD51 had no effect. Double depletion also did not reveal any additional effect. This is surprising, especially since HR is available in the G2 phase. Like in G1 phase before, in G2 phase the c-NHEJ is the main repair pathway for the induced breaks.

The results on the formation and repair of DSBs after H_2O_2 treatment demonstrated that break induction mainly occures in S phase. In addition, break induction several hours after the removal of H_2O_2 and dependence on the repair via the HR pathway was demonstrated. Formation via secondary processes, as occurring in replication-associated breaks, was thereby assumed. To further validate this conclusion, the process of DSB formation in S phase was investigated in more detail.

4.2 Characterization of the processes involved in DSB induction after H_2O_2

The occurrence of replication-associated breaks represents a major threat to the genomic integrity. If the replication process collapses, one-ended DSBs are formed that lack the second break end, thereby promoting the formation of chromosomal aberrations (Gómez-González and Aguilera, 2019). One-ended DSBs arise when replication interferes with obstacles that prevent unhindered progression originating from structural obstacles in the DNA, the transcription process, or the formation of DNA lesions. The replication-dependent generation of DSBs by H_2O_2 should be investigated and the further processes contributing to break induction should be determined.

4.2.1 Involvement of replication and transcription on DSBs induced by H_2O_2

As shown in the previous results, the S-phase specific breaks are repaired by HR and remain unrepaired for up to 4 hours (**Figure 4.2 B**). Even an increase was observed in this period of time, suggesting the formation of replication-associated secondary breaks. To investigate the possible involvement of replication in the abovementioned DSB formation, the replication inhibitor aphidicolin was used. This inhibitor blocks Pol α and δ specifically in eukaryotes and provides an arrest of replication. In order to label S-phase cells, EdU treatment was performed prior to the addition of aphidicolin. This allowed for the identification of cells being in S phase during the aphidicolin and subsequent treatment with 250 μM H_2O_2. 4 h was chosen

as the fixation time point, since the highest fraction of additional in S phase generated DSBs was expected here. Inhibition of replication resulted in decreased γH2AX foci numbers in S-phase cells (**Figure 4.3 A**). For all tested H_2O_2 concentrations the number of induced γH2AX foci was reduced almost by half, revealing a significant difference from the control. Interestingly, not all S-phase specific breaks could be prevented from inhibition by aphidicolin, leaving a fraction of breaks unaffected. In contrast, in both G1 and G2 phases, inhibition of replication was shown to have no effect on the γH2AX foci induced at these cell cycle stages. Consequently, a partial dependence on replication was demonstrated for breaks induced in S phase, which was further investigated.

One possible cause for break induction associated with replication is the occurrence of interferences with the transcription process. The emergence of replication-transcription conflicts has been studied intensively in recent years and provided new insights into replication-associated DSB induction (Helmrich et al., 2011; Prado and Aguilera, 2005). The formation of replication-transcription conflicts is triggered by obstacles in the DNA that prevent unhindered progression of replication or transcription. Oxidative stress has the potential to cause such a hindrance due to its DNA damaging effect.

To investigate whether transcription is involved in H_2O_2-induced break formation, the transcription inhibitor DRB was used. DRB is an inhibitor of cyclin-dependent kinase 9, which associates with P-TEFb. This inhibits the elongation initiation of Pol II mediated by P-TEFb. To achieve efficient inhibition of transcription, DRB treatment was performed for 3 h before H_2O_2 treatment and led to a reduced induction of γH2AX foci in S phases (**Figure 4.3 B**). The number was significantly reduced approximately by half at all concentrations, showing great similarity with inhibition of replication. As for aphidicolin, treatment with DRB had no effect on breaks induced in G1 and G2 phases.

To confirm the previously obtained results, an additional inhibitor was used. The choice was made for triptolide, which specifically binds to TFIIH and inhibits the helicase activity required for the first step of transcription to open the dsDNA. Consequently, the transcription bubble cannot be formed and the onset of transcription is inhibited. Triptolide was added 1 h before H_2O_2 treatment to achieve transcription inhibition. Triptolide treatment resulted in reduced γH2AX foci in S phases comparable to an inhibition by DRB (**Figure 4.3 C**). However, the reduction was less pronounced and resulted in a lower significance compared to the control. As with the inhibitors before, there was no effect on G1 or G2 phases. These results suggest that, in addition to replication, transcription is also required for the formation of a subset of S-phase specific breaks.

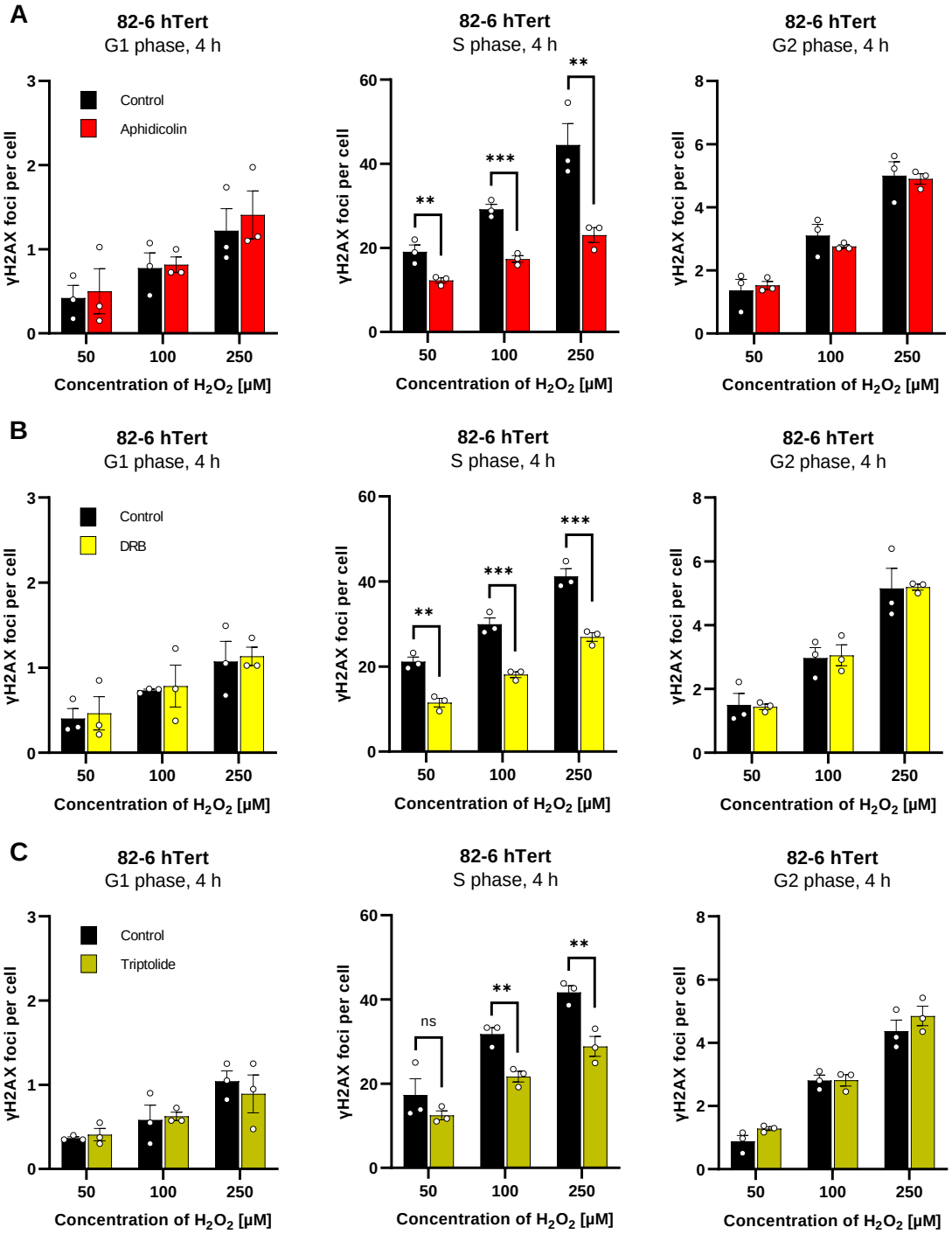

Figure 4.3 H_2O_2-induced γH2AX foci formation and inhibition of replication and transcription
(**A**) 82-6 hTert cells were treated with EdU for 30 min, followed by 30 min with aphidicolin. (**B**) To inhibit transcription, a 3 h treatment with DRB was performed. EdU was added in the last 30 min of DRB treatment. (**C**) Triptolide was added for 1 h and EdU in the last 30 min of triptolide treatment. The following steps were identical for all samples. After inhibitor treatment, damage induction for 30 min with H_2O_2 followed. Subsequently, H_2O_2 was removed and replaced by fresh medium and were indicated inhibitors were added. Fixation was conducted 4 h thereafter and staining with anti-γH2AX antibodies, DAPI, and EdU followed. Samples were scanned using Metafer software and 40 cells per cell cycle phase were scored for each individual experiment. Background γH2AX foci of the 0 μM H_2O_2 treatment were subtracted from all data (values see appendix **Table 1**). Data points show individual experiments. Mean ± SEM (n=3). **P<0.01, ***P<0.001 and ns, not significant (Student's t-test).

4.2.2 BER contribution to the induction of S-phase specific DSBs after H_2O_2 treatment

For S-phase specific induction of DSBs after MMS treatment, initiation of BER was shown to be crucial (Ensminger et al., 2014). It was demonstrated that replication forks interfere with SSBs that are formed as an intermediate of BER and that this is causativ for one-ended DSB formation. H_2O_2 also has the potential to generate base modifications that are repaired via BER. The most common one is the oxidation of guanine to 8-oxoG due to the lowest redox potential of this base (Burrows and Muller, 1998). BER, in turn, is initiated by a lesion-specific glycosylase that recognizes and removes the base modification, in the case of 8-oxoG by OGG1. In this work, it was shown that besides replication, transcription also contributes to the S-phase specific DSB formation after H_2O_2 treatment. Interestingly, studies on oxidative base modification 8-oxoG have revealed an involvement in transcriptional blockage (Kitsera et al., 2011). The base modification 8-oxoG itself has no blocking ability, neither on replication nor on transcription. However, 8-oxoG can be processed into a transcription-blocking intermediate by forming a SSB during the BER process. As a result, blocked transcription could promote a collision with the replication fork.

To determine whether BER contributes to the formation of S-phase specific DSBs after H_2O_2 treatment, initiation of repair was prevented by using an OGG1-deficient MEF cell line. Here, the oxidized base 8-oxoG cannot be recognized and consequently cannot be removed from the DNA. As a result, the modified base remains in the DNA and the BER process cannot be initiated. To define S-phase cells, MEFs were treated with EdU for 30 min before damage induction with H_2O_2 followed. For a better comparison with previous results, cells were fixed 4 h after H_2O_2 treatment. $OGG1^{-/-}$ MEFs showed, compared to wild type (WT) MEFs, a reduced γH2AX foci formation in S phase after treatment with H_2O_2 (**Figure 4.4 A**). The number of γH2AX foci was reduced by half and showed a significant difference between the two cell lines. However, treatment with H_2O_2 revealed no differences between the cell lines in G1 or G2 phases.

The recent development of OGG1 specific inhibitors, such as O8, allowed to confirm the results in the previously analyzed cell line 82-6 hTert. By using O8, the active site of OGG1 is blocked and the removal of 8-oxoG is omitted. For this, 82-6 hTert cells were treated for 1 h with inhibitor O8. Treatment with EdU and H_2O_2 was performed as previously described and fixation was conducted after 4 h. Inhibition of OGG1 resulted in a significant difference compared to control treated cells (**Figure 4.4 B**). The number of induced γH2AX foci was thereby specifically reduced in S phase, comparable to the inhibition of replication and transcription (**Figure 4.3**).

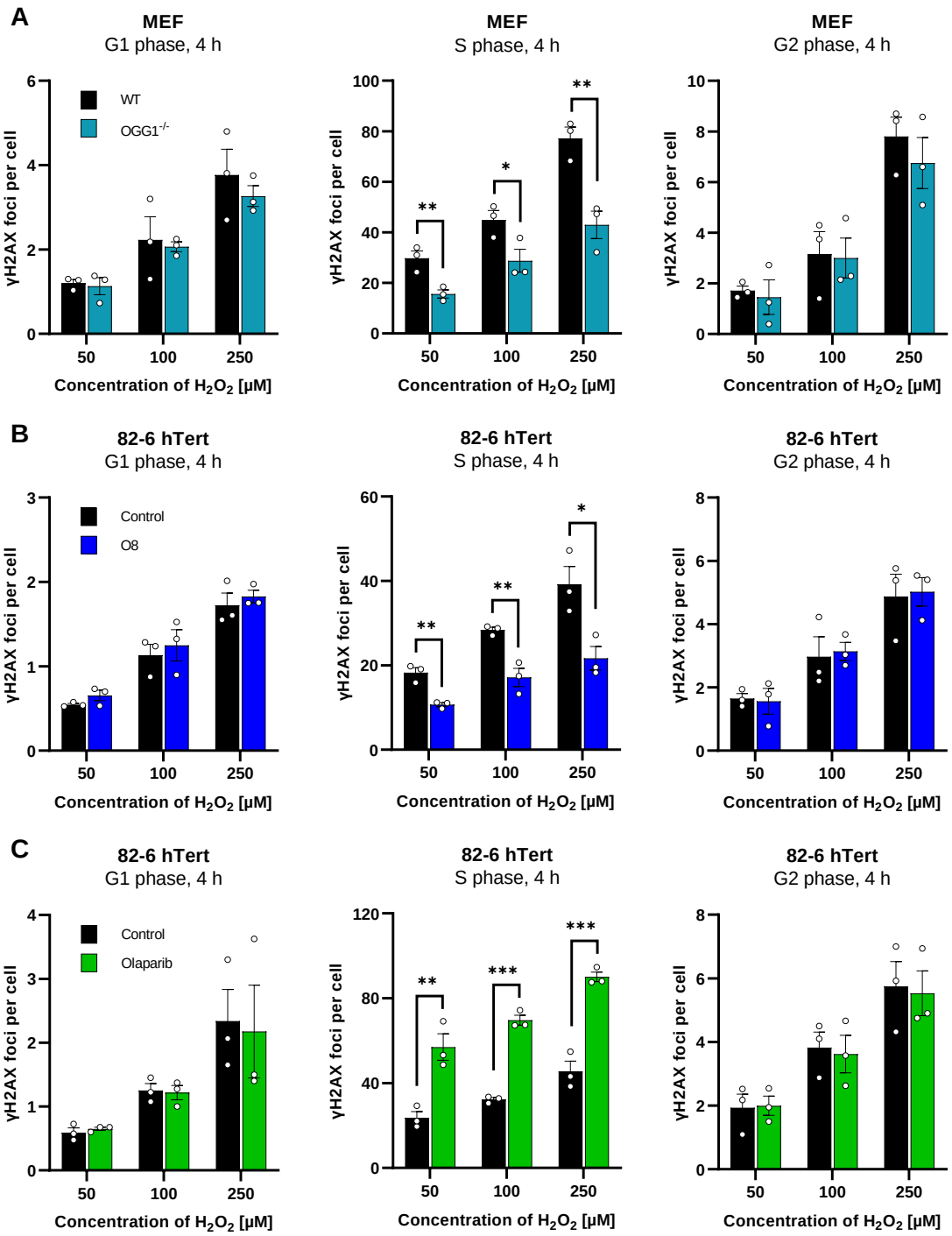

Figure 4.4 γH2AX foci formation after H_2O_2 treatment and modulation of BER
(**A**) WT and OGG1$^{-/-}$ MEFs were treated with EdU for 30 min before damage induction. (**B**) OGG1 inhibitor O8 was added to 82-6 hTert cells for 1 h and EdU was added for the last 30 min of incubation time. (**C**) For inhibition of PARP1, 1 h treatment with olaparib was performed with 82-6 hTert cells. EdU was added in the last 30 min of olaparib treatment. The following steps were identical for all samples. Damage induction was performed by treatment with H_2O_2 for 30 min. Fixation of cells was done 4 h after H_2O_2 was removed and replaced with fresh medium and were indicated inhibitors were added. This was followed by staining with anti-γH2AX antibodies, DAPI, and EdU. Samples were subsequently scanned using Metafer software and 40 cells per cell cycle phase were scored for each individual experiment. Background γH2AX foci of the 0 μM H_2O_2 treatment were subtracted from all data (values see appendix **Table 2**). Data points show individual experiments. Mean ± SEM (n=3). *P<0.05, **P<0.01 and ***P<0.001 (Student's t-test).

Again, inhibitor treatment had no effect on H_2O_2-induced breaks in G1 or G2 phase. These results indicate that the repair of oxidized bases via BER contributes to the formation of S-phase specific DSBs after H_2O_2 treatment.

As previously described, the induction of DSBs in S phase can be associated with the formation of SSBs during BER (Ensminger et al., 2014). The transcriptional blocking potential of 8-oxoG is also due to a SSB formed as a BER intermediate (Kitsera et al., 2011). If the SSB is indeed causative for the formation of DSBs, then unrepaired SSBs should lead to increased DSBs numbers. To further test whether SSBs are responsible for DSB induction in S phase, the PARP1 inhibitor olaparib was used. The PARP family consists of 17 members, with PARP1 being the most abundant and best-studied one. PARP1 is involved in diverse DNA repair processes, including the religation of the DNA backbone during BER (Caldecott, 2007; Fisher et al., 2007). If PARP1 is inhibited, BER is initiated, but the DNA backbone cannot be re-ligated resulting in an accumulation of SSBs generated by the BER process.

Inhibition of PARP1 by olaparib led to an opposite effect compared to the inhibitors used before (**Figure 4.4 C**). It significantly increased the number of γH2AX foci induced in S phase at all concentrations, whereas the number induced in G1 or G2 remained at the control level. These results demonstrate that BER can contribute to the formation of DSBs after H_2O_2 treatment and that SSBs represent the most critical structure of this process.

4.2.3 Investigation of the interplay between replication, transcription, and BER

The previous results demonstrated that three distinct cellular processes contribute to the induction of S-phase specific breaks after H_2O_2 treatment: replication, transcription, and BER. Inhibition of these processes alone resulted in a comparable, although not complete, decrease in foci numbers. It is assumed that only a subpopulation of S-phase specific breaks could be affected by the respective processes. To exclude that the reductions by the inhibitors affect different subpopulations and to verify the presence of an associated induction mechanism, combinational treatment of the inhibitors was performed. For this purpose, the previously mentioned method of cell cycle-specific γH2AX foci analysis was aplied.

Inhibition of replication, transcription, or BER alone could reproduce the previously obtained reduction in γH2AX foci numbers described earlier (**Figure 4.5 A**). Strikingly, any combination of two of these inhibitors did not show an additive effect. In fact, dual inhibition had the same effect on significantly reducing γH2AX foci numbers as single depletion indicating that all three processes are epistatic and operate on the same mechanism.

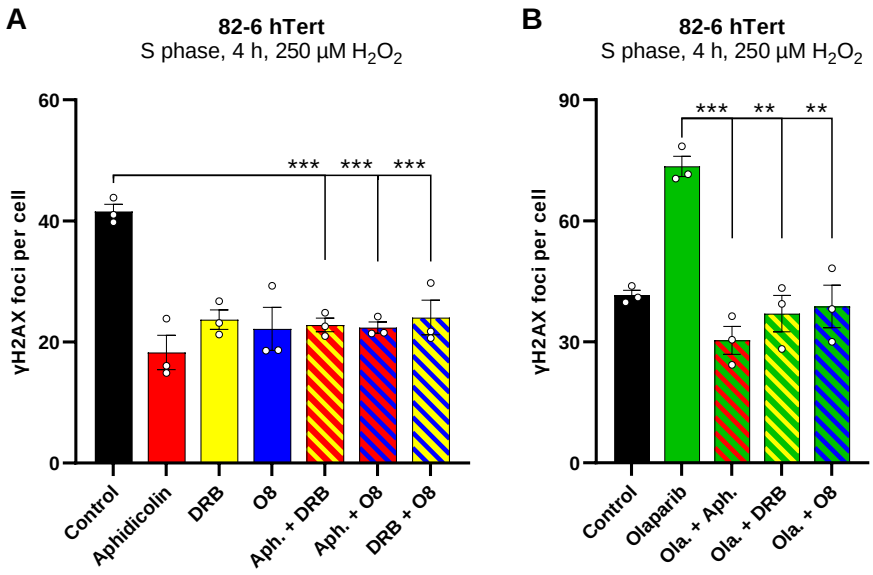

Figure 4.5 Combined inhibitor treatment and H_2O_2-induced γH2AX foci formation
(**A**) Inhibitor treatment of 82-6 hTert cells was performed as previously described. The combination of the different inhibitors followed the same treatment scheme as the single treatment. Briefly, the incubation period of DRB was 3 h and for O8 1 h. When aphidicolin was included, EdU treatment was performed for 30 minutes before aphidicolin was added for 30 minutes. Without aphidicolin, EdU treatment occurred during the last 30 minutes of the inhibitor incubation period. Damage induction was performed for all samples by treatment with 250 μM H_2O_2 for 30 min. After H_2O_2 was removed fresh medium with the indicated inhibitors was added until fixation. The cells were fixed after a total time of 4 h after damage induction. This was followed by staining with anti-γH2AX antibodies, DAPI, and EdU. Samples were subsequently scanned using Metafer software and 40 EdU-positive S-phase cells were scored for each individual experiment. (**B**) 82-6 hTert cells were treated with Inhibitors as previously described. The incubation period of olaparib and O8 was 1 h whereas DRB was incubated for 3 h. EdU was added for the last 30 min of the incubation period. For the combination of olaparib and aphidicolin the cells were treated with olaparib for 1 h and EdU was added simultaneously. Aphidicolin was then added 30 min before the end of incubation. Damage induction was performed for all samples by treatment with 250 μM H_2O_2 for 30 min. Fixation, staining, and analysis were as in (**A**). Background γH2AX foci of the 0 μM H_2O_2 treatment were subtracted from all data (values see appendix **Table 3**). The control values originate from the same experiment. Data points show individual experiments. Mean ± SEM (n=3). **P<0.01 and ***P<0.001 (Student's t-test).

Inhibition of PARP1 by the specific inhibitor olaparib, on the other hand, led to an increase in S-phase specific γH2AX foci (**Figure 4.5 B**). The effect based on the accumulation of SSBs should be prevented if any of the three aforementioned processes is inhibited. Inhibition of PARP1 in combination with replication, transcription, or BER resulted in decreased γH2AX foci numbers compared to olaparib treatment alone. However, the reduction obtained could not be reduced to the same level as the inhibition of replication, transcription, or BER before. A decrease equivalent to the level of the control without inhibitors was though achieved resulting in significantly reduced γH2AX foci compared to the olaparib treatment alone.

Nevertheless, partial reduction and thus involvement of SSBs in S-phase specific break induction related to replication, transcription, and BER was observed.

4.2.4 H_2O_2 treatment causes replication-transcription conflicts

From the previously obtained results, it was evident that S-phase specific DSBs after H_2O_2 treatment are partly dependent on both replication and transcription (**Figure 4.3**). Further investigations revealed an epistatic behavior when both processes were inhibited, indicating that both processes contribute to break induction via the same mechanism (**Figure 4.5 A**). To investigate the role of both processes in more details, the question was asked if S-phase specific break induction is caused by replication-transcription conflicts. A useful tool to investigate this question is the proximity ligation assay (PLA) (Alam, 2018). The PLA was developed to detect, amongst others, the interaction of two proteins. Specific primary antibodies are used to label the proteins of interest, in this case, PCNA (replication) and Pol II (transcription). The primary antibodies are in turn bound by specific PLA probes. These have an attached oligonucleotide sequence that forms a closed circular DNA template via hybridizing connector oligos and ligase activity. This process is only possible when the target proteins are in close proximity (< 40 nm) and thus interaction is assumed. The DNA template is used to amplify the signal up to 1,000-fold by a rolling circle amplification and labeling via fluorescently marked oligos. Thus, this technique enables the detection of interactions of individual molecules.

Since replication-transcription conflicts have to take place before the induction of a DSB, the cells were fixed after a H_2O_2 treatment time of 10, 20, and 30 min. EdU treatment was performed as previously described, and only EdU-positive cells were included in the analysis. **Figure 4.6 A** shows representative images of a PLA experiment. As negative controls, the primary antibodies were incubated alone, giving rise to no detectable PLA signals. In contrast, treatment with both antibodies shows the typical foci of a PLA experiment. The PLA foci number increased with the H_2O_2 concentration and showed the highest numbers after a short H_2O_2 treatment of 10 min (**Figure 4.6 B**). This suggests that treatment with H_2O_2 immediately increased the probability of replication-transcription conflicts. Aditionally, it supports the idea of a conflict between replication and transcription during H_2O_2-induced break induction.

Furthermore, the effects of the previously used inhibitors of replication, transcription, and BER were also analyzed by the PLA approach (**Figure 4.6 C**). Here, aphidicolin, DRB, and O8 had the same reducing effect on PLA foci formation as previously seen in the detection of γH2AX foci.

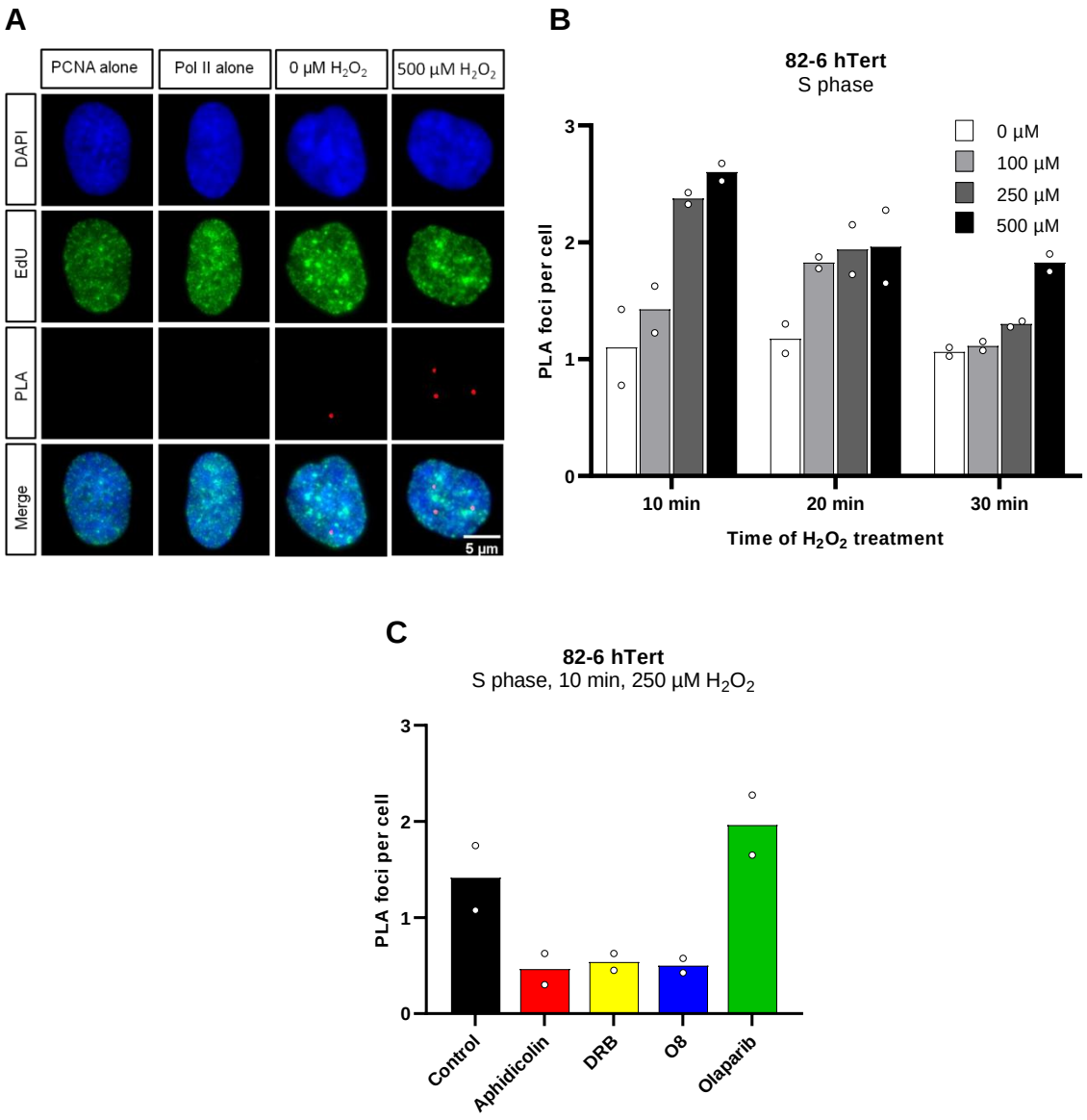

Figure 4.6 Detection of replication-transcription conflicts after H_2O_2 treatment by proximity ligation assay

(**A**-**B**) 82-6 hTert cells were treated with EdU for 30 min to identify S-phase cells. This was followed by damage induction using H_2O_2 for 10, 20, or 30 min. After washing out H_2O_2, pre-extraction and subsequent fixation was performed directly. This was followed by PLA staining with anti-PCNA and anti-Pol II antibodies, DAPI, and EdU. Samples were subsequently scanned using Metafer software. (**A**) Representative images of a PLA with PCNA and Pol II antibodies alone as controls and both antibodies in combination either in the absence of damage or 10 min after H_2O_2 treatment. (**B**) Obtained PLA foci numbers after evaluating different H_2O_2 treatment times. For each individual experiment, 40 EdU-positive S-phase cells were evaluated. (**C**) Inhibitor treatment of 82-6 hTert cells was performed as previously described. Briefly, for replication inhibition, treatment with EdU for 30 min was followed by aphidicolin treatment for 30 min. The incubation period of DRB was 3 h, for O8 and olaparib 1 h. EdU was added in the last 30 min of incubation time. Damage induction was performed with 250 μM H_2O_2 for 10 min. Fixation, staining, and analysis were as in (**B**) except for background subtraction of PLA foci of 0 μM H_2O_2 treatment from all data (values see appendix **Table 4**). Data points show individual experiments. Mean (n=2).

In contrast, inhibition by olaparib led to an increased number of PLA foci. The effect was not as pronounced as observed at the γH2AX level, but it should be mentioned that only the conflicts occurring at the time of fixation can be detected by the PLA. An overall accumulation of events as for DSBs using the the γH2AX foci assay is not possible here, which can also be seen in the generally lower numbers. Nevertheless, the same behavior for the occurrence of replication-transcription conflicts after H_2O_2 treatment could be detected on the PLA level as before for DSB induction.

These results supported the idea that replication-transcription conflicts are involved in the formation of DSBs after H_2O_2 treatment. It was shown that the conflicts are dependent on the same three processes and that SSBs generated by BER promote the occurrence of conflicts.

4.2.5 Effects of replication, transcription, and BER on CPT-induced S-phase specific DSBs

The occurrence of replication-associated breaks can be attributed, amongst others, to the formation of SSBs. These are converted into a one-ended break by ongoing replication and pose a major threat to the genomic integrity (Zeman and Cimprich, 2014). However, transcription seems to play no role in the induction of these breaks, in contrast to the results presented here. To test whether transcription is involved in the formation of S-phase specific one-ended breaks induced via a different drug, topoisomerase 1 (Top1) was inhibited via CPT. Top1 overcomes topological stress resulting from replication or transcription by inducing a SSB in the DNA backbone. This allows for the unwinding of the DNA and promotes subsequent re-ligation of the broken strand. CPT, on the other hand, stabilizes the Top1 bound to the DNA and prevents re-ligation of the DNA backbone. The result is a persistent SSB that can be converted into a one-ended DSB by a replication fork, independent of the occurrence of base modifications (Strumberg et al., 2000). To generate the replication-associated breaks using CPT, the EdU treatment was performed for 30 min, followed by addition of CPT for 1 h. The inhibitors were added as described previously and the number of CPT-induced γH2AX foci was determined for EdU-positive S-phase cells.

Treatment with 20 nM CPT led to an induction of γH2AX foci in S-phase cells (**Figure 4.7**). The induction of these γH2AX foci was almost completely prevented by inhibiting replication using aphidicolin, resulting in a highly significant difference compared to the control. Inhibition of transcription or BER of 8-oxoG had no effect on the amount of γH2AX foci numbers by CPT treatment. While inhibition of PARP1 led to a massive increase in γH2AX foci after treatment with H_2O_2 (**Figure 4.4 C**), no such effect was seen in combination with CPT treatment (**Figure 4.7**). A slight increase in γH2AX foci was noted, but not to the same extent

as with PARP1 inhibition in combination with H_2O_2 treatment. This suggests that CPT induces breaks in a manner independent of transcription and BER demonstrating that these breaks differ from the ones induced by H_2O_2. Thus, the breaks induced by H_2O_2 represent a special class that is dependent on the three processes of replication, transcription, and BER.

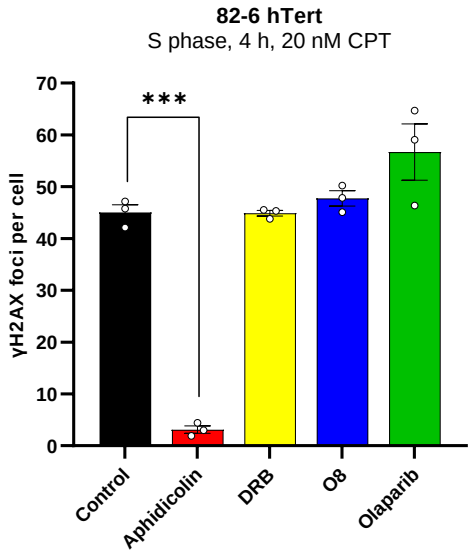

Figure 4.7 S-phase specific DSB induction by CPT and effects of replication, transcription, and BER inhibition
EdU treatment was performed for 30 min, followed by damage induction with 20 nM CPT for 1 h. Aphidicolin treatment was performed for 30 min after EdU and before CPT treatment. DRB was added 3 h before CPT treatment. O8 and olaparib was added 1 h before CPT treatment. After damage induction cells were washed and fresh medium was added. Where indicated inhibitors were added until fixation. Fixation of the cells was performed 4 h after CPT treatment. This was followed by staining with anti-γH2AX antibodies, DAPI, and EdU. Samples were subsequently scanned using Metafer software and 40 EdU-postive S-phase cells were scored for each individual experiment. Background γH2AX foci of 0 nM CPT treatment were subtracted from all data (values see appendix **Table 5**). Data points show individual experiments. Mean ± SEM (n=3). ***P<0.001 (Student's t-test).

In summary, investigations on the processes involved in S-phase specific DSB induction after H_2O_2 treatment demonstrated a strong dependence on replication, transcription, and BER, thus revealing a mechanism of DSB formation that is different to other S-phase damaging agents such as CPT. The involvement of BER confirmed that the processing of oxidative base modifications can also lead to the formation of replication-dependent DSBs, as previously shown for methylated base modifications. Moreover, transcriptional involvement in the induction of these breaks was demonstrated, and subsequent experiments support the idea that replication-transcription conflicts are causative for break induction. Since replication-transcription conflicts can only occur in regions of active transcription, more detailed investigations on the distribution of DSBs in the genome should be performed in the following.

4.3 Investigations on the genome-wide distribution of H_2O_2-induced DSBs

The γH2AX data of this work demonstrated the involvement of replication as well as transcription in the formation of S-phase specific DSBs after treatment with H_2O_2 (**Figure 4.3**). Moreover, the occurrence of replication-transcription conflicts after H_2O_2 treatment was confirmed using PLA indicating that these conflicts could contribute to DSB formation (**Figure 4.6**). Consequently, these breaks could only occur in regions of the genome of actively transcribed genes. For this reason, further investigations should give insight into the regions of the genome where H_2O_2-induced DSBs occur. A method that has been established to identify such regions at the whole genome level is the chromatin immunoprecipitation followed by massive parallel sequencing (ChIP-Seq). In this approach, the interaction of DNA damage markers with DNA can be used to identify those regions of the genome where DSBs occur. This approach should elucidate where in the genome DSBs occur after H_2O_2 treatment and whether a dependence on replication, transcription, and BER can be confirmed for these breaks. For this reason, the aim was to first establish the ChIP-Seq method in this laboratory.

4.3.1 Establishment of the ChIP-Seq method using the DIvA cell system

Establishing the ChIP-Seq method based on H_2O_2-induced breaks turned out to be difficult and extremely complex. For this reason, the cell system of DIvA cells was chosen, which is particularly suitable for the optimization and validation of the ChIP approach. These cells possess an A*si*SI restriction enzyme fused to a modified oestrogen receptor hormone-binding domain (Iacovoni et al., 2010). Treatment with 4-OHT allows the enzyme located in the cytoplasm to enter the nucleus, where it cuts DNA at its specific 8 bp recognition sequence. As a result, approximately 100 annotated DSBs are generated throughout the human genome. The advantage of this cell system is the defined break sites, which can be effectively analyzed by qPCR and thus differs from the H_2O_2 approach, in which breaks are more randomly distributed in the genome.

For ChIP, the DIvA cells were treated with 4-OHT for 2 h and immunoprecipitation was performed with the DSB marker γH2AX. Phosphorylation of H2AX after 4-OHT treatment has been previously demonstrated for DIvA cells and was used here for analysis of the cell system (Iacovoni et al., 2010). Based on these data, primers were designed for evaluation by qPCR and used to optimize the ChIP approach. The results show the use of primers of two annotated cutting sites (DSB 12, DSB II) and two non-cutting regions of several Mbp (NC A,

NC B) (**Figure 4.8 A** and **B**). In the optimized protocol, 4-OHT treatment resulted in a distinct increase in γH2AX-ChIP DNA for the cutting sites DSB 12 and DSB II. In contrast, the NC A and NC B primer pairs showed no detectable increase compared to the controls. The additional use of an IgG antibody revealed low values and confirmed the specificity of the pull-down. This suggests successful break induction at the annotated sites and successful validation of the ChIP approach using DIvA cells.

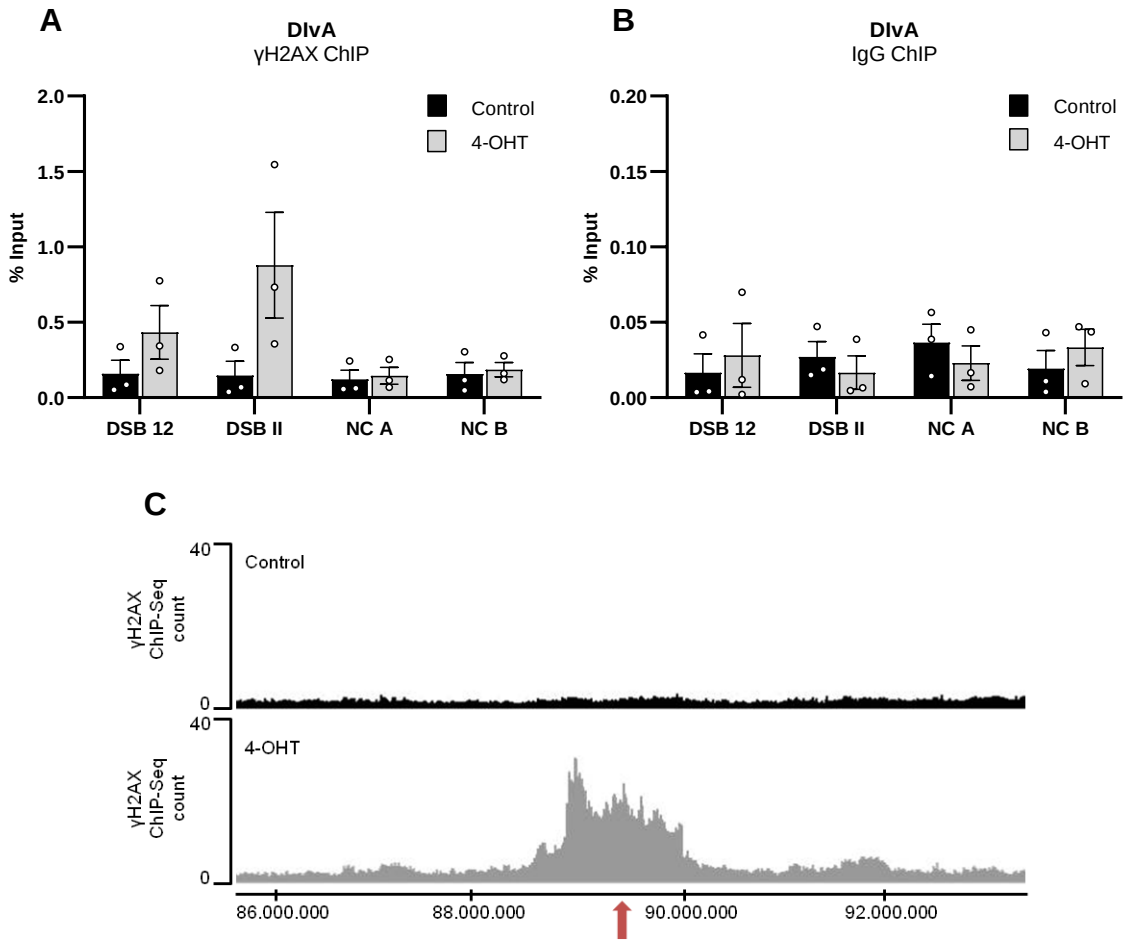

Figure 4.8 ChIP-qPCR and ChIP-Seq after damage induction using 4-OHT in DIvA cells
DIvA cells were treated with 4-OHT for 2 h and fixed. After lysation the cells were sonicated to obtain 200 to 500 bp fragments. Pre-clearing with magnetic beads was followed by antibody incubation with anti-γH2AX or anti-IgG overnight. After several washing steps, the samples were eluted and the DNA was purified on columns. (**A-B**) qPCR was performed using primers specific for cutting sites (DSB 12, DSB II) or non-cutting sites (NC A, NC B). Mean ± SEM (n=3). (**C**) Library preparation and sequencing of the purified DNA were performed at the IMB in Mainz. Bioinformatic analysis was conducted using the open, web-based platform Galaxy. Profiles of γH2AX ChIP-Seq reads of control and 4-OHT treated samples. A*si*SI cutting site is indicated by a red arrow.

However, for the determination of the break sites on whole genome level, the evaluation by qPCR is not sufficient. Primer design requires prior knowledge of the region of interest in the genome. Therefore, for the determination on whole genome level, sequencing of the ChIP-DNA is required. To verify the quality of the DNA obtained by γH2AX ChIP, sequencing was performed using Ilumina NextSeq 500 technology at the IMB in Mainz. The obtained data were bioinformatically processed and could confirm the occurrence of breaks at the annotated cutting sites (**Figure 4.8 C**). These are characterized by an increased density of DNA fragments around the break site. The results are consistent with previously published data and confirmed additional validation of the execution and evaluation of the sequencing (Aymard et al., 2014; Iacovoni et al., 2010).

By using the DIvA cell system, a successful optimization and validation of the ChIP-Seq approach was achieved. The results obtained were comparable to those from published studies and the protocol could then be transferd to investigate the 82-6 hTert cells and a break induction by H_2O_2.

4.3.2 γH2AX ChIP-Seq of H_2O_2-induced DSBs

The previously established method of ChIP-Seq could now be used to determine the regions of DSB induction after H_2O_2 treatment. The aim was to prove the notion that H_2O_2-induced DSBs predominantely arise in actively transcribes regions. For this purpose, the previously described γH2AX damage marker was chosen also for the H_2O_2 studies, due to its universal labeling of DSBs and persistence until the break is repaired. This ensured that all S-phase DSBs were included in the analysis following an incubation period of 4 h after 500 μM H_2O_2 treatment. In addition, the contribution of DSBs arising in the G1 and G2 phases was low at this time point (**Figure 4.1 D**). Besides, no publicly available data sets on the transcriptome of the 82-6 hTert cell line used were available. In order to obtain precise information about the actively transcribed regions, an RNA-Seq analysis was performed in parallel. For this purpose, the RNA-Seq service of BGI geomics could be used, which provides sample preparation and sequencing.

Bioinformatic evaluation revealed a correlation between RNA and γH2AX ChIP-DNA content (**Figure 4.9**). To achieve this, the human genome was divided into 0.5 Mbp windows and the log2 values of RNA-Seq and γH2AX ChIP-Seq were plotted against each other (**Figure 4.9 A).** The data cloud "kinked" to the right, into the region with increased RNA-Seq and γH2AX ChIP-Seq values. This indicates that areas with increased presence of γH2AX were also those with higher transcription rates. For a better visualization, 200 of the 0.5 Mbp windows

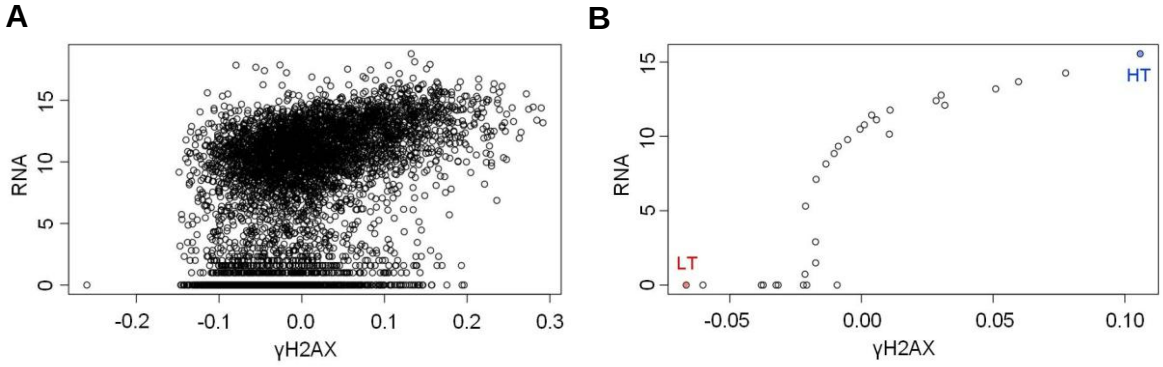

C

Region	GC (%)	Average	Genes	Average
HT1	0.56		40	
HT2	0.53		24	
HT3	0.52	0.537	34	32.7
LT1	0.47		2	
LT2	0.35		7	
LT3	0.38	0.400	3	4.0

Figure 4.9 γH2AX ChIP-Seq of 82-6 hTert cells after treatment with H_2O_2
For ChIP-Seq, 82-6 hTert cells were treated with 500 μM H_2O_2 for 30 min. After 4 h, the cells were fixed and lysed, followed by sonification to obtain 200 to 500 bp fragments. Pre-clearing with magnetic beads was followed by antibody incubation with anti-γH2AX overnight. After several washing steps, the samples were eluted and the DNA was purified on columns. Library preparation and sequencing of the purified DNA were performed at the IMB in Mainz. RNA isolation and RNA-Seq were performed by BGI Genomics. (**A**) Plot of log2 values of RNA-Seq and ChIP-Seq results. The genome was divided into 0.5 Mbp sections. (**B**) As in (**A**), except data from 200 of the 0.5 Mbp windows were grouped according to their RNA content to one data point. The datapoint with the highest and a low RNA expression were defined as HT and LT, respectively. (**C**) Three exemplary 0.5 Mbp windows from the HT and LT datapoints from (**B**) were checked for their GC content and gene density. Bioinformatic analysis was performed by Ilaria Ghiro (AG Löbrich).

were grouped according to their RNA content (**Figure 4.9 B)**. Here, the areas with the highest RNA expression were also found to have the highest values of γH2AX ChIP-DNA. The amount of γH2AX ChIP-DNA decreased with dropping RNA expression until it reached a range of low RNA content, where the amount of γH2AX ChIP-DNA was more variable. For a more detailed analysis, three 0.5 Mbp windows each were chosen from the datapoint with the highest and from a low RNA expression (**Figure 4.9 B** and **C**). It was observed that the regions with a high transcription (HT) rate showed a higher GC content of 53.7 % in comparison to an average GC content of 40 % in the low transcription (LT) regions indicating increased genetic regions. Accordingly, gene density was also increased with an average of 32.7 genes per 0.5 Mbp in

the HT regions compared to 4 in the LT regions. Thus, the sequencing results indicate a dependence on the occurrence of DSBs after H_2O_2 treatment with the regions of actively transcribed genes in 82-6 hTert cells.

4.3.3 Impact of replication, transcription, and BER inhibition on DSB formation in HT and LT regions after H_2O_2 treatment

Since both the γH2AX and PLA results showed a dependence on the three processes of replication, transcription, and BER, the question arose whether this dependence also applied to the breaks analysed in the ChIP approach. For this purpose, the information obtained by sequencing was used to design selective primers. The previously investigated HT and LT regions served as reference and primers were used for ChIP-qPCR analyses. Strikingly, treatment with 500 μM H_2O_2 resulted in an increase of γH2AX ChIP-DNA mainly in the HT regions, as shown in a representative experiment in **Figure 4.10 A** (confirmation by second experiment see appendix **Figure 6.2**). In contrast, there was little to no increase in the LT regions. This result confirms that mainly the actively transcribed regions of the genome contribute to DSB induction after H_2O_2 treatment.

Since representative primers for the induction of breaks after H_2O_2 treatment were now available, the effects of the inhibitors on replication, transcription, and BER were examined. 82-6 hTert cells were treated with inhibitors and H_2O_2 as previously described. In undamaged cells (0 μM H_2O_2), inhibition by any of the above-mentioned inhibitors had no effect on the amount of DNA precipitated compared to control cells (**Figure 4.10 A)**. In contrast, a different behavior for the samples was observed after additional treatment with 500 μM H_2O_2. Despite the increase in the HT regions of the control sample, inhibiting replication, transcription, as well as BER via OGG1, had a reducing effect on the amount of DNA precipitated after γH2AX ChIP. As in previous experiments, PARP1 inhibitor treatment had the opposite effect, leading to an increase in the amount of γH2AX ChIP-DNA in HT regions. Interestingly, the LT regions showed almost no additional increase compared to the 0 μM H_2O_2 samples. To validate the results obtained by γH2AX, additional control ChIP were performed using non-specific IgG antibodies. Elevated values were not detected in any condition, confirming that the ChIP by γH2AX was specific (**Figure 4.10 B**). The results suggest that mainly the HT regions contribute to the formation of DSBs after treatment with H_2O_2. Moreover, it was confirmed that this induction depends on three processes: replication, transcription, and BER. Additionally, the involvement of SSBs in break induction after H_2O_2 was also demonstrated here.

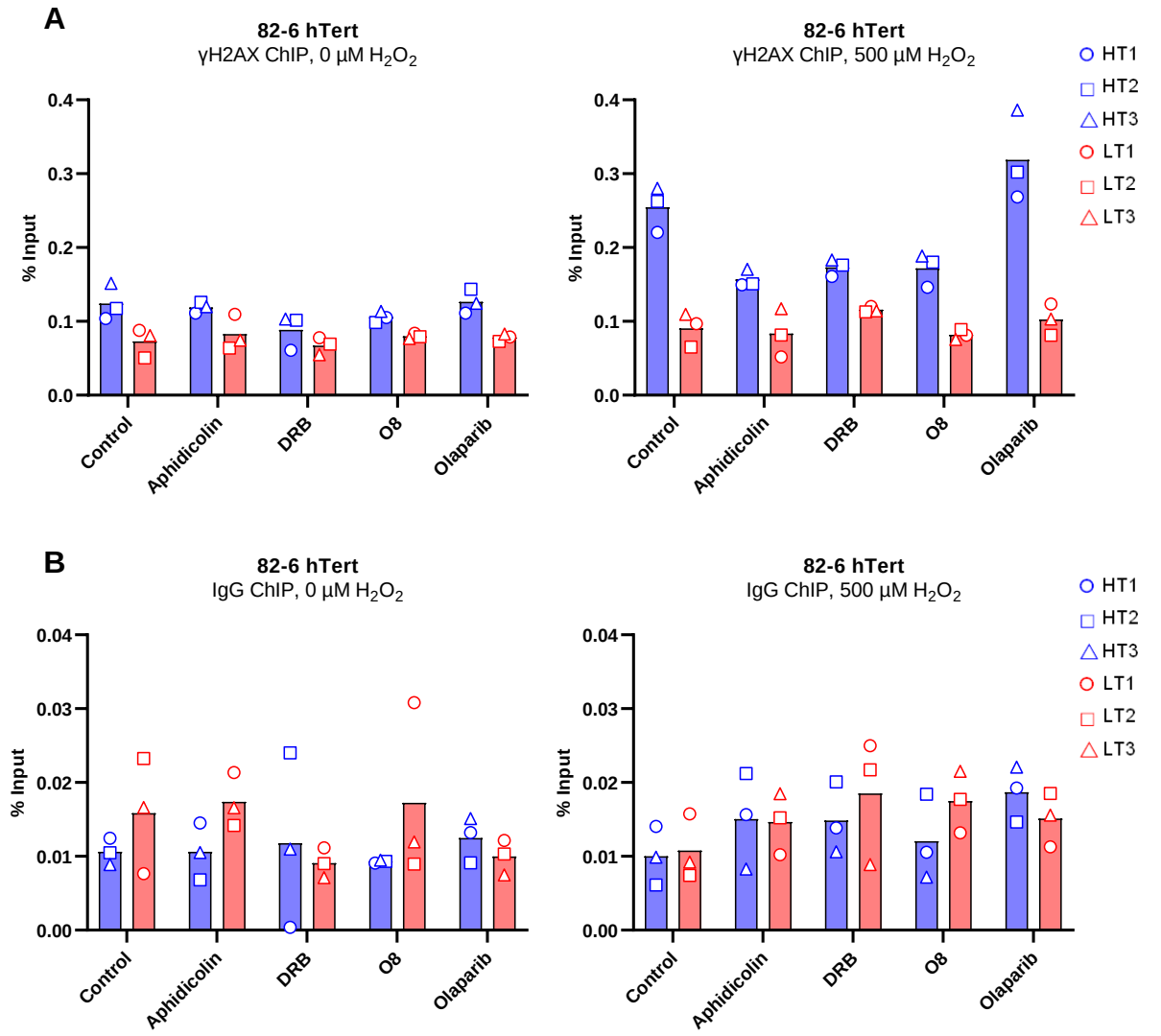

Figure 4.10 ChIP-qPCR of 82-6 hTert cells after H_2O_2 and inhibitor treatment
82-6 hTert cells were treated with inhibitors for 3 h (DRB), 1 h (O8, olaparib), or 30 min (aphidicolin). This was followed by damage induction with 500 μM H_2O_2 for 30 min. After 4 h, the cells were fixed and lysed. Afterwards, sonification was performend to obtain 200 to 500 bp fragments. Pre-clearing with magnetic beads was followed by antibody incubation with anti-γH2AX or anti-IgG overnight. After various washing steps, samples were eluted and DNA was purified over columns. A qPCR was performed with different primers based on the sequencing results. (**A**) γH2AX ChIP of 0 μM and 500 μM H_2O_2 treated samples. (**B**) IgG ChIP of 0 μM and 500 μM H_2O_2 treated samples to validate the specificity of ChIP. Mean of HT or LT primers (n=1).

In conclusion, the establishment of the ChIP method using DIvA cells allowed for the investigation of the effects of H_2O_2 on 82-6 hTert cells using ChIP-Seq, as well as ChIP-qPCR. A correlation between the occurring DSBs with the regions of active transcription could be established. In addition, by designing specific primers, the dependence of the DSBs generated in the HT regions on the three processes of replication, transcription, as well as BER could be revealed.

4.4 Evaluation of endogenous and H_2O_2-induced DSBs during S phase progression

4.4.1 Formation of H_2O_2-induced DSBs in different S-phase stages

The previously obtained results demonstrated that replication-transcription conflicts can contribute to the formation of DSBs in S phase (**Figure 4.6**). In addition, ChIP experiments revealed the increased occurrence of DSBs in the areas of high transcription rate (**Figure 4.9**). Replication itself proceeds according to a particular order. Especially the euchromatic regions and thereby those of active transcription are replicated first. This is related to the open chromatin structure, which allows easier and faster accumulation of replication factors at the replication origins (White et al., 2004; Woodfine et al., 2004). Since the H_2O_2-induced DSBs occur in a replication-dependent manner in actively transcribed regions, it was questioned, wheter these DSBs are predominantely formed in an early S-phase stage.

To investigate this, double labeling with Edu/BrdU was applied, which allows to define different stages in S phase more precisely (early/mid/late) and to follow them throughout the cell cycle. With this approach the formation and repair of DSBs can be investigated for different S-phase stages. As recently described in *Llorens Agost et al. 2021*, a 1 hr treatment with EdU is first performed to label all cells in S phase. After washing off EdU, BrdU is added to the cells for 2 hours. This results in three distinctive S-phase populations: cells positive for EdU but not BrdU, cells positive for both EdU and BrdU, and cells only positive for BrdU (**Figure 4.11 A**). The $EdU^-/BrdU^+$-cells were defined as early S-phase cells since these cells were in G1 phase during the EdU treatment and have transitioned to S phase during the BrdU treatment. Additional staining of chromatin-bound PCNA determined the transition of $EdU^-/BrdU^+$-cells from S to G2 phase. PCNA binds to chromatin only during S phase and a decreased signal is indicative of transition to G2 phase. A transition of $EdU^-/BrdU^+$-cells between 5 and 6 h after BrdU removal was detected (**Figure 4.11 B**).

Using the EdU/BrdU double labeling approach, it was possible to investigate in which stage of S phase H_2O_2-induced DSBs predominantly arise. Based on the observation before that cells start entering G2 phase at 5 to 6 h after BrdU removal, H_2O_2 treatment was performed at 0h, 2h, or 4h after EdU/BrdU labeling to specifically treat cells in early, mid, or late S phase, respectively (**Figure 4.11 A**). Aditional staining for γH2AX allowed for the evaluation of arising DSBs. If the H_2O_2 treatment was carried out in the early S phase, an increase in γH2AX foci numbers was detected compared to control treated cells (**Figure 4.11 C**). However, when treated in the mid S phase, the number of induced γH2AX foci was greatly reduced, and almost no γH2AX foci were observed after treatment in late S phase.

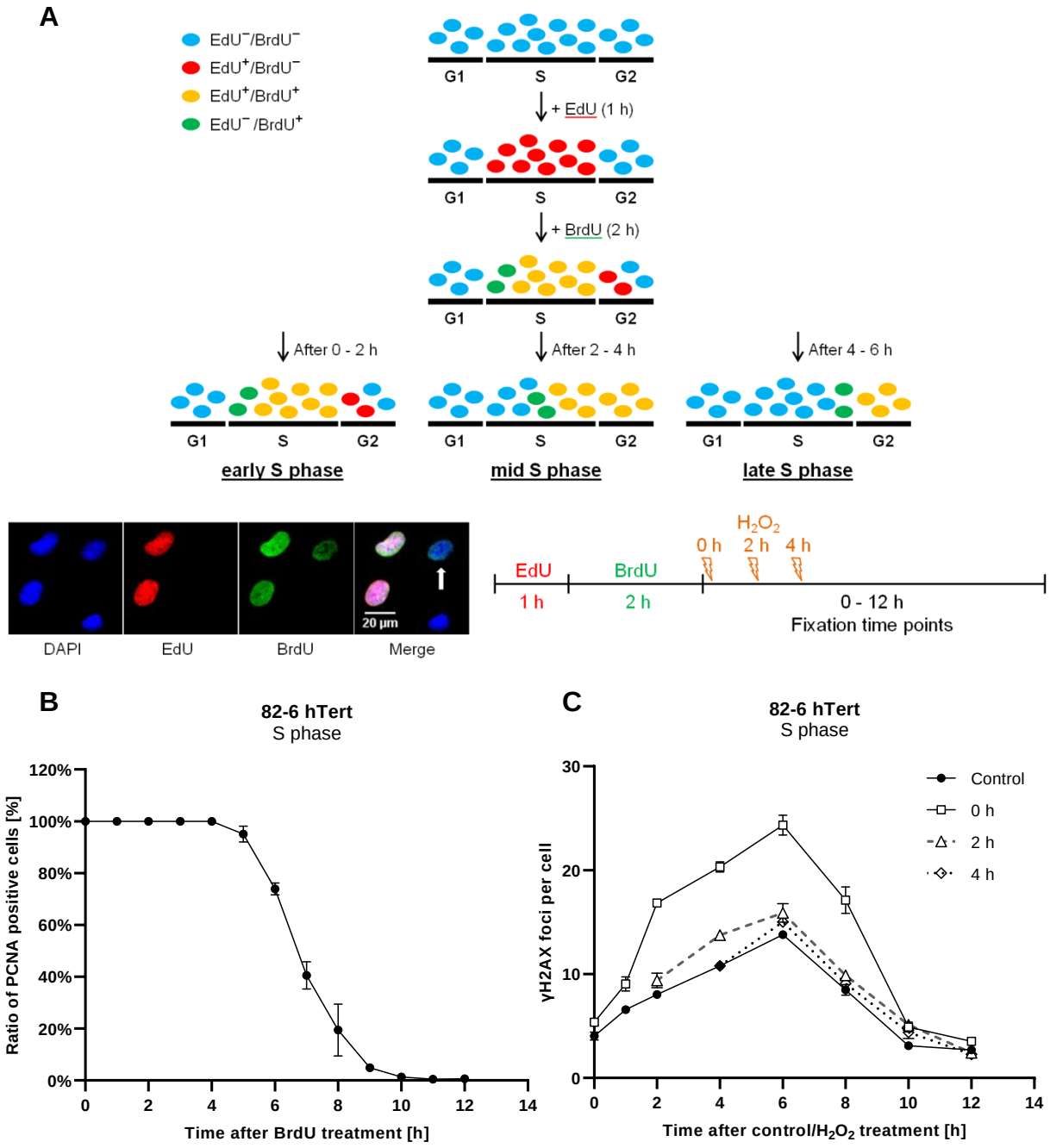

Figure 4.11 EdU/BrdU double labeling approach and H_2O_2-induced DSBs throughout S phase
(**A**) Schematic illustration of EdU/BrdU double labeling with progression of $EdU^-/BrdU^+$-cells into early, mid, and late S phase (top). Representative images of 82-6 hTert cells after EdU/BrdU double labeling. Cells were treated for 1 h with EdU and for 2 h with BrdU. An $EdU^-/BrdU^+$-cell is marked with an arrow (bottom left). Treatment scheme to study the the induction of DSBs by H_2O_2 at different stages of S phase (bottom right). (**B**) 82-6 hTert cells were treated for 1 h with EdU and for 2 h with BrdU. Pre-extraction and subsequent fixation was performed at different time points after BrdU removal. Staining with anti-PCNA and anti-BrdU antibodies, DAPI, and EdU followed. Samples were subsequently scanned using Metafer software and the percentage of PCNA-positive cells was determined for the population of $EdU^-/BrdU^+$-cells. Experiments were performed by Michael Ensminger (AG Löbrich). (**C**) EdU/BrdU labeling was performed as described before. H_2O_2 treatment followed 0 h, 2 h, or 4 h after BrdU removal or control treatment was performed. Cells were fixed at different time points and staining with anti-γH2AX and anti-BrdU antibodies, DAPI, and EdU followed. Samples were subsequently scanned using Metafer software and analyzed for their γH2AX foci levels. For each individual experiment, 40 $EdU^-/BrdU^+$-cells were scored per time point. Mean ± SEM (n=3).

This indicates that H_2O_2 treatment induces breaks mainly in early S phase and to a lesser extent in later stages of S phase. This is consistent with previously obtained results that breaks occur in actively transcribed regions of the genome after H_2O_2 treatment.

4.4.2 Dependency of early S-phase DSBs on transcription and BER

Using the EdU/BrdU double labeling approach, it was possible to identify the early S phase as the stage where H_2O_2-induced DSBs predominantly arise. When the whole S phase was analyzed in prevous experiments, a dependency on replication, transcription, as well as BER could be identified using specific inhibitors. In order to confirm these dependencies specifically for early S-phase cells, the EdU/BrdU double labeling approach was performed in the presence of the above-mentioned inhibitors. In these experiments, the cells were first treated with EdU for 1 h. This was followed by treatment with BrdU for 2 hours and damage induction with 25 μM H_2O_2 for 30 min. To analyse the break induction the cells were fixed at different time points after H_2O_2 removal. The contribution of transcription and BER for the formation of H_2O_2-induced DSBs was examined by adding the inhibitors DRB, O8, and olaparib as previously described.

As observed before, H_2O_2 treatment in early S phase resulted in an increase of γH2AX foci numbers above control levels (**Figure 4.12 A**). The number of γH2AX foci increased steadily until 6 h after H_2O_2 treatment, when a rapid decrease was observed. This can be explained by the transition from the S to the G2 phase and the initiation of repair of replication-associated DSBs. Interestingly, the additional inhibition of transcription by using DRB diminished the γH2AX foci inducing effect of the H_2O_2 treatment (**Figure 4.12 A**). This is in line with the previous results that the transcription process contributes to the S-phase specific induction of DSBs by H_2O_2 treatment. Comparable results were obtained by the inhibition of OGG1 with the specific inhibitor O8 (**Figure 4.12 A**). Preventing the initiation of BER reduced the number of γH2AX foci, indicating the need for base removal for DSB formation. In previous experiments, an increased damage induction after H_2O_2 treatment was observed after PARP1 inhibition by olaparib. Using the EdU/BrdU double labeling approach, this observation was confirmed as treatment with olaparib increased the number of γH2AX foci induced after H_2O_2 treatment (**Figure 4.12 B**). The results indicate that the occurrence of SSBs is essential for the S-phase specific breaks induced after H_2O_2 treatment.

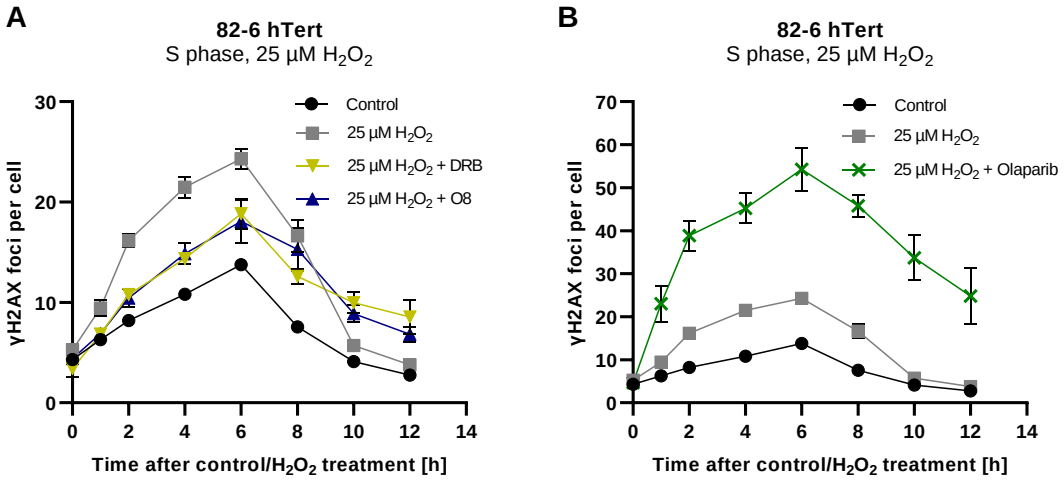

Figure 4.12 Formation of γH2AX foci in early S phases after H_2O_2 and inhibitor treatment
(**A**-**B**) 82-6 hTert cells were treated for 1 h with EdU, followed by 2 h with BrdU. If indicated, treatment with inhibitors for 3 h (DRB) or 1 h (O8 and olaparib) occurred simultaneously with EdU/BrdU treatment. H_2O_2 or control treatment was conducted for 30 min and followed by fixation at different time points. Staining with anti-γH2AX and anti-BrdU antibodies, as well as DAPI and EdU labeling followed. Samples were subsequently scanned using Metafer software and analyzed for their γH2AX foci levels. For each individual experiment, 40 $EdU^-/BrdU^+$-cells were scored per time point. Control and 25 μM H_2O_2 sample shown in (**A**-**B**) are from the same experiment. Mean ± SEM (n=3).

In summary, by specifically analyzing early S-phase cells using the EdU/BrdU double labeling approach very similar results were obtained as in the experiments performed before. In particular, a dependence of H_2O_2-induced break formation on transcription and initiation of BER was confirmed for early S-phase cells. Thus, it can be assumed that the processes of break induction investigated above are mainly arising during early S phase.

4.4.3 Investigations on endogenous DSBs and characterization of the processes involved

The studies on the involvement of different S-phase stages in DSB induction after H_2O_2 treatment revealed not only an increase in γH2AX foci in treated cells but also a steady rise over the course of S phase for untreated control cells (**Figure 4.11 C** and **Figure 4.12**). This can be attributed to the formation of endogenous DSBs. The occurrence of endogenous DSBs is found primarily in S phases, as these breaks arise in a replication-dependent manner. This is supported by the fact that considerably less endogenous DSBs are present in the G1 and G2 phases. Interestingly, oxidative stress is commonly considered a major contributor to the formation of endogenous DNA lesions (Lindahl and Barnes, 2000; Tubbs and Nussenzweig, 2017). Since oxidative base modifications are one of the most common oxidative

stress-induced lesion, the question arises whether a subset of endogenous DSBs rely on the same processes as DSBs induced after H_2O_2 treatment. For this study, the previously used method of EdU/BrdU double labeling was applied. In contrast to the previous experiments, no break induction was performed for all samples, so that only the endogenously occurring DSBs were analyzed. This method was combined with inhibitor treatment and once more γH2AX staining was used to quantify the DSBs.

As seen previously, control cells accumulate γH2AX foci during S phase, peaking 6 h after removal of BrdU (**Figure 4.13**). Thereafter, the number of γH2AX foci in the cells decreased, which can again be explained by the transition to the G2 phase and the superposition of the repair process over the induction of new DSBs. To investigate the contribution of oxidative stress on the accumulation of endogenous breaks during S phase, the antioxidant NAC was used. NAC is not an active radical scavenger, but rather a supporting chemical that keeps glutathione levels high in cells. Treatment with NAC leads to reduced ROS levels in cells and decreases oxidative stress-induced DNA damage (Aruoma et al., 1989). The treatment with NAC resulted in a decreased γH2AX foci formation over the course of S phase (**Figure 4.13**). This confirmes that oxidative stress is a major contributor to the formation of endogenous breaks in S phase. Interestingly, a similar reduction in γH2AX foci numbers was observed when cells were treated with the OGG1 glycosylase inhibitor O8 (**Figure 4.13**). As previously mentioned, 8-oxoG is the most common base modification induced by ROS (Epe, 1996). Accordingly, inhibition of OGG1 could prevent the formation of breaks in untreated S-phase cells in a similar manner as after treatment with H_2O_2. No further reduction was observed with combined treatment of NAC with O8 inhibitor (**Figure 4.13**). This suggests that the breaks prevented by OGG1 inhibition correspond to the same class prevented by NAC treatment. Thus, the formation of endogenous breaks in S phase after oxidative stress could be mainly caused by 8-oxoG.

The induction of replication-dependent DSBs after H_2O_2 treatment required the formation of a SSB by BER. To test whether this also affected the formation of endogenous breaks, olaparib was used. The treatment with olaparib resulted in an increase in γH2AX foci numbers (**Figure 4.13**). It can be concluded that SSBs generated during BER can lead to DSBs during replication, especially if they persist. Investigation with the PLA assay have additionally confirmed the increased occurrence of replication-transcription conflicts after H_2O_2 treatment and identified them as the cause of break induction (**Figure 4.6**). Since inhibition of replication was not possible for the EdU/BrdU double labeling approach, only the effect of transcriptional inhibition could be tested. A comparable reduction of the γH2AX foci numbers to the inhibition of OGG1 could be obtained (**Figure 4.13**). This confirmed that the same

processes involved in the S-phase-specific induction of DSBs after H_2O_2 are also responsible for the formation of endogenous breaks.

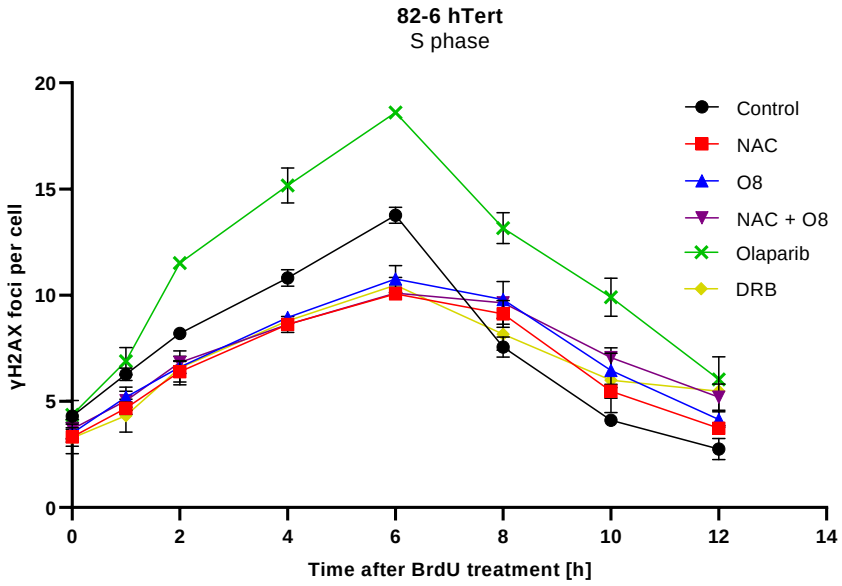

Figure 4.13 Formation of endogenous breaks in S phase and their dependence on different cellular processes
82-6 hTert cells were treated for 1 h with EdU, followed by 2 h with BrdU. If indicated, treatment with inhibitors for 3 h (DRB) or 1 h (NAC, O8, DRB, and olaparib) occurred simultaneously with EdU/BrdU treatment. Cells were then fixed at different time points and staining with anti-γH2AX and anti-BrdU antibodies, as well as DAPI and EdU labeling followed. Samples were subsequently scanned using Metafer software and analyzed for their γH2AX foci levels. For each individual experiment, 40 $EdU^-/BrdU^+$-cells were scored per time point. Mean ± SEM (n=3).

In summary, by using the EdU/BrdU double labeling assay, it was shown that DSBs induced by H_2O_2 mainly arise during early S phase when replication of actively transcribed regions takes place. In addition, EdU/BrdU double labeling also revealed a dependence on transcription and BER for this H_2O_2-induced DSBs. Interestingly, this approach also demonstrated the formation of endogenous DSBs and their partial dependency on the same processes. Thus, the break formation in dependency of replication, transcription, and BER also occurs in untreated cells without H_2O_2 treatment.

5 Discussion

The preservation and safe transfer of genetic information is an essential survival process of every living being. However, DNA, as the carrier of this information, is exposed to a variety of damages, which is why specific repair processes have evolved. Oxidative stress, for example, possesses a constant threat to genomic integrity. DNA damage induced by ROS is diverse and insufficient repair can have severe consequences for an organism, such as cancer development or cell death. Surprinsingly, the results of this work demonstrate that the repair processes of relatively common DNA lesions induced by ROS, oxidative base modifications, have the potential to cause far more deleterious lesions: DSBs.

The work presented in this thesis is based on research findings by *Ensminger et al. 2014*. There, it was shown that base modifications induced by the methylating agent MMS lead to the S-phase specific induction of DSBs (Ensminger et al., 2014). However, oxidative base modifications, due to the presence of ROS, occur more frequently and represent one of the most common damages in our genome (Marnett, 2000). For this reason, the aim was to establish a treatment that primarily induces oxidative base modifications, to better reflect the physiological damage profile. Subsequent studies were designed to determine whether these base modifications could also lead to the formation of DSBs as defined by *Ensminger et al. 2014*. Furthermore, it was important to keep the level of additionally induced DNA lesions low, as ROS in high concentrations also lead to the induction of direct DSBs. For this purpose, the peroxide H_2O_2 was used, which is a widely used agent for the induction of oxidative stress. Previous studies of this research group already demonstrated that treatment with H_2O_2 in the range below 500 μM barely contributes to the formation of direct DSBs (Löbrich et al., 2010). Other studies have also shown the γH2AX inducing effect of H_2O_2, but these were performed without considering the cell cycle and the associated effects of S phase (Li et al., 2006; Ye et al., 2016). Therefore, starting from this knowledge, different concentrations of H_2O_2 were used and their DSB-inducing potential was investigated.

5.1 The replication process is involved in the formation of DSBs after H_2O_2 treatment

Treatment with H_2O_2 resulted in the formation of DSBs mainly in the S phase of cell cycle (**Figure 4.1**). A much lower induction of DSBs was observed in both G1 and G2 phases, arising particularly at an early time point of 15 min and at higher H_2O_2 concentrations. However, since the number of DSBs is significantly lower than in S phase, it can be concluded

that H_2O_2 can induce S-phase specific DSBs. The fundamental difference between the gap phases and the synthesis phase is the duplication of DNA. This process of DNA replication defines the S phase and has been the subject of research in numerous studies investigating genome instability (Gadaleta and Noguchi, 2017; Kaushal and Freudenreich, 2019; Zeman and Cimprich, 2014). Since the very stable and protective form of the DNA double helix structure must be opened for the purpose of replication and is duplicated via a complex process, there is a constant risk of compromising the structure of the DNA. Even relatively common DNA lesions such as base modifications and SSBs can thereby interact with the replication fork, leading to replication fork collapse and thus DSBs. Although it is known that oxidative stress can lead to the formation of oxidative base modifications and SSBs, studies on S-phase specific induction of DSBs and investigations of the underlying mechanism are lacking. Interestingly, inhibition of replication in the approaches used in this work resulted in a partial reduction of induced DSBs in S phase. Both the number of γH2AX foci and the amount of DNA obtained by a γH2AX-ChIP were reduced, suggesting a direct involvement of the replication process in the induction of DSBs after H_2O_2 treatment in S-phase cells (**Figure 4.3** and **Figure 4.10)**. Furthermore, the involvement of replication can also explain the recorded increase in DSBs several hours after H_2O_2 treatment. Persistent DNA lesions can interact with the replication process even after H_2O_2 was removed and contribute to the induction of replication-dependent DSBs. This proved that a specific class of DSBs is induced in S phase after H_2O_2 treatment that is directly dependent on replication, demonstrating the importance of the cell cycle for DSB induction.

DSBs that arise specifically in S phase are usually one-ended breaks that lack the second break end. This is due to the replication process, which can convert a SSB into a DSB end by ongoing synthesis or is caused by a collapse of the replication fork (Zeman and Cimprich, 2014). Replication is terminated at this point and the second end, until it is generated by an adjacent replication fork, is missing for ligation by end-joining processes. If the repair of the break end would be performed via the c-NHEJ pathway, this could have serious consequences, as the absence of the second break end would lead to a ligation of two mismatched ends. As recently shown by our group, HR deficient cells delay repair of one-ended breaks even until mitosis (Llorens-Agost et al., 2021). This allows for the presence of the second break end, and the additional condensation of chromatin leads to the juxtaposition of ends, resulting in a lower incidence of chromosomal aberrations for repair via end-joining processes. Consequently, one-ended DSBs are a hallmark of S-phase specific breaks and require repair via HR for error-free re-ligation. The classical pathway that is considered to repair one-ended DSBs is BIR (Ensminger and Löbrich, 2020). Here, the open break end performs strand

invasion as known from repair via the dHJ or SDSA pathway. Due to the lack of a second break end, the synthesis of new DNA can now proceed to the end of the chromosome or until another replication fork is encountered. However, studies in this laboratory have also revealed an alternative way to repair such one-ended breaks. Here, the repair process of HR is initiated but repair is not proceeded and finished until late S phase or upon entry into G2 phase, ensuring that the sister chromatid is available for repair by HR via dHJ or SDSA (Spies et al., 2016). This could counteract the BIRs high error-proneness and allow repair via an error-free mechanism.

As the results from **Figure 4.2** show, the H_2O_2-induced breaks in S phase are repaired exclusively via HR. By inhibiting the HR core component RAD51, an almost complete suppression of the break repair in S phase was achieved. Thus, as breaks in S phase must be repaired via the HR process, it is reasonable to assume that one-ended DSBs are formed after H_2O_2 treatment. In agreement with the previous results, there is a steady increase in γH2AX foci until approximately 4 h after H_2O_2 treatment, indicating break induction by the replication process, which can lead to the formation of DSBs even several hours after H_2O_2 treatment. After a repair time of 4 h, the number of γH2AX foci in the S phase starts to decrease. This might be related to the transition from the S phase into the G2 phase and could support the idea that the DSB repair is not finished until G2 phase entry. In summary, the formation of H_2O_2-induced DSBs in S phase was shown to be replication-associated and HR dependent, representing a similar induction mechanism as described by *Ensminger et al. 2014*.

5.2 The transcription machinery collides with replication after H_2O_2 treatment

By treatment with MMS, it was shown by *Ensminger et al. 2014* that the S-phase specific induction of DSBs is dependent on the formation of SSBs (Ensminger et al., 2014). Here, it was assumed that the replication fork encounters a SSB induced by the BER process leading to a so-called replication fork run-off. This model of break induction has also been postulated for the inhibition of Top1 by CPT (Strumberg et al., 2000). However, it remains questionable whether the replication process has no efficient control mechanism for the occurrence of a SSB to avoid deleterious break formation. It is well known that oxidative base modifications and SSBs are the most frequently occurring lesions in the genome (Epe, 1996; Marnett, 2000). Consequently, the replication fork must overcome a not inconsiderable number of SSBs each time the replication is initiated without inducing a DSB. Regardless of the idea that SSBs can cause S-phase specific breaks, increasing knowledge of the conflict between replication and transcription brought into play an additional component for the induction of

breaks in S phase (Bermejo et al., 2012; Prado and Aguilera, 2005). In this context, a negative effect on the unhindered progress of either replication or transcription, such as obstacles in the DNA, will cause the occurrence of collisions. For instance, it has been shown that under conditions of mild replication stress, there is an increased frequency of conflicts between replication and transcription (Helmrich et al., 2011). DNA lesions can also contribute to the formation of replication-transcription conflicts by, for example, providing a blockage of Pol II (Trautinger et al., 2005). Numerous studies have addressed the phenomenon of replication-transcription conflicts in recent years. These studies have repeatedly confirmed the occurrence of DSBs and demonstrated their involvement in chromosome instability (Domínguez-Sánchez et al., 2011). Thus, both the occurrence of DSBs at common fragile sites and DSB induction by overexpression of oncogenes has been shown to involve replication-transcription conflicts (Helmrich et al., 2011; Jones et al., 2013).

Interestingly, the results from **Figure 4.3** and **Figure 4.10** suggest that breaks induced by H_2O_2 are also transcription dependent. Inhibition of Pol II and the transcription process was able to reduce the formation of DSBs in S phase. This supports the idea that a specific class of breaks is induced in S phase that depends on transcription in addition to replication. Moreover, epistasis analysis confirmed that both processes together are needed for the formation of this class of DSBs (**Figure 4.5**). The interaction between replication and transcription was also demonstrated using the PLA and confirmed the observed effects. This technique has been established in recent years as a method to detect replication-transcription conflicts (Hamperl et al., 2017; Sanchez et al., 2020). The results in this work show that increased conflicts occur in S-phase cells after H_2O_2 treatment (**Figure 4.6**). It should be noted that the maximum level of PLA foci was already detected 10 min after H_2O_2 addition. This is a clear indication that replication and transcription run into a state of conflict immediately after H_2O_2 treatment. This is also evident from the already high level of γH2AX foci immediately after H_2O_2 treatment (**Figure 4.1** and **Figure 4.2**). The rapid induction of γH2AX foci suggests that as a direct consequence of the conflict of replication and transcription DSBs are formed and, for example, replication forks arrested for a prolonged period of time do not initially contribute to DSB formation. Thus, it has already been shown that arrested replication forks do not lead to the formation of distinct γH2AX foci and that enzymatic processing into a DSB usually requires several hours (Ensminger et al., 2014; Petermann et al., 2010). The extent to which the conflict between replication and transcription can lead to the direct formation of a DSB is not yet fully elucidated. For instance, it is currently unknown whether both processes collide directly or are stopped ahead of time due to increasing torsional stress (García-Muse and Aguilera, 2016). However, in this regard,

further studies are needed to better understand the mechanism of the conflict between replication and transcription and to understand the process of break induction.
Additionally, inhibition of transcription or replication after H_2O_2 treatment results in reduced formation of PLA foci (**Figure 4.6**). This supports the idea that inhibition of the two processes alone does not lead to the formation of replication-transcription conflicts. This has already been demonstrated in previous studies (Hamperl et al., 2017; Sanchez et al., 2020). The appearance of additional structures such as R-loops or G-quadruplexes could be a crucial and supporting element for the formation of a conflict. For example, it has already been shown that the occurrence of R-loops results in a greater risk for break formation (Hamperl et al., 2017). Furthermore, studies of the process of replication in transcribed regions show that replication can dissociate Pol II from DNA (Pomerantz and O'Donnell, 2008). Transcription can subsequently be restarted, by the reassembly of transcription factors. However, this process is inhibited when a backtracked Pol II occurs, triggering the occurrence of conflicts (Nudler, 2012). These Pol II are prevented from progression over a prolonged time and co-occur with secondary structures such as R-loops, representing a replication-blocking obstacle.

5.3 BER has the potential to block Pol II after H_2O_2 treatment

Treatment with the H_2O_2 concentrations used in this work mainly induces the oxidative base modification 8-oxoG (Epe, 1996). However, an 8-oxoG is usually not an obstacle for any of the polymerases. Both transcription and replication can incorporate an adenine opposite to the 8-oxoG, contributing to point mutations. In the case of transcription, it has been shown that adenine is incorporated in 10 % of cases, leading to mutagenic transcripts (Brégeon et al., 2009). These lead to so-called transcriptional mutagenesis and can result in abnormal proteins that limit cell viability. However, this process has no blocking properties on transcription. In contrast, the research group led by Khobta was able to show that 8-oxoG is capable of blocking Pol II (Kitsera et al., 2011). It was confirmed that 8-oxoG itself does not block transcription, only the onset of BER converts the base modification into a transcription-blocking intermediate. In this process, the modified base must be recognized by the specific glycosylase OGG1 and removed from the DNA backbone. Thus, unhindered transcription was observed in OGG1-deficient mouse fibroblasts, whereas a functional OGG1 led to increased transcriptional blockages. It was hypothesized that 8-oxoG is converted to a BER intermediate by the function of OGG1, which blocks transcription.

The results obtained in this work support the hypothesis that transcription can be blocked by BER intermediates. It was shown that the induction of the majority of DSBs after H_2O_2 treatment was dependent on BER initiation by OGG1. Inhibition of OGG1 resulted in decreased DSBs in S phase and a lower amount of DNA detected in the γH2AX-ChIP, as validated by qPCR (**Figure 4.4** and **Figure 4.10**). Accordingly, retention of the oxidized base 8-oxoG in the DNA strand does not lead to DSB induction. However, if the base is removed by OGG1, the risk of a DSB induction is increased. Apparently, an intermediate of BER generated by OGG1 leads to a blockage of Pol II, which in turn can lead to a replication-transcription conflict. This is also demonstrated by the decreased frequency of replication-transcription conflicts after OGG1 inhibition as measured by PLA (**Figure 4.6)**.

For both transcriptional block by 8-oxoG and DSB induction after MMS treatment, SSBs generated during BER were considered to be implicated (Ensminger et al., 2014; Kitsera et al., 2011). Also in this work, S-phase specific DSBs after H_2O_2 treatment were shown to be dependent on the formation of SSBs. This was achieved by experiments using a PARP1 specific inhibitor. Inhibition of PARP1 prevents repair of SSBs and leads to accumulation of unrepaired SSBs (Murai et al., 2014). Under these circumstances, a strong increase in γH2AX and PLA foci, as well as an increase measured by qPCR, was observed (**Figure 4.4, Figure 4.6,** and **Figure 4.10**). As in the previous studies, SSBs represent the key intermediate leading to DSB formation and transcriptional blockade in this case.

To what extent this effect is solely due to SSBs generated by BER is difficult to assess. Inhibition of PARP1 also prevents repair of directly generated SSBs, since repair occurs by the same mechanism at the moment the DNA backbone is broken (Caldecott, 2007; Fisher et al., 2007). In addition, there are studies stating that a SSB alone can lead to a transcription block (Kathe et al., 2004). However, it should be noted that in this study the blocking effect of Pol II was only observed when the SSB was present on the transcribed strand. Whether this Pol II can in turn block replication or can be removed by it remains unclear. Further studies on transcriptional blocking by the 8-oxoG/BER process revealed a direct dependence on the activity of OGG1 and that it did not matter whether the lesion occurred in the transcribed or non-transcribed DNA strand (Allgayer et al., 2013). This suggests a more complex structure leading to blocking of transcription, which could also promote the occurrence of conflicts. Interestingly, treatment with MMS has no such effect after inhibition of transcription. In the course of a bachelor's thesis, no reduced induction of DSBs after MMS could be demonstrated for inhibition by DRB (Bachelor thesis Johanna Ertl). One reason for this could be the different processing of the breaks via the specific glycosylases (Huffman et al., 2005; Jacobs and Schär, 2012). Damage by MMS is detected via the monofunctional N-methylpurine DNA

glycosylases. This glycosylase recognizes the base modifications and removes them. The DNA backbone is subsequently cut by APE1 to allow the insertion of a new nucleotide. In contrast, 8-oxoG is recognized and removed by the bifunctional glycosylase OGG1. This has an additional AP lyase activity that cuts the DNA backbone. Although APE1 is also required here, it is only needed to generate the 3'-OH end. Nevertheless, the break in the DNA backbone is already present. However, whether and to what extent this explains the different results must be further investigated and confirmed.

5.4 Induction of replication-independent DSBs after H_2O_2 treatment

The DSB inducing effect of H_2O_2 was assumed so far to be mainly related to the induction of direct SSBs. If two SSBs are induced on opposite strands of the DNA in close proximity this may lead to the break of the DNA backbone, resulting in a DSB (Bradley and Kohn, 1979). This process should generally be able to occur in all cell cycle phases, although ssDNA is more prone to such lesions and is more prevalent in S phase (Saini and Gordenin, 2020). However, unlike replication-associated breaks, these DSBs should also be repairable via c-NHEJ repair processes, given the presence of the second break end (Ensminger and Löbrich, 2020). The results from **Figure 4.2** would confirm this notion, since repair of DSBs induced in G1 and G2 occurred rapidly and was exclusively due to c-NHEJ processes. Inhibition of HR here had no effect on repair behavior after H_2O_2 treatment. Moreover, most DSBs were formed specifically in the cells of S phase, while the induction was lower in G1 and G2 phases. In general, DSB formation appeared to be different from the S-phase specific DSBs. No effects were observed in the gap phases of treatments with replication, transcription, or BER inhibitors, indicating a different process of break induction (**Figure 4.3** and **Figure 4.4**). This supports the idea that, to a certain extent, breaks can occur via a direct mechanism by H_2O_2.

Furthermore, a DSB inducing effect was suggested for OGG1, which is also supposed to take place via the occurrence of two SSBs in spatial proximity (Sharma et al., 2016). The damaging effect of OGG1 was explained by the induction of SSBs in clustered lesions generated by ROS. Here, different DNA lesions are produced in a short section of the DNA under which 8-oxoG could be one of them. If OGG1 removes the modified base from the DNA and incises the backbone a SSB is induced. This would be a comparable situation to directly induced SSBs, since multiple 8-oxoG could arise in the clustered lesion, including on opposing DNA strands. However, other results show that OGG1 has greatly reduced activity in DNA regions that have an increased number of additional lesions such as mismatches, AP-sites, or SSBs (David-Cordonnier et al., 2001; Sassa et al., 2012). This is thought to suppress the

induction of DSBs by the activity of OGG1 in nearby base modifications on opposite DNA strands. This characteristic is in a better concordance with the results obtained in this work. Here, it is shown that inhibition of OGG1 has no effect on the formation of γH2AX foci in G1 or G2 phase (**Figure 4.4**). If the breaks would occur in regions of clustered lesions depending on OGG1 activity, this should also reduce DSB formation in G1 and G2 phases, as these DSBs could occur in all cell cycle phases. Accordingly, it can be assumed that replication-independent breaks can occur via a direct mechanism, whereas a specific class of DSBs is formed in S phase when replication and BER interfere.

5.5 H_2O_2-induced DSBs are located in actively transcribed regions of the genome

The results on DSB induction after H_2O_2 treatment in S-phase cells revealed a process characterized by the involvement of replication and transcription. Accordingly, break induction should only be able to take place in regions of actively transcribed genes. Gene regions generally have an increased risk for the induction of DNA damage, including DSBs, due to their open chromatin structure. Several studies demonstrate that transcription start sites, promoter regions, and gene bodies are particularly prone to DSB formation (Amente et al., 2019; Wei et al., 2016). These studies become possible by the development and continuous optimization of next-generation sequencing technologies. In these, millions of short DNA fragments are sequenced and the information obtained is bioinformatically processed, allowing an accurate map of the occurrence of proteins or DNA alterations at whole-genome scale. Therefore, for the studies performed in this work, the method of ChIP-Seq was established in our laboratory (**Figure 4.8**). Here, chromatin immunoprecipitation against the target protein γH2AX was combined with massive parallel sequencing of the obtained DNA fragments. This allowed for the detection of genomic regions with enriched γH2AX and thus sites of break induction.

With this approach it was possible to detect a correlation between the transcription rate and the occurrence of γH2AX in H_2O_2 treated cells, as shown in **Figure 4.9**. The regions with a higher rate of RNA-Seq signal also had more DNA precipitated with γH2AX antibody. This correlation was even more evident once the regions were grouped according to their RNA-Seq signal. In this case, the group of regions that possessed the highest signal in the ChIP-Seq approach also had the highest RNA-Seq signal. These results are supported by qPCR experiments in which primers were designed based on sequencing results (**Figure 4.10**). Here, an increased level of precipitated DNA is shown after H_2O_2 treatment in regions with an increased transcription rate. In comparison, regions with low transcription rates do not show

increased precipitated DNA levels. These results could confirm that the breaks after H_2O_2 treatment occur mainly in actively transcribed regions of the genome.

However, as previously described, euchromatic regions are inherently more susceptible to the induction of a DSB. Thus, the results obtained by H_2O_2 treatment could also simply reflect the natural damage profile of cells instead of representing any specific damage dependency. This notion, however, is contradicted by results optained in the Artemis-deficient cell line Callum Jones hTert that was used in the course of establishing the ChIP-Seq. These are deficient in the resection-dependent repair of the c-NHEJ, therefore showing a repair defect. Artemis-dependent breaks are thought to occur mainly in heterochromatin and thus in transcriptionally inactive regions (Löbrich and Jeggo, 2017). **Figure 6.1** in the appendix shows a sequencing experiment of this cell line 3 days after break induction by X-rays. The breaks remaining after 3 days are those dependent on Artemis and as can be seen, the profile shows an inverse behavior compared to the H_2O_2 treated 82-6 hTert (**Figure 4.9**). The remaining breaks are found in transcriptionally inactive regions of the genome, confirming the detection of additionally generated breaks for this method. This proved the general validity of the analysis used.

In the context of oxidative stress, it has become common in recent years to detect the established marker 8-oxoG in the genome. This has revealed a correlation with those regions that also exhibit an increased risk for the formation of breaks. Thus, 8-oxoG was shown to be more abundant in regions of common fragile sites but also in regions with increased GC content and active Pol II (Amente et al., 2019; Gorini et al., 2020). Gene regions generally have higher levels of guanines and cytosines than the rest of the genome. Distributed over the entire genome, approximately 41 % of all bases occur as GC (Lander et al., 2001). A closer examination of three regions from the group of the most highly transcribed regions in this work revealed an average GC content of 53.7 % (**Figure 4.9**). This is clearly above the average and can be explained by regulatory elements such as CpG islands or G4 quadruplexes, which occur more frequently in gene regulatory regions. This is further supported by the number of genes in these regions, which is 32.7 genes per 0.5 Mbp, well above the average of about 7 genes per 0.5 Mbp (Pertea et al., 2018). Furthermore, an equal number of regions from a group with low transcription were found to have an average GC content of 40 % and a decreased gene density of only 4 genes per 0.5 Mbp. Thus, the regions of increased break induction described above are in a region of high gene density, high GC content, and high transcription rate. These are also the regions which have been associated with increased levels of 8-oxoG in recent studies (Fang and Zou, 2020; Gorini et al., 2020). Oxidative stress and the

formation of 8-oxoG is thus directly related to the formation of breaks in gene regions that are susceptible to break induction.

In general, actively transcribed domains of the genome are the first regions that are replicated in S phase. This is related to the open chromatin structure that is more easily accessible for replication initiation factors (White et al., 2004; Woodfine et al., 2004). In a recently published study of this group, the method of EdU/BrdU double labeling was presented, which allows to distinguish the S phase sub-populations more precisely and to follow its progression (Llorens-Agost et al., 2021). By combining the two thymidine analogs, it is possible to define an early S phase population and to follow its progression through the synthesis phase. This allows for a more accurate evaluation of the different S phase stages and their involvement in DSB induction.

This method confirmed the previously obtained evidence of γH2AX foci induction in S phase by treatment with H_2O_2. For these breaks, like before, a dependency on transcription as well as BER could be confirmed (**Figure 4.12**). Interestingly though, was that treatment with H_2O_2 revealed a specific progression of γH2AX foci induction. For example, the biggest increase in foci numbers was observed directly in the first 2 h after treatment, whereas only a smaller increase is observed at later times in S phase. Further investigations showed that H_2O_2 treatment at later stages of the S phase had a significantly reduced potential for γH2AX foci formation (**Figure 4.11**). Accordingly, it can be assumed that the breaks induced by H_2O_2 mainly occur at an early time point of the S phase. This again confirms the assumption that the DSBs studied in this work occur in actively transcribed regions that are also replicated at the beginning of S phase. Interestingly, a class of fragile sites has been identified in recent years that, contrary to common fragile sites, are located in gene clusters and are replicated in early S phase. Because of these properties and the localization near origins of replication, these regions have been named early replicative fragile sites (Barlow et al., 2013). In addition, these early replicative fragile sites occurred in regions of the genome that had elevated levels of GC as measured by CpG islands. It is also assumed here that there may be a conflict between replication and transcription that results in the formation of a DSB. Since the DSBs induced after H_2O_2 treatment also arise in regions of active transcription at the beginning of S phase, the breaks observed in this study may be consistent with the DSBs induced after H_2O_2 in this work.

Ideally, the detection of breaks induced by H_2O_2 would not only be limited to chromatin regions of active transcription, but also to the region of gene bodies. Unfortunately, the sequencing results presented in this work could not provide a more precise indication of the localization of the breaks. This may be because γH2AX represents a very broad signal around

the break. H2AX is phosphorylated in a region of approximately 2 Mbp around the break site. The result is not a sharp peak of DNA fragments at the break but broad signals that attenuate away from the break site. In addition, treatment with H_2O_2 creates an individual damage profile in each cell that is different from a profile of an enzyme-induced break as seen by the DIvA cell line (**Figure 4.8**). Thus, each cell is expected to have DSBs generated at different locations in the genome. As a result, it is not possible to define break sites on the specific genome location but only higher-order regions with similar properties. With the emerging establishment of new methods to identify the regions of breaks in the genome, the accuracy of the results obtained is constantly improving. Methods that can visualize the break site at the nucleotide level are becoming increasingly available, but they usually have a high degree of specificity, which means that they are not always suitable for every application (Rybin et al., 2021).

5.6 Interplay between replication, transcription, and BER is needed for the S-phase specific induction of DSBs

Both by analysis of γH2AX foci and qPCR results, a similar response to inhibitor treatment after H_2O_2 was observed (**Figure 4.3, Figure 4.4**, and **Figure 4.10**). The inhibition of replication by aphidicolin, transcription by DRB, as well as BER by O8 all resulted in a decrease in the number of DSBs. In contrast, more DSBs were detected after inhibition of PARP1 using olaparib. Moreover, the results obtained by PLA assay could demonstrate the same dependence for the occurrence of replication-transcription conflicts (**Figure 4.6**). These outcomes led to the assumption that all three processes are involved in the same mechanism of break induction. This is supported by the analysis of the inhibitors used in a combined treatment, which did not have an additive effect at the γH2AX foci level (**Figure 4.5**). Any combination of replication, transcription, and BER inhibition resulted in a reduction, as did single inhibitor treatments. The opposite behavior was again obtained by inhibition with the PARP1 inhibitor olaparib. Here, inhibition led to an increase in detected breaks. The effect by PARP inhibitor could be reversed by co-inhibition. Interestingly, not quite the same extent of reduction was achieved as in the experiments without olaparib. As previously discussed, inhibition of PARP1 also impairs repair of directly induced SSBs (Caldecott, 2007; Fisher et al., 2007; Murai et al., 2014). The accumulation of SSBs could lead to an increased risk of inducing a DSB in S phase, which in turn is not dependent on replication progression, transcription, and BER. How exactly this process may occur remains unanswered from the results obtained in this work and requires more detailed investigations.

It is also striking that individual or combined inhibition of any of the three processes never reduces the number of γH2AX foci, as well as the qPCR results, to the control level (**Figure 4.3, Figure 4.4**, and **Figure 4.10**). However, the breaks that remain unaffected by inhibition appear to arise specifically in S phases since these breaks do not occur in either G1 or G2 phase (**Figure 4.2, Figure 4.3**, and **Figure 4.4**). One way to explain this is that these breaks occur at single-stranded regions of the replication fork. Thus, these ssDNA regions are particularly susceptible to the induction of lesions such as SSBs (Saini and Gordenin, 2020). If a SSB is induced in the ssDNA of a replication fork, this would lead to the formation of a one-ended DSB as replication is terminated and collapses. As can be seen from the results in **Figure 4.2**, all S-phase specific breaks are repaired via HR after H_2O_2 treatment. Repair via c-NHEJ would now only be possible via the ligation of two mismatched ends and consequently repair via HR would be the error-free option. Inhibition of replication by aphidicolin in this case would also have no reducing effect. Aphidicolin inhibits the activity of polymerase α and δ, but not the formation of replication forks. Thus, these could form despite aphidicolin treatment, thereby maintaining susceptibility to break induction. Moreover, the results obtained in this work suggest direct SSB induction to be responsible for this process. Involvement of secondary SSBs generated, for example, by OGG1 activity can be excluded by the results of OGG1 deficient cells and OGG1 inhibition (**Figure 4.4**). If such secondary SSBs were involved, they could no longer be generated under inactive OGG1 conditions and, consequently, such conditions would have to lead to a reduced induction of DSBs to control levels. Such a reduction could be demonstrated neither in OGG1 deficient cells nor by O8 treatment. In addition, greatly reduced activity of OGG1 in regions of ssDNA in, for example, secondary structures has been proven to counteract the generation of cytotoxic secondary damage, indicating that OGG1 has no role in the induction of these DSBs (Jarem et al., 2009; Kirpota et al., 2011; Rhee et al., 2011).

In contrast, replication, transcription, as well as BER have the same impact on the break induction of a specific class of breaks in S phase. Thus, the model for the induction of these breaks could be as follows (**Figure 5.1**). The base guanine is oxidized by ROS and an 8-oxoG is formed. This is recognized and removed by the specific glycosylase OGG1, initiating the BER process. A SSB is generated representing the BER intermediate that has the potential to block transcription. The process of Pol II backtracking may now present an obstacle to the pregression of replication, resulting in a replication-transcription conflict. The result is the formation of a DSB that is dependent on all three processes. The exact process that ultimately leads to the formation of the DSB is still unclear. Various possibilities, such as replication fork run-off, collapsed replication fork, active induction of a DSB to resolve the conflict, are

generally possible. Based on the results obtained in this work that DSB formation occurs directly after H_2O_2 treatment, the possibilities such as an enzymatic processing would be less likely and argue for a direct induction of the breaks. Nevertheless, further investigations are necessary to describe the process of break formation in more detail.

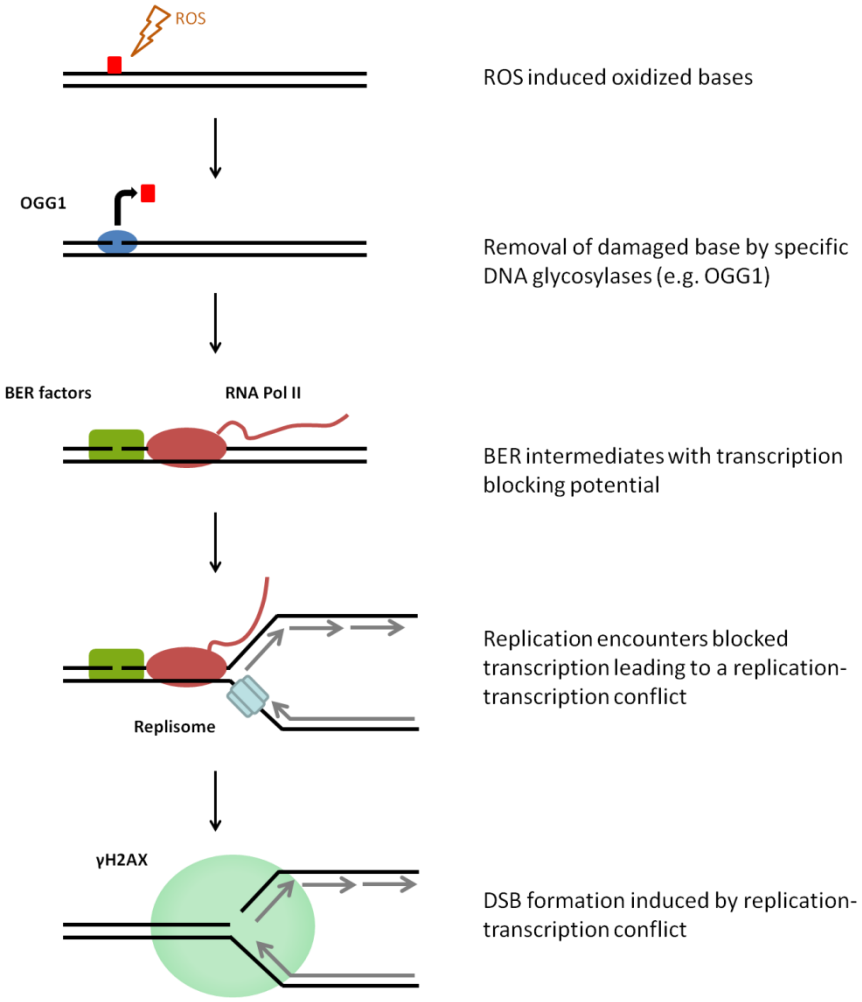

Figure 5.1 Model for the S-phase specific induction of DSBs after oxidative stress
Oxidative base modifications are generated in the DNA by ROS reactivity and recognized via specific glycosylases. Removal of the modified base by glycosylases initiates repair via BER. The processes of BER generates a SSB, which in turn has the potential to block transcription. Stalled transcription can lead to a conflict with replication, resulting in the conversion to a DSB.

This mechanism for DSB induction by ROS differs from the induction of other S-phase specific DSBs. In this work, it could be shown that no dependence on transcription or BER prevails by treatment with CPT (**Figure 4.7**). Only the already known dependence on replication was confirmed. DSB induction by CPT is commonly assumed to be a process of replication fork run-off (Strumberg et al., 2000). This process was initially also assumed for induction after

MMS treatment (Ensminger et al., 2014). However, in this work, the component of transcription and the associated replication-transcription conflicts were additionally linked to DSB induction by ROS. Thus, the formation of one-ended DSBs after oxidative stress and CPT rely on distinct processes.

5.7 The mechanism of break induction after H_2O_2 is present in unperturbed cells

The mechanism described above seems to be an adverse concatenation of several processes that have a crucial function for survival. This mechanism is triggered by the repair of an oxidative base modification via BER, resulting in a deleterious DSB. Interestingly, a basic level of oxidative base modifications is already present in every cell of our body. These are generated by ROS which are mainly by-products of the metabolism. For example, a study that considered multiple detection methods and sample origins found an average value of 0.3 to 4.2 8-oxoG per 10^6 guanines in healthy men between the age of 20 and 30 years (Gedik and Collins, 2005). With a human genome size of 3.2 billion bp, this results in a background level averaging approximately 3,000 8-oxoG in the DNA of each cell. It is estimated that the number of base modifications that occur daily in a single cell is well over 10,000, requiring constant repair by the BER mechanism (Lindahl, 1993). For this reason, it is an important question whether the previously described mechanism of DSB formation could also occur in untreated cells.

By using the previously described EdU/BrdU double labeling approach it was possible to follow an early S phase population during its progression through S phase and to asses endogenously arising DSBs. The results showed a steady increase in DSBs over the course of S phase (**Figure 4.13**). The detected γH2AX foci peak at 6 h, followed by repair of the induced DSBs. This progression is explained by the duration of the S phase and the subsequent transition into the G2 phase as confirmed by PCNA staining (**Figure 4.11**). This repair behavior has been seen in different studies in this group and confirm the aforementioned idea that the repair of one-ended breaks is not finished until G2 entry (see discussion in section 5.1). As a consequence, also endogenous breaks arising in a replication-dependent manner can accumulate during S phase and are not repaired until they are in G2 phase.

Besides that, it is already known that a higher level of endogenous breaks prevails during S phase. This is mostly attributed to the DNA processing mechanisms of topoisomerases (Tubbs and Nussenzweig, 2017). Topoisomerases specifically induce SSBs and DSBs to reduce the torsional stress that occurs during replication. However, DNA damaging sources, such as

ROS, can also have more severe effects in S phase, as increased secondary structures and ssDNA are formed that are more susceptible to DNA damage induction (Saini and Gordenin, 2020). As shown in the results of **Figure 4.13**, treatment with the antioxidant NAC had a reducing effect on endogenously arising γH2AX foci. Treatment with NAC reduces the level of ROS and thereby the prevailing oxidative stress. Oxidative stress is thus an essential contributor to endogenously occurring breaks during S phase progression, which may also explain the mutagenic effect of ROS. As mentioned before, 8-oxoG is the most abundant base modification occurring in the context of oxidative stress (Epe, 1996). In addition, a study showed that not only oxidative stress, but also the occurrence 8-oxoG increased during S phase, implying its role in endogenously arising DNA damage (Baquero et al., 2021). To verify the involvement of 8-oxoG for endogenously generated DSBs in S phase, undamaged cells were examined with the inhibitor against OGG1. As shown in **Figure 4.13**, inhibition of the 8-oxoG-specific glycosylase OGG1 resulted in a strong reduction of endogenously formed γH2AX foci. A reduction almost similar to that observed with treatment with the antioxidant NAC was observed. From these results, it can be concluded that the oxidative base modification 8-oxoG is the primary oxidative lesion responsible for the endogenously occurring DSBs in S phase. In this context, 8-oxoG seems to play a key role for the induction of endogenous breaks, confirming the importance for the outcomes of oxidative stress induced effects.

Interestingly, a screening approach on genes involved in genome stabilization revealed that processes involved in transcription processing are one of the main groups preventing DSB formation (Paulsen et al., 2009). Here, downregulation of the genes observed resulted in an increase of endogenous H2AX phosphorylation. Additionally, these functions were connected to the processing of R-loops, showing the relevance of transcription processes for the occurrence of endogenous DSBs. In this work, an inhibition of transcription led to a similar reducing effect on the formation of endogenous γH2AX foci as shown previously (**Figure 4.13**). This confirms the involvement of transcription observed by the EdU/BrdU double labeling approach and thereby by the same processes as demonstrated for H_2O_2 treatment. Accordingly, breaks are also generated in untreated cells during S phase, which are dependent on transcription as well as BER. It can therefore be assumed that the previously described mechanism also leads to the formation of endogenous DSBs.

5.8 Cancer and the contribution of oxidative stress

Oxidative stress is associated with a whole range of diseases, with different mechanisms and responses contributing to their development (Pizzino et al., 2017; Rajendran et al., 2014). One example is the mutagenic effect of ROS in the development and promotion of cancer. An accumulation of mutations is an essential step for the tumorigenic process (Hao et al., 2016). In this context, the discovery of the so-called oncogenes is of particular importance (Nenclares and Harrington, 2020). These genes, when constitutively activated by a mutation, have the potential to promote the fate of a cell towards a cancer cell. Examples of these oncogenes include cyclin E, RAS, or c-Myc. Interestingly, the reason for the tumor-promoting effect of these genes is often associated with a deregulation of replication. This results in chromosomal aberrations associated with the occurrence of replication-transcription conflicts (Jones et al., 2013; Kotsantis et al., 2016). In addition, cancer cells generally have elevated levels of ROS, which is due to the deregulated metabolism of the cells (Perillo et al., 2020). All these points suggest that elevated ROS levels as well as deregulated replication and transcription pose an increased risk for the occurrence of replication-transcription conflicts, as in the model proposed in this work. Since it is important for cancer cells to accumulate mutations, the previously described mechanism could contribute to the development of cancer in two ways. One way is by generating initial mutations in oncogenes, which subsequently promote the formation of cancer cells, and another way is by triggering further mutations in already deregulated cells. Interestingly, the results in this work were obtained predominantly in somatic cells. Thus, the occurrence of these breaks cannot be solely attributed to increased ROS levels or abnormal replication/transcription as prevalent in cancer cells. Still, an increased number of DSBs was detected in S-phase cancer cell lines after H_2O_2 treatment compared with 82-6 hTert cells (**Figure 4.1**). This supports the idea that in cancer cells in general there is an increased risk for the occurrence of replication-transcription conflicts and DSBs under the previously discussed aspects. However, this process may occur in all replicating cells and thus contribute significantly to mutagenesis and carcinogenesis.

In addition, the increased ROS level in tumor cells compared to the healthy cells of a body opens up new strategies in cancer therapy. In this context, a specific approach concerning the occurrence and repair of 8-oxoG is elaborated. As previously described, the cellular protection system consists of three enzymes, with MTH1 responsible for removing 8-oxod-GTP from the DNA pool (see section 2.2). As shown by a study, inhibition of MTH1 leads to an increased number of 8-oxoG in the DNA, as 8-oxod-GTP is no longer removed from the DNA pool (Gad et al., 2014). Surprisingly, normal cells remained unaffected by this intervention, whereas an

increased mortality rate was demonstrated in cancer cells. It was shown that due to the increased ROS level in tumor cells, the number of incorporated 8-oxoG is also significantly higher, resulting in a DNA-damaging effect. A recently published study showed that the deleterious effect of MTH1 inhibition can be reversed by co-inhibition of OGG1 (Zhang et al., 2021). It was hypothesized that the glycosylase function of OGG1 is required for the DNA-damaging effects. An increased DSB formation with the mechanism for S-phase specific break induction presented in this work would explain the results. As mentioned earlier, tumor cells possess an increased proliferation rate in addition to an increased ROS level. Inhibition of MTH1 increases the number of 8-oxoG in DNA and the occurrence of replication-transcription conflicts could increase in an OGG1-BER-dependent manner. Various inhibitors against MTH1 are currently being investigated for their potential cancer-killing effects, highlighting the relevance of oxidative stress and associated DNA damage to cancer development and therapy (Berglund et al., 2016; Zhou et al., 2019).

5.9 Outlook

In this work, a new mechanism for S-phase specific break induction was presented, which is triggered by the base modification 8-oxoG, frequently occurring in our genome. In this process, the oxidized base is recognized and removed by the specific glycosylase OGG1 and initiates repair via BER. The repair intermediate involves a SSB which has transcriptional blocking potential and, in turn, leads to replication-transcription conflicts resulting in the conversion of a simple base modification into the far more dangerous DNA lesion of a DSB.

Although the results of this work suggest a conflict between replication and transcription as a trigger of break induction, there are still some open questions to be answered. For example, it is still unclear to what extent secondary structures are involved in the process of break induction. As several studies have already shown, these secondary structures in the dissociated DNA strand of a transcription bubble are able to stabilize stalled Pol II and are also increasingly found at the sites leading to DSBs (Domínguez-Sánchez et al., 2011; Skourti-Stathaki et al., 2011). Studies revealing the occurrence of R-loops or G4-quadruplexes could provide insight into whether they are also involved in break induction in this case. Furthermore, it is unclear what the directionality of the replication-transcription conflicts is. Although previous studies saw more severe consequences associated with head-to-head collisions, now, there are several studies showing the occurrence of DSBs with co-directional orientation (Dutta et al., 2011; Hamperl et al., 2017). Here, blocked Pol II and the presence of secondary structures such as R-loops are mainly involved in break induction. The use of

constructs such as those utilized in *Hamperl et al. 2017* could allow a more detailed analysis of the directionality of the conflict and thus provide more precise information about the process leading to break induction.

This and other publications in the field of oxidative stress confirm the paradoxical situation that, for example, treatment with H_2O_2 makes the repair process of BER part of the induction of a much more toxic lesion, the DSB. When cells are exposed to elevated levels of ROS, the oxidized base modifications must be removed from the DNA to prevent the development of point mutations. Interestingly, multiple studies have investigated the occurrence of cancer in $OGG1^{-/-}$ mice showing no increase in cancer development (Klungland et al., 1999; Minowa et al., 2000). Thus, although these studies detected increased levels of 8-oxoG in DNA and point mutations by several folds, there was no higher tumorigenesis than in wild-type mice. The tolerance of both 8-oxoG and the resulting point mutations appears to be much higher than initially thought. In contrast, knock-out mice of the other two enzymes of the GO system, MUTYH and MTH1, showed increased tumorigenesis (Sieber et al., 2003; Tsuzuki et al., 2002; Xie et al., 2004). The crucial role of OGG1 was demonstrated by its overexpression, which led to increased mortality in mice. Further studies confirmed the DSB-inducing effect depending on OGG1, thus demonstrating the key function emanating from the glycosylase (Priestley et al., 2010; Wang et al., 2018). Although point mutations caused by 8-oxoG have long been considered as the primary force of mutagenesis, a mutational signature attributable to oxidative base modification has not been found in primary cancers or mitochondrial DNA (Helleday et al., 2014; Kennedy et al., 2013). For this reason, the question arises whether it is not the point mutation caused by 8-oxoG but the activity of OGG1 and the related DSB induction that is responsible for the mutagenic effects of oxidative stress.

Appendix

Table 1 Background subtracted values from Figure 4.3

	Control	Aphidicolin	Control	DRB	Control	Triptolide
G1	0.363	0.425	0.500	0.500	0.400	0.500
	0.475	0.325	0.300	0.375	0.375	0.475
	0.475	0.325	0.425	0.400	0.300	0.325
S	10.850	10.450	10.350	10.325	9.850	9.575
	10.225	9.225	9.925	10.050	10.100	9.150
	10.950	9.675	10.375	10.250	9.675	8.550
G2	2.347	2.175	1.175	1.100	1.525	0.950
	1.700	1.750	1.944	1.200	1.575	1.250
	1.053	1.725	1.053	1.175	1.150	1.705

Table 2 Background subtractes values from Figure 4.4

	MEF WT	MEF OGG1$^{-/-}$	Control	O8	Control	Olaparib
G1	2.744	2.550	0.488	0.425	0.300	0.325
	2.000	1.000	0.350	0.375	0.400	0.400
	2.200	2.000	0.325	0.350	0.325	0.325
S	24.800	23.842	9.925	10.450	9.350	10.075
	21.100	17.675	10.675	10.775	10.375	9.975
	29.850	19.075	10.650	10.175	10.175	10.325
G2	4.825	4.778	1.450	2.175	1.550	1.759
	4.700	5.010	2.075	1.950	1.400	1.450
	5.650	3.625	1.725	1.541	2.900	1.600

Table 3 Background subtractes values from Frigure 4.5

Control	Aph.	DRB	O8	Aph. +DRB	Aph. +O8	O8 +DRB	Ola.	Ola. +Aph.	Ola. +DRB	Ola. +OGG1
10.435	11.875	10.875	11.975	9.525	10.475	9.800	11.100	10.275	12.075	10.700
10.955	10.450	12.675	11.250	9.125	9.250	9.500	9.675	10.225	10.750	10.175
10.225	11.525	11.100	12.325	9.525	9.725	9.425	10.000	10.625	11.725	10.500

Table 4 Background subtractes values from Figure 4.6

Control	Aphidicolin	DRB	O8	Olaparib
1.000	0.975	1.225	1.000	1.475
1.075	1.025	1.300	0.900	1.350

Table 5 Background subtracted values from Figure 4.7

Control	Aphidicolin	DRB	O8	Olaparib
9.650	9.450	9.450	9.575	11.875
10.100	9.300	10.075	9.475	10.500
10.050	9.975	9.750	10.250	12.225

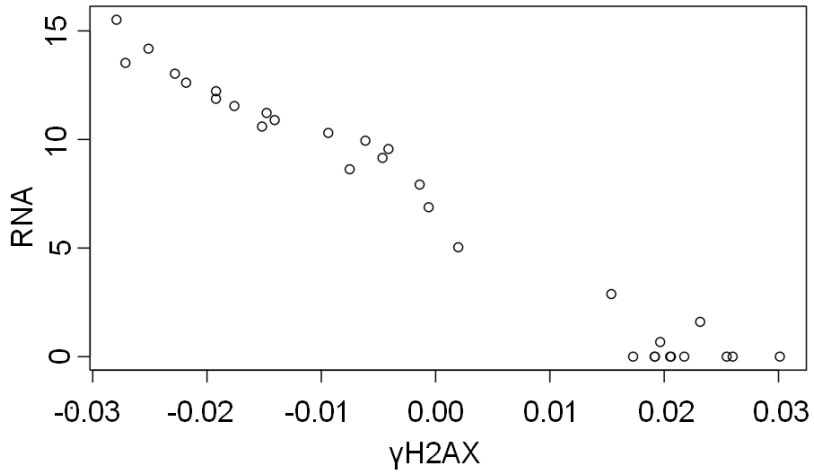

Figure 6.1 Sequencing Experiment of Callum Jones hTert cells.
For ChIP-Seq, Callum Jones hTert cells were irradiated with 20 Gy X-rays. After 3 days, the cells were fixed and lysed, followed by sonification to obtain 200 to 500 bp fragments. Pre-clearing with magnetic beads was followed by antibody incubation with anti-γH2AX overnight. After several washing steps, the samples were eluted and the DNA was purified on columns. Library preparation and sequencing of the purified DNA were performed at the IMB in Mainz. RNA isolation and RNA-Seq were performed by BGI Genomics. Plot of log2 values of RNA-Seq and ChIP-Seq results. The genome was divided into 0.5 Mbp sections. Datapoints represent 200 of the 0.5 Mbp windows combined according to the RNA-Seq signal.

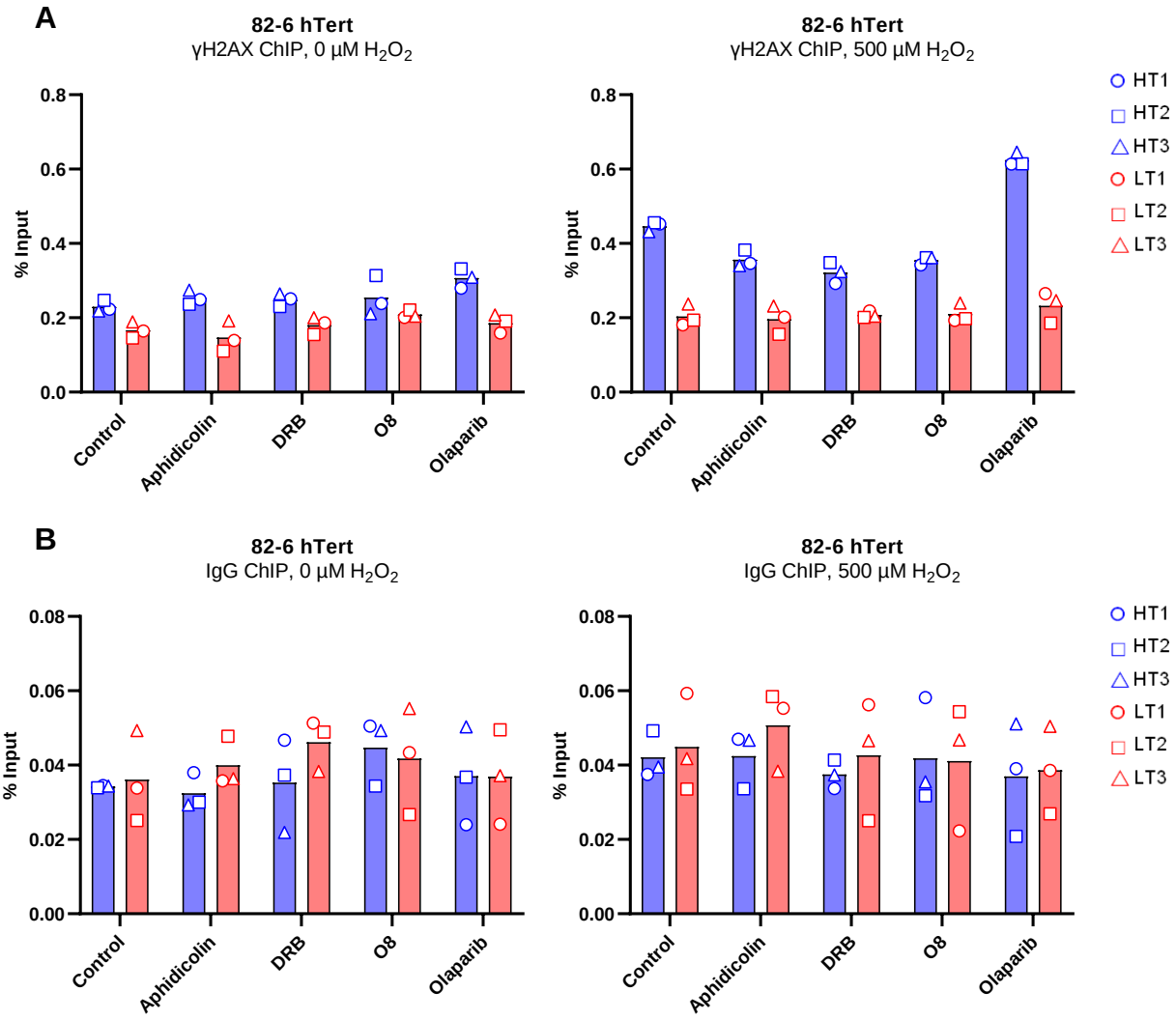

Figure 6.2 ChIP followed by qPCR of 82-6 hTert cells after H_2O_2 and inhibitor treatment
82-6 hTert cells were treated with inhibitors for 3 h (DRB), 1 h (O8, olaparib), or 30 min (aphidicolin). This was followed by damage induction with 500 μM H_2O_2 for 30 min. After 4 h, the cells were fixed and lysed. Afterwards sonification was performend to obtain 200 to 500 bp fragments. Pre-clearing with magnetic beads was followed by antibody incubation with anti-γH2AX or anti-IgG overnight. After various washing steps, samples were eluted and DNA was purified over columns. A qPCR was performed with different primers based on the sequencing results. (**A**) γH2AX ChIP of 0 μM and 500 μM H_2O_2 treated samples. (**B**) IgG ChIP of 0 μM and 500 μM treated samples to validate the specificity of ChIP. Mean of HT or LT primers (n=1).

References

Abraham, R.T., 2001. Cell cycle checkpoint signaling through the ATM and ATR kinases. Genes Dev. 15, 2177–2196. https://doi.org/10.1101/gad.914401

Akbari, M., Peña-Diaz, J., Andersen, S., Liabakk, N.B., Otterlei, M., Krokan, H.E., 2009. Extracts of proliferating and non-proliferating human cells display different base excision pathways and repair fidelity. DNA Repair (Amst). 8, 834–843. https://doi.org/10.1016/j.dnarep.2009.04.002

Akiyama, M., Maki, H., Sekiguchi, M., Horiuchi, T., 1989. A specific role of MutT protein: to prevent dG.dA mispairing in DNA replication. Proc. Natl. Acad. Sci. U. S. A. 86, 3949–52. https://doi.org/10.1073/pnas.86.11.3949

Alam, M.S., 2018. Proximity Ligation Assay (PLA). Curr. Protoc. Immunol. 123. https://doi.org/10.1002/cpim.58

Alfonso-Prieto, M., Biarnés, X., Vidossich, P., Rovira, C., 2009. The molecular mechanism of the catalase reaction. J. Am. Chem. Soc. 131, 11751–11761. https://doi.org/10.1021/ja9018572

Allgayer, J., Kitsera, N., Von Der Lippen, C., Epe, B., Khobta, A., 2013. Modulation of base excision repair of 8-oxoguanine by the nucleotide sequence. Nucleic Acids Res. 41, 8559 8571. https://doi.org/10.1093/nar/gkt620

Amente, S., Di Palo, G., Scala, G., Castrignanò, T., Gorini, F., Cocozza, S., Moresano, A., Pucci, P., Ma, B., Stepanov, I., Lania, L., Pelicci, P.G., Dellino, G.I., Majello, B., 2019. Genome-wide mapping of 8-oxo-7,8-dihydro-2′-deoxyguanosine reveals accumulation of oxidatively-generated damage at DNA replication origins within transcribed long genes of mammalian cells. Nucleic Acids Res. 47, 221–236. https://doi.org/10.1093/nar/gky1152

Amir Aslani, B., Ghobadi, S., 2016. Studies on oxidants and antioxidants with a brief glance at their relevance to the immune system. Life Sci. 146, 163–73. https://doi.org/10.1016/j.lfs.2016.01.014

Andegeko, Y., Moyal, L., Mittelman, L., Tsarfaty, I., Shiloh, Y., Rotman, G., 2001. Nuclear Retention of ATM at Sites of DNA Double Strand Breaks. J. Biol. Chem. 276, 38224–38230. https://doi.org/10.1074/jbc.m102986200

Aruoma, O.I., Halliwell, B., Hoey, B.M., Butler, J., 1989. The antioxidant action of N-acetylcysteine: Its reaction with hydrogen peroxide, hydroxyl radical, superoxide, and hypochlorous acid. Free Radic. Biol. Med. 6, 593–597. https://doi.org/10.1016/0891-5849(89)90066-X

Audry, J., Maestroni, L., Delagoutte, E., Gauthier, T., Nakamura, T.M., Gachet, Y., Saintomé, C., Géli, V., Coulon, S., 2015. RPA prevents G-rich structure formation at lagging-strand telomeres to allow maintenance of chromosome ends . EMBO J. 34, 1942–1958. https://doi.org/10.15252/embj.201490773

Aymard, F., Bugler, B., Schmidt, C.K., Guillou, E., Caron, P., Briois, S., Iacovoni, J.S., Daburon, V., Miller, K.M., Jackson, S.P., Legube, G., 2014. Transcriptionally active chromatin recruits homologous recombination at DNA double-strand breaks. Nat. Struct. Mol. Biol. 21, 366–74. https://doi.org/10.1038/nsmb.2796

Bakkenist, C.J., Kastan, M.B., 2003. DNA damage activates ATM through intermolecular autophosphorylation and dimer dissociation. Nature 421, 499–506. https://doi.org/10.1038/nature01368

Banin, S., Moyal, L., Shieh, S., Taya, Y., Anderson, C.W., Chessa, L., Smorodinsky, N.I., Prives, C., Reiss, Y., Shiloh, Y., Ziv, Y., 1998. Enhanced phosphorylation of p53 by ATM in response to DNA damage. Science 281, 1674–7. https://doi.org/10.1126/science.281.5383.1674

Baquero, J.M., Benítez-Buelga, C., Rajagopal, V., Zhenjun, Z., Torres-Ruiz, R., Müller, S., Hanna, B.M.F., Loseva, O., Wallner, O., Michel, M., Rodríguez-Perales, et al., 2021. Small molecule inhibitor of OGG1 blocks oxidative DNA damage repair at telomeres and potentiates methotrexate anticancer effects. Sci. Rep. 11, 3490. https://doi.org/10.1038/s41598-021-82917-7

Barja, G., 2004. Free radicals and aging. Trends Neurosci. 27, 595–600. https://doi.org/10.1016/j.tins.2004.07.005

Barlow, J.H., Faryabi, R.B., Callén, E., Wong, N., Malhowski, A., Chen, H.T., Gutierrez-Cruz, G., Sun, H.W., McKinnon, P., Wright, G., Casellas, R., Robbiani, D.F., et al., 2013. Identification of early replicating fragile sites that contribute to genome instability. Cell 152, 620–632. https://doi.org/10.1016/j.cell.2013.01.006

Bartek, J., Lukas, J., 2001. Mammalian G1- and S-phase checkpoints in response to DNA damage. Curr. Opin. Cell Biol. 13, 738–47. https://doi.org/10.1016/s0955-0674(00)00280-5

Beard, W.A., Horton, J.K., Prasad, R., Wilson, S.H., 2019. Eukaryotic base excision repair: New approaches shine light on mechanism. Annu. Rev. Biochem. 88, 137–162. https://doi.org/10.1146/annurev-biochem-013118-111315

Berglund, U.W., Sanjiv, K., Gad, H., Kalderén, C., Koolmeister, T., Pham, T., Gokturk, C., Jafari, R., Maddalo, G., Seashore-Ludlow, B., Chernobrovkin, A., et al., 2016. Validation and development of MTH1 inhibitors for treatment of cancer. Ann. Oncol. 27, 2275–2283. https://doi.org/10.1093/annonc/mdw429

Bermejo, R., Capra, T., Gonzalez-Huici, V., Fachinetti, D., Cocito, A., Natoli, G., Katou, Y., Mori, H., Kurokawa, K., Shirahige, K., Foiani, M., 2009. Genome-Organizing Factors Top2 and Hmo1 Prevent Chromosome Fragility at Sites of S phase Transcription. Cell 138, 870–884. https://doi.org/10.1016/j.cell.2009.06.022

Bermejo, R., Capra, T., Jossen, R., Colosio, A., Frattini, C., Carotenuto, W., Cocito, A., Doksani, Y., Klein, H., Gómez-González, B., Aguilera, A., Katou, Y., et al., 2011. The replication checkpoint protects fork stability by releasing transcribed genes from nuclear pores. Cell 146, 233–246. https://doi.org/10.1016/j.cell.2011.06.033

Bermejo, R., Lai, M.S., Foiani, M., 2012. Preventing replication stress to maintain genome stability: resolving conflicts between replication and transcription. Mol. Cell 45, 710–8. https://doi.org/10.1016/j.molcel.2012.03.001

Bernstein, C., Bernstein, H., Payne, C.M., Garewal, H., 2002. DNA repair/pro-apoptotic dual-role proteins in five major DNA repair pathways: fail-safe protection against carcinogenesis. Mutat. Res. 511, 145–78. https://doi.org/10.1016/s1383-5742(02)00009-1

Birben, E., Sahiner, U.M., Sackesen, C., Erzurum, S., Kalayci, O., 2012. Oxidative stress and antioxidant defense. World Allergy Organ. J. 5, 9–19. https://doi.org/10.1097/WOX.0b013e3182439613

Bjelakovic, G., Nikolova, D., Gluud, L.L., Simonetti, R.G., Gluud, C., 2007. Mortality in randomized trials of antioxidant supplements for primary and secondary prevention: systematic review and meta-analysis. JAMA 297, 842–57. https://doi.org/10.1001/jama.297.8.842

Bochman, M.L., Paeschke, K., Zakian, V.A., 2012. DNA secondary structures: stability and function of G-quadruplex structures. Nat. Rev. Genet. 13, 770–80. https://doi.org/10.1038/nrg3296

Bradley, M.O., Kohn, K.W., 1979. X-ray induced DNA double strand break production and repair in mammalian cells as measured by neutral filter elution. Nucleic Acids Res. 7, 793–804. https://doi.org/10.1093/nar/7.3.793

Braithwaite, E.K., Prasad, R., Shock, D.D., Hou, E.W., Beard, W.A., Wilson, S.H., 2005. DNA polymerase λ mediates a back-up base excision repair activity in extracts of mouse embryonic fibroblasts. J. Biol. Chem. 280, 18469–18475. https://doi.org/10.1074/jbc.M411864200

Brégeon, D., Peignon, P.A., Sarasin, A., 2009. Transcriptional mutagenesis induced by 8-oxoguanine in mammalian cells. PLoS Genet. 5. https://doi.org/10.1371/journal.pgen.1000577

Brewer, B.J., 1988. When polymerases collide: replication and the transcriptional organization of the E. coli chromosome. Cell 53, 679–86. https://doi.org/10.1016/0092-8674(88)90086-4

Buettner, G.R., 1993. The pecking order of free radicals and antioxidants: lipid peroxidation, alpha-tocopherol, and ascorbate. Arch. Biochem. Biophys. 300, 535–43. https://doi.org/10.1006/abbi.1993.1074

Bullock, P.A., Seo, Y.S., Hurwitz, J., 1991. Initiation of simian virus 40 DNA synthesis in vitro. Mol. Cell. Biol. 11, 2350–61. https://doi.org/10.1128/mcb.11.5.2350-2361.1991

Buratowski, S., Hahn, S., Guarente, L., Sharp, P.A., 1989. Five intermediate complexes in transcription initiation by RNA polymerase II. Cell 56, 549–61. https://doi.org/10.1016/0092-8674(89)90578-3

Burgers, P.M.J., Kunkel, T.A., 2017. Eukaryotic DNA Replication Fork. Annu. Rev. Biochem. 86, 417–438. https://doi.org/10.1146/annurev-biochem-061516-044709

Burma, S., Chen, B.P., Murphy, M., Kurimasa, A., Chen, D.J., 2001. ATM Phosphorylates Histone H2AX in Response to DNA Double-strand Breaks. J. Biol. Chem. 276, 42462–42467. https://doi.org/10.1074/jbc.C100466200

Burrows, C.J., Muller, J.G., 1998. Oxidative Nucleobase Modifications Leading to Strand Scission. Chem. Rev. 98, 1109–1152. https://doi.org/10.1021/cr960421s

Bzymek, M., Thayer, N.H., Oh, S.D., Kleckner, N., Hunter, N., 2010. Double holliday junctions are intermediates of DNA break repair. Nature 464, 937–941. https://doi.org/10.1038/nature08868

Cadoret, J.-C., Meisch, F., Hassan-Zadeh, V., Luyten, I., Guillet, C., Duret, L., Quesneville, H., Prioleau, M.-N., 2008. Genome-wide studies highlight indirect links between human replication origins and gene regulation. Proc. Natl. Acad. Sci. U. S. A. 105, 15837–42. https://doi.org/10.1073/pnas.0805208105

Cahill, D., Connor, B., Carney, J.P., 2006. Mechanisms of eukaryotic DNA double strand break repair. Front. Biosci. 11, 1958–76. https://doi.org/10.2741/1938

Caldecott, K.W., 2007. Mammalian single-strand break repair: Mechanisms and links with chromatin. DNA Repair (Amst). 6, 443–453. https://doi.org/10.1016/j.dnarep.2006.10.006

Canman, C.E., Lim, D.S., Cimprich, K.A., Taya, Y., Tamai, K., Sakaguchi, K., Appella, E., Kastan, M.B., Siliciano, J.D., 1998. Activation of the ATM kinase by ionizing radiation and phosphorylation of p53. Science (80-.). 281, 1677–1679. https://doi.org/10.1126/science.281.5383.1677

Cardoso, B.R., Hare, D.J., Bush, A.I., Roberts, B.R., 2017. Glutathione peroxidase 4: a new player in neurodegeneration? Mol. Psychiatry 22, 328–335. https://doi.org/10.1038/mp.2016.196

Chang, H.H.Y., Lieber, M.R., 2016. Structure-Specific nuclease activities of Artemis and the Artemis: DNA-PKcs complex. Nucleic Acids Res. 44, 4991–7. https://doi.org/10.1093/nar/gkw456

Chen, H., Lisby, M., Symington, L.S., 2013. RPA Coordinates DNA End Resection and Prevents Formation of DNA Hairpins. Mol. Cell 50, 589–600. https://doi.org/10.1016/j.molcel.2013.04.032

Chilkova, O., Stenlund, P., Isoz, I., Stith, C.M., Grabowski, P., Lundström, E.B., Burgers, P.M., Johansson, E., 2007. The eukaryotic leading and lagging strand DNA polymerases are loaded onto primer-ends via separate mechanisms but have comparable processivity in the presence of PCNA. Nucleic Acids Res. 35, 6588–6597. https://doi.org/10.1093/nar/gkm741

Cimprich, K.A., Cortez, D., 2008. ATR: an essential regulator of genome integrity. Nat. Rev. Mol. Cell Biol. 9, 616–27. https://doi.org/10.1038/nrm2450

Conomos, D., Pickett, H.A., Reddel, R.R., 2013. Alternative lengthening of telomeres: Remodeling the telomere architecture. Front. Oncol. 3 FEB. https://doi.org/10.3389/fonc.2013.00027

Costantino, L., Sotiriou, S.K., Rantala, J.K., Magin, S., Mladenov, E., Helleday, T., Haber, J.E., Iliakis, G., Kallioniemi, O.P., Halazonetis, T.D., 2014. Break-induced replication repair of damaged forks induces genomic duplications in human cells. Science (80-.). 343, 88–91. https://doi.org/10.1126/science.1243211

D'Amours, D., Desnoyers, S., D'Silva, I., Poirier, G.G., 1999. Poly(ADP-ribosyl)ation reactions in the regulation of nuclear functions. Biochem. J. 342 (Pt 2), 249–68.

Danis, E., Brodolin, K., Menut, S., Maiorano, D., Girard-Reydet, C., Méchali, M., 2004. Specification of a DNA replication origin by a transcription complex. Nat. Cell Biol. 6, 721–730. https://doi.org/10.1038/ncb1149

David-Cordonnier, M.H., Boiteux, S., O'Neill, P., 2001. Efficiency of excision of 8-oxo-guanine within DNA clustered damage by XRS5 nuclear extracts and purified human OGG1 protein. Biochemistry 40, 11811–11818. https://doi.org/10.1021/bi0112356

Davis, A.P., Symington, L.S., 2004. RAD51-Dependent Break-Induced Replication in Yeast. Mol. Cell. Biol. 24, 2344–2351. https://doi.org/10.1128/mcb.24.6.2344-2351.2004

de Jager, M., van Noort, J., van Gent, D.C., Dekker, C., Kanaar, R., Wyman, C., 2001. Human Rad50/Mre11 is a flexible complex that can tether DNA ends. Mol. Cell 8, 1129–35. https://doi.org/10.1016/s1097-2765(01)00381-1

Dizdaroglu, M., 1985. Formation of 8-hydroxyguanine moiety in deoxyribonucleic acid on .gamma.-irradiation in aqueous solution. Biochemistry 24, 4476–4481. https://doi.org/10.1021/bi00337a032

Domínguez-Sánchez, M.S., Barroso, S., Gómez-González, B., Luna, R., Aguilera, A., 2011. Genome instability and transcription elongation impairment in human cells depleted of THO/TREX. PLoS Genet. 7. https://doi.org/10.1371/journal.pgen.1002386

Dueva, R., Iliakis, G., 2013. Alternative pathways of non-homologous end joining (NHEJ) in genomic instability and cancer. Transl. Cancer Res. 2, 163–177. https://doi.org/10.3978/j.issn.2218-676X.2013.05.02

Durocher, D., Jackson, S.P., 2001. DNA-PK, ATM and ATR as sensors of DNA damage: variations on a theme? Curr. Opin. Cell Biol. 13, 225–31. https://doi.org/10.1016/s0955-0674(00)00201-5

Dutta, D., Shatalin, K., Epshtein, V., Gottesman, M.E., Nudler, E., 2011. Linking RNA polymerase backtracking to genome instability in E. coli. Cell 146, 533–543. https://doi.org/10.1016/j.cell.2011.07.034

Ensminger, M., Iloff, L., Ebel, C., Nikolova, T., Kaina, B., Löbrich, M., 2014. DNA breaks and chromosomal aberrations arise when replication meets base excision repair. J. Cell Biol. 206, 29–43. https://doi.org/10.1083/jcb.201312078

Ensminger, M., Löbrich, M., 2020. One end to rule them all: Non-homologous end-joining and homologous recombination at DNA double-strand breaks. Br. J. Radiol. 93, 20191054. https://doi.org/10.1259/bjr.20191054

Epe, B., 1996. DNA damage profiles induced by oxidizing agents. Rev. Physiol. Biochem. Pharmacol. 127, 223–49. https://doi.org/10.1007/BFb0048268

Fang, Y., Zou, P., 2020. Genome-Wide Mapping of Oxidative DNA Damage via Engineering of 8-Oxoguanine DNA Glycosylase. Biochemistry 59, 85–89. https://doi.org/10.1021/acs.biochem.9b00782

Fisher, A.E.O., Hochegger, H., Takeda, S., Caldecott, K.W., 2007. Poly(ADP-Ribose) Polymerase 1 Accelerates Single-Strand Break Repair in Concert with Poly(ADP-Ribose) Glycohydrolase. Mol. Cell. Biol. 27, 5597–5605. https://doi.org/10.1128/mcb.02248-06

Frei, B., England, L., Ames, B.N., 1989. Ascorbate is an outstanding antioxidant in human blood plasma. Proc. Natl. Acad. Sci. U. S. A. 86, 6377–81. https://doi.org/10.1073/pnas.86.16.6377

Gad, H., Koolmeister, T., Jemth, A.S., Eshtad, S., Jacques, S.A., Ström, C.E., Svensson, L.M., Schultz, N., Lundbäck, T., Einarsdottir, B.O., Saleh, A., Göktürk, C., et al., 2014. MTH1 inhibition eradicates cancer by preventing sanitation of the dNTP pool. Nature 508, 215–221. https://doi.org/10.1038/nature13181

Gadaleta, M., Noguchi, E., 2017. Regulation of DNA Replication through Natural Impediments in the Eukaryotic Genome. Genes (Basel). 8, 98. https://doi.org/10.3390/genes8030098

Galanos, P., Vougas, K., Walter, D., Polyzos, A., Maya-Mendoza, A., Haagensen, E.J., Kokkalis, A., Roumelioti, F.M., Gagos, S., Tzetis, M., Canovas, B., Igea, A., Ahuja, A.K., et al., 2016. Chronic p53-independent p21 expression causes genomic instability by deregulating replication licensing. Nat. Cell Biol. 18, 777–789. https://doi.org/10.1038/ncb3378

García-Muse, T., Aguilera, A., 2016. Transcription-replication conflicts: how they occur and how they are resolved. Nat. Rev. Mol. Cell Biol. 17, 553–63. https://doi.org/10.1038/nrm.2016.88

Garg, P., Stith, C.M., Sabouri, N., Johansson, E., Burgers, P.M., 2004. Idling by DNA polymerase δ maintains a ligatable nick during lagging-strand DNA replication. Genes Dev. 18, 2764–2773. https://doi.org/10.1101/gad.1252304

Gedik, C.M., Collins, A., 2005. Establishing the background level of base oxidation in human lymphocyte DNA: results of an interlaboratory validation study. FASEB J. 19, 82–84. https://doi.org/10.1096/fj.04-1767fje

Genestra, M., 2007. Oxyl radicals, redox-sensitive signalling cascades and antioxidants. Cell. Signal. 19, 1807–19. https://doi.org/10.1016/j.cellsig.2007.04.009

Gómez-González, B., Aguilera, A., 2019. Transcription-mediated replication hindrance: a major driver of genome instability. Genes Dev. 33, 1008–1026. https://doi.org/10.1101/gad.324517.119

Goodarzi, A.A., Yu, Y., Riballo, E., Douglas, P., Walker, S.A., Ye, R., Härer, C., Marchetti, C., Morrice, N., Jeggo, P.A., Lees-Miller, S.P., 2006. DNA-PK autophosphorylation facilitates Artemis endonuclease activity. EMBO J. 25, 3880–3889. https://doi.org/10.1038/sj.emboj.7601255

Gorini, F., Scala, G., Di Palo, G., Dellino, G.I., Cocozza, S., Pelicci, P.G., Lania, L., Majello, B., Amente, S., 2020. The genomic landscape of 8-oxodG reveals enrichment at specific inherently fragile promoters. Nucleic Acids Res. 48, 4309–4324. https://doi.org/10.1093/nar/gkaa175

Grawunder, U., Wilm, M., Wu, X., Kulesza, P., Wilson, T.E., Mann, M., Lieber, M.R., 1997. Activity of DNA ligase IV stimulated by complex formation with XRCC4 protein in mammalian cells. Nature 388, 492–495. https://doi.org/10.1038/41358

Grollman, A.P., Moriya, M., 1993. Mutagenesis by 8-oxoguanine: an enemy within. Trends Genet. 9, 246–9. https://doi.org/10.1016/0168-9525(93)90089-z

Grünberg, S., Warfield, L., Hahn, S., 2012. Architecture of the RNA polymerase II preinitiation complex and mechanism of ATP-dependent promoter opening. Nat. Struct. Mol. Biol. 19, 788–796. https://doi.org/10.1038/nsmb.2334

Gu, H., Marth, J.D., Orban, P.C., Mossmann, H., Rajewsky, K., 1994. Deletion of a DNA polymerase beta gene segment in T cells using cell type-specific gene targeting. Science 265, 103–6. https://doi.org/10.1126/science.8016642

Halazonetis, T.D., Gorgoulis, V.G., Bartek, J., 2008. An Oncogene-Induced DNA Damage Model for Cancer Development. Science (80-.). 319, 1352–1355. https://doi.org/10.1126/science.1140735

Hamperl, S., Bocek, M.J., Saldivar, J.C., Swigut, T., Cimprich, K.A., 2017. Transcription-Replication Conflict Orientation Modulates R-Loop Levels and Activates Distinct DNA Damage Responses. Cell 170, 774-786.e19. https://doi.org/10.1016/j.cell.2017.07.043

Hamperl, S., Cimprich, K.A., 2016. Conflict Resolution in the Genome: How Transcription and Replication Make It Work. Cell 167, 1455–1467. https://doi.org/10.1016/j.cell.2016.09.053

Hansen, J.M., Go, Y.-M., Jones, D.P., 2006. Nuclear and mitochondrial compartmentation of oxidative stress and redox signaling. Annu. Rev. Pharmacol. Toxicol. 46, 215–34. https://doi.org/10.1146/annurev.pharmtox.46.120604.141122

Hanssen-Bauer, A., Solvang-Garten, K., Sundheim, O., Peña-Diaz, J., Andersen, S., Slupphaug, G., Krokan, H.E., Wilson, D.M., Akbari, M., Otterlei, M., 2011. XRCC1 coordinates disparate responses and multiprotein repair complexes depending on the nature and context of the DNA damage. Environ. Mol. Mutagen. 52, 623–635. https://doi.org/10.1002/em.20663

Hao, D., Wang, L., Di, L.J., 2016. Distinct mutation accumulation rates among tissues determine the variation in cancer risk. Sci. Rep. 6. https://doi.org/10.1038/srep19458

Hegde, M.L., Hazra, T.K., Mitra, S., 2008. Early steps in the DNA base excision/single-strand interruption repair pathway in mammalian cells. Cell Res. 18, 27–47. https://doi.org/10.1038/cr.2008.8

Helleday, T., Eshtad, S., Nik-Zainal, S., 2014. Mechanisms underlying mutational signatures in human cancers. Nat. Rev. Genet. 15, 585–98. https://doi.org/10.1038/nrg3729

Heller, R.C., Kang, S., Lam, W.M., Chen, S., Chan, C.S., Bell, S.P., 2011. Eukaryotic origin-dependent DNA replication in vitro reveals sequential action of DDK and S-CDK kinases. Cell 146, 80–91. https://doi.org/10.1016/j.cell.2011.06.012

Helmrich, A., Ballarino, M., Tora, L., 2011. Collisions between Replication and Transcription Complexes Cause Common Fragile Site Instability at the Longest Human Genes. Mol. Cell 44, 966–977. https://doi.org/10.1016/j.molcel.2011.10.013

Heyer, W.-D., Ehmsen, K.T., Liu, J., 2010. Regulation of homologous recombination in eukaryotes. Annu. Rev. Genet. 44, 113–39. https://doi.org/10.1146/annurev-genet-051710-150955

Hirano, T., 2008. Repair system of 7, 8-dihydro-8-oxoguanine as a defense line against carcinogenesis. J. Radiat. Res. 49, 329–40. https://doi.org/10.1269/jrr.08049

Hu, Y., Raynard, S., Sehorn, M.G., Lu, X., Bussen, W., Zheng, L., Stark, J.M., Barnes, E.L., Chi, P., Janscak, P., Jasin, M., Vogel, H., Sung, P., Luo, G., 2007. RECQL5/Recql5 helicase regulates homologous recombination and suppresses tumor formation via disruption of Rad51 presynaptic filaments. Genes Dev. 21, 3073–3084. https://doi.org/10.1101/gad.1609107

Huertas, P., Aguilera, A., 2003. Cotranscriptionally formed DNA:RNA hybrids mediate transcription elongation impairment and transcription-associated recombination. Mol. Cell 12, 711–21. https://doi.org/10.1016/j.molcel.2003.08.010

Huffman, J.L., Sundheim, O., Tainer, J.A., 2005. DNA base damage recognition and removal: new twists and grooves. Mutat. Res. 577, 55–76. https://doi.org/10.1016/j.mrfmmm.2005.03.012

Iacovoni, J.S., Caron, P., Lassadi, I., Nicolas, E., Massip, L., Trouche, D., Legube, G., 2010. High-resolution profiling of gammaH2AX around DNA double strand breaks in the mammalian genome. EMBO J. 29, 1446–57. https://doi.org/10.1038/emboj.2010.38

Jacobs, A.L., Schär, P., 2012. DNA glycosylases: in DNA repair and beyond. Chromosoma 121, 1–20. https://doi.org/10.1007/s00412-011-0347-4

Jarem, D.A., Wilson, N.R., Delaney, S., 2009. Structure-dependent DNA damage and repair in a trinucleotide repeat sequence. Biochemistry 48, 6655–6663. https://doi.org/10.1021/bi9007403

Jones, R.M., Mortusewicz, O., Afzal, I., Lorvellec, M., García, P., Helleday, T., Petermann, E., 2013. Increased replication initiation and conflicts with transcription underlie Cyclin E-induced replication stress. Oncogene 32, 3744–3753. https://doi.org/10.1038/onc.2012.387

Kadyk, L.C., Hartwell, L.H., 1992. Sister chromatids are preferred over homologs as substrates for recombinational repair in Saccharomyces cerevisiae. Genetics 132, 387–402. https://doi.org/10.1093/genetics/132.2.387

Kathe, S.D., Shen, G.P., Wallace, S.S., 2004. Single-Stranded Breaks in DNA but Not Oxidative DNA Base Damages Block Transcriptional Elongation by RNA Polymerase II in HeLa Cell Nuclear Extracts. J. Biol. Chem. 279, 18511–18520. https://doi.org/10.1074/jbc.M313598200

Kaushal, S., Freudenreich, C.H., 2019. The role of fork stalling and DNA structures in causing chromosome fragility. Genes. Chromosomes Cancer 58, 270–283. https://doi.org/10.1002/gcc.22721

Kennedy, S.R., Salk, J.J., Schmitt, M.W., Loeb, L.A., 2013. Ultra-Sensitive Sequencing Reveals an Age-Related Increase in Somatic Mitochondrial Mutations That Are Inconsistent with Oxidative Damage. PLoS Genet. 9. https://doi.org/10.1371/journal.pgen.1003794

Khanna, K.K., Jackson, S.P., 2001. DNA double-strand breaks: signaling, repair and the cancer connection. Nat. Genet. 27, 247–54. https://doi.org/10.1038/85798

Kim, M., Krogan, N.J., Vasiljeva, L., Rando, O.J., Nedea, E., Greenblatt, J.F., Buratowski, S., 2004. The yeast Rat1 exonuclease promotes transcription termination by RNA polymerase II. Nature 432, 517–22. https://doi.org/10.1038/nature03041

Kirpota, O.O., Endutkin, A. V., Ponomarenko, M.P., Ponomarenko, P.M., Zharkov, D.O., Nevinsky, G.A., 2011. Thermodynamic and kinetic basis for recognition and repair of 8-oxoguanine in DNA by human 8-oxoguanine-DNA glycosylase. Nucleic Acids Res. 39, 4836–4850. https://doi.org/10.1093/nar/gkq1333

Kitsera, N., Stathis, D., Lühnsdorf, B., Müller, H., Carell, T., Epe, B., Khobta, A., 2011. 8-Oxo-7,8-dihydroguanine in DNA does not constitute a barrier to transcription, but is converted into transcription-blocking damage by OGG1. Nucleic Acids Res. 39, 5926–5934. https://doi.org/10.1093/nar/gkr163

Klungland, A., Rosewell, I., Hollenbach, S., Larsen, E., Daly, G., Epe, B., Seeberg, E., Lindahl, T., Barnes, D.E., 1999. Accumulation of premutagenic DNA lesions in mice defective in removal of oxidative base damage. Proc. Natl. Acad. Sci. U. S. A. 96, 13300–5. https://doi.org/10.1073/pnas.96.23.13300

Komarnitsky, P., Cho, E.J., Buratowski, S., 2000. Different phosphorylated forms of RNA polymerase II and associated mRNA processing factors during transcription. Genes Dev. 14, 2452–2460. https://doi.org/10.1101/gad.824700

Kotsantis, P., Silva, L.M., Irmscher, S., Jones, R.M., Folkes, L., Gromak, N., Petermann, E., 2016. Increased global transcription activity as a mechanism of replication stress in cancer. Nat. Commun. 7, 13087. https://doi.org/10.1038/ncomms13087

Kozlov, S., Gueven, N., Keating, K., Ramsay, J., Lavin, M.F., 2003. ATP activates Ataxia-telangiectasia Mutated (ATM) in vitro: Importance of autophosphorylation. J. Biol. Chem. 278, 9309–9317. https://doi.org/10.1074/jbc.M300003200

Kramara, J., Osia, B., Malkova, A., 2018. Break-Induced Replication: The Where, The Why, and The How. Trends Genet. 34, 518–531. https://doi.org/10.1016/j.tig.2018.04.002

Kunst, F., Ogasawara, N., Moszer, I., Albertini, A.M., Alloni, G., Azevedo, V., Bertero, M.G., Bessières, P., Bolotin, A., Borchert, S., Borriss, R., Boursier, L., Brans, A., et al., 1997. The complete genome sequence of the gram-positive bacterium Bacillus subtilis. Nature 390, 249–56. https://doi.org/10.1038/36786

Lander, E.S., Linton, L.M., Birren, B., Nusbaum, C., Zody, M.C., Baldwin, J., Devon, K., Dewar, K., Doyle, M., et al., International Human Genome Sequencing Consortium, 2001. Initial sequencing and analysis of the human genome. Nature 409, 860–921. https://doi.org/10.1038/35057062

Lehmann, F., Wennerberg, J., 2021. Evolution of Nitrogen-Based Alkylating Anticancer Agents. Processes 9, 377. https://doi.org/10.3390/pr9020377

Letessier, A., Millot, G.A., Koundrioukoff, S., Lachagès, A.M., Vogt, N., Hansen, R.S., Malfoy, B., Brison, O., Debatisse, M., 2011. Cell-type-specific replication initiation programs set fragility of the FRA3B fragile site. Nature 470, 120–124. https://doi.org/10.1038/nature09745

Li, X., Fang, P., Mai, J., Choi, E.T., Wang, H., Yang, X., 2013. Targeting mitochondrial reactive oxygen species as novel therapy for inflammatory diseases and cancers. J. Hematol. Oncol. 6, 19. https://doi.org/10.1186/1756-8722-6-19

Li, Z., Yang, J., Huang, H., 2006. Oxidative stress induces H2AX phosphorylation in human spermatozoa. FEBS Lett. 580, 6161–6168. https://doi.org/10.1016/j.febslet.2006.10.016

Lindahl, T., 1993. Instability and decay of the primary structure of DNA. Nature 362, 709–15. https://doi.org/10.1038/362709a0

Lindahl, T., Barnes, D.E., 2000. Repair of endogenous DNA damage. Cold Spring Harb. Symp. Quant. Biol. 65, 127–33. https://doi.org/10.1101/sqb.2000.65.127

Liu, J., Doty, T., Gibson, B., Heyer, W.D., 2010. Human BRCA2 protein promotes RAD51 filament formation on RPA-covered single-stranded DNA. Nat. Struct. Mol. Biol. 17, 1260–1262. https://doi.org/10.1038/nsmb.1904

Llorens-Agost, M., Ensminger, M., Le, H.P., Gawai, A., Liu, J., Cruz-García, A., Bhetawal, S., Wood, R.D., Heyer, W.-D., Löbrich, M., 2021. POLθ-mediated end joining is restricted by RAD52 and BRCA2 until the onset of mitosis. Nat. Cell Biol. 23, 1095–1104. https://doi.org/10.1038/s41556-021-00764-0

Löbrich, M., Shibata, A., Beucher, A., Fisher, A., Ensminger, M., Goodarzi, A.A., Barton, O., Jeggo, P.A., 2010. gammaH2AX foci analysis for monitoring DNA double-strand break repair: strengths, limitations and optimization. Cell Cycle 9, 662–9. https://doi.org/10.4161/cc.9.4.10764

Löbrich, M., Jeggo, P., 2017. A Process of Resection-Dependent Nonhomologous End Joining Involving the Goddess Artemis. Trends Biochem. Sci. 42, 690–701. https://doi.org/10.1016/j.tibs.2017.06.011

Lydeard, J.R., Jain, S., Yamaguchi, M., Haber, J.E., 2007. Break-induced replication and telomerase-independent telomere maintenance require Pol32. Nature 448, 820–823. https://doi.org/10.1038/nature06047

Lydeard, J.R., Lipkin-Moore, Z., Sheu, Y.-J., Stillman, B., Burgers, P.M., Haber, J.E., 2010. Break-induced replication requires all essential DNA replication factors except those specific for pre-RC assembly. Genes Dev. 24, 1133–44. https://doi.org/10.1101/gad.1922610

Ma, X., Tang, T.-S., Guo, C., 2020. Regulation of translesion DNA synthesis in mammalian cells. Environ. Mol. Mutagen. 61, 680–692. https://doi.org/10.1002/em.22359

Ma, Y., Lu, H., Tippin, B., Goodman, M.F., Shimazaki, N., Koiwai, O., Hsieh, C.L., Schwarz, K., Lieber, M.R., 2004. A biochemically defined system for mammalian nonhomologous DNA end joining. Mol. Cell 16, 701–713. https://doi.org/10.1016/j.molcel.2004.11.017

Malik, S., Roeder, R.G., 2000. Transcriptional regulation through Mediator-like coactivators in yeast and metazoan cells. Trends Biochem. Sci. 25, 277–83. https://doi.org/10.1016/s0968-0004(00)01596-6

Marnett, L.J., 2000. Oxyradicals and DNA damage. Carcinogenesis 21, 361–70. https://doi.org/10.1093/carcin/21.3.361

Marshall, N.F., Price, D.H., 1995. Purification of P-TEFb, a transcription factor required for the transition into productive elongation. J. Biol. Chem. 270, 12335–8. https://doi.org/10.1074/jbc.270.21.12335

Martin, M.M., Ryan, M., Kim, R.G., Zakas, A.L., Fu, H., Lin, C.M., Reinhold, W.C., Davis, S.R., Bilke, S., Liu, H., Doroshow, J.H., Reimers, M.A., Valenzuela, M.S., et al., 2011. Genome-wide depletion of replication initiation events in highly transcribed regions. Genome Res. 21, 1822–1832. https://doi.org/10.1101/gr.124644.111

Matsui, T., Segall, J., Weil, P.A., Roeder, R.G., 1980. Multiple factors required for accurate initiation of transcription by purified RNA polymerase II. J. Biol. Chem. 255, 11992–11996. https://doi.org/10.1016/s0021-9258(19)70232-4

McCulloch, S.D., Kunkel, T.A., 2008. The fidelity of DNA synthesis by eukaryotic replicative and translesion synthesis polymerases. Cell Res. 18, 148–61. https://doi.org/10.1038/cr.2008.4

Meek, K., Dang, V., Lees-Miller, S.P., 2008. DNA-PK: the means to justify the ends? Adv. Immunol. 99, 33–58. https://doi.org/10.1016/S0065-2776(08)00602-0

Michaels, M.L., Miller, J.H., 1992. The GO system protects organisms from the mutagenic effect of the spontaneous lesion 8-hydroxyguanine (7,8-dihydro-8-oxoguanine). J. Bacteriol. 174, 6321–5. https://doi.org/10.1128/jb.174.20.6321-6325.1992

Minocherhomji, S., Ying, S., Bjerregaard, V.A., Bursomanno, S., Aleliunaite, A., Wu, W., Mankouri, H.W., Shen, H., Liu, Y., Hickson, I.D., 2015. Replication stress activates DNA repair synthesis in mitosis. Nature 528, 286–290. https://doi.org/10.1038/nature16139

Minowa, O., Arai, T., Hirano, M., Monden, Y., Nakai, S., Fukuda, M., Itoh, M., Takano, H., Hippou, Y., Aburatani, H., Masumura, K., Nohmi, T., Nishimura, S., Noda, T., 2000. Mmh/Ogg1 gene inactivation results in accumulation of 8-hydroxyguanine in mice. Proc. Natl. Acad. Sci. U. S. A. 97, 4156–61. https://doi.org/10.1073/pnas.050404497

Mladenov, E., Magin, S., Soni, A., Iliakis, G., 2016. DNA double-strand-break repair in higher eukaryotes and its role in genomic instability and cancer: Cell cycle and proliferation-dependent regulation. Semin. Cancer Biol. 37–38, 51–64. https://doi.org/10.1016/j.semcancer.2016.03.003

Mourón, S., Rodriguez-Acebes, S., Martínez-Jiménez, M.I., García-Gómez, S., Chocrón, S., Blanco, L., Méndez, J., 2013. Repriming of DNA synthesis at stalled replication forks by human PrimPol. Nat. Struct. Mol. Biol. 20, 1383–1389. https://doi.org/10.1038/nsmb.2719

Moyer, S.E., Lewis, P.W., Botchan, M.R., 2006. Isolation of the Cdc45/Mcm2-7/GINS (CMG) complex, a candidate for the eukaryotic DNA replication fork helicase. Proc. Natl. Acad. Sci. U. S. A. 103, 10236–10241. https://doi.org/10.1073/pnas.0602400103

Murai, J., Huang, S.Y.N., Renaud, A., Zhang, Y., Ji, J., Takeda, S., Morris, J., Teicher, B., Doroshow, J.H., Pommier, Y., 2014. Stereospecific PARP trapping by BMN 673 and comparison with olaparib and rucaparib. Mol. Cancer Ther. 13, 433–443. https://doi.org/10.1158/1535-7163.MCT-13-0803

Nathan, C., Shiloh, M.U., 2000. Reactive oxygen and nitrogen intermediates in the relationship between mammalian hosts and microbial pathogens. Proc. Natl. Acad. Sci. U. S. A. 97, 8841–8. https://doi.org/10.1073/pnas.97.16.8841

Nenclares, P., Harrington, K.J., 2020. The biology of cancer. Medicine (Baltimore). 48, 67–72. https://doi.org/10.1016/j.mpmed.2019.11.001

Nickoloff, J.A., Sharma, N., Taylor, L., Allen, S.J., Hromas, R., 2021. The Safe Path at the Fork: Ensuring Replication-Associated DNA Double-Strand Breaks are Repaired by Homologous Recombination. Front. Genet. 12, 1–9. https://doi.org/10.3389/fgene.2021.748033

Nikolova, T., Ensminger, M., Löbrich, M., Kaina, B., 2010. Homologous recombination protects mammalian cells from replication-associated DNA double-strand breaks arising in response to methyl methanesulfonate. DNA Repair (Amst). 9, 1050–1063. https://doi.org/10.1016/j.dnarep.2010.07.005

Nudler, E., 2012. RNA polymerase backtracking in gene regulation and genome instability. Cell 149, 1438–45. https://doi.org/10.1016/j.cell.2012.06.003

Núñez-Ramírez, R., Klinge, S., Sauguet, L., Melero, R., Recuero-Checa, M.A., Kilkenny, M., Perera, R.L., García-Alvarez, B., Hall, R.J., Nogales, E., Pellegrini, L., Llorca, O., 2011. Flexible tethering of primase and DNA Pol α in the eukaryotic primosome. Nucleic Acids Res. 39, 8187–8199. https://doi.org/10.1093/nar/gkr534

Ochi, T., Blackford, A.N., Coates, J., Jhujh, S., Mehmood, S., Tamura, N., Travers, J., Wu, Q., Draviam, V.M., Robinson, C. V, Blundell, T.L., Jackson, S.P., 2015. DNA repair. PAXX, a paralog of XRCC4 and XLF, interacts with Ku to promote DNA double-strand break repair. Science 347, 185–188. https://doi.org/10.1126/science.1261971

Okazaki, R., Okazaki, T., Sakabe, K., Sugimoto, K., Sugino, A., 1968. Mechanism of DNA chain growth. I. Possible discontinuity and unusual secondary structure of newly synthesized chains. Proc. Natl. Acad. Sci. U. S. A. 59, 598–605. https://doi.org/10.1073/pnas.59.2.598

Paliwal, S., Kanagaraj, R., Sturzenegger, A., Burdova, K., Janscak, P., 2014. Human RECQ5 helicase promotes repair of DNA double-strand breaks by synthesis-dependent strand annealing. Nucleic Acids Res. 42, 2380–2390. https://doi.org/10.1093/nar/gkt1263

Paulsen, R.D., Soni, D. V., Wollman, R., Hahn, A.T., Yee, M.-C., Guan, A., Hesley, J.A., Miller, S.C., Cromwell, E.F., Solow-Cordero, D.E., Meyer, T., Cimprich, K.A., 2009. A genome-wide siRNA screen reveals diverse cellular processes and pathways that mediate genome stability. Mol. Cell 35, 228–39. https://doi.org/10.1016/j.molcel.2009.06.021

Pearce, A.K., Humphrey, T.C., 2001. Integrating stress-response and cell-cycle checkpoint pathways. Trends Cell Biol. 11, 426–33. https://doi.org/10.1016/s0962-8924(01)02119-5

Perillo, B., Di Donato, M., Pezone, A., Di Zazzo, E., Giovannelli, P., Galasso, G., Castoria, G., Migliaccio, A., 2020. ROS in cancer therapy: the bright side of the moon. Exp. Mol. Med. 52, 192–203. https://doi.org/10.1038/s12276-020-0384-2

Pertea, M., Shumate, A., Pertea, G., Varabyou, A., Chang, Y.C., Madugundu, A.K., Pandey, A., Salzberg, S.L., 2018. Thousands of large-scale RNA sequencing experiments yield a comprehensive new human gene list and reveal extensive transcriptional noise. bioRxiv. https://doi.org/10.1101/332825

Petermann, E., Orta, M.L., Issaeva, N., Schultz, N., Helleday, T., 2010. Hydroxyurea-Stalled Replication Forks Become Progressively Inactivated and Require Two Different RAD51-Mediated Pathways for Restart and Repair. Mol. Cell 37, 492–502. https://doi.org/10.1016/j.molcel.2010.01.021

Pizzino, G., Irrera, N., Cucinotta, M., Pallio, G., Mannino, F., Arcoraci, V., Squadrito, F., Altavilla, D., Bitto, A., 2017. Oxidative Stress: Harms and Benefits for Human Health. Oxid. Med. Cell. Longev. 2017, 8416763. https://doi.org/10.1155/2017/8416763

Pomerantz, R.T., O'Donnell, M., 2008. The replisome uses mRNA as a primer after colliding with RNA polymerase. Nature 456, 762–767. https://doi.org/10.1038/nature07527

Prado, F., Aguilera, A., 2005. Impairment of replication fork progression mediates RNA polII transcription-associated recombination. EMBO J. 24, 1267–1276. https://doi.org/10.1038/sj.emboj.7600602

Prasad, R., Dianov, G.L., Bohr, V.A., Wilson, S.H., 2000. FEN1 stimulation of DNA polymerase β mediates an excision step in mammalian long patch base excision repair. J. Biol. Chem. 275, 4460–4466. https://doi.org/10.1074/jbc.275.6.4460

Priestley, C.C., Green, R.M., Fellows, M.D., Doherty, A.T., Hodges, N.J., O'Donovan, M.R., 2010. Anomalous genotoxic responses induced in mouse lymphoma L5178Y cells by potassium bromate. Toxicology 267, 45–53. https://doi.org/10.1016/j.tox.2009.10.012

Quinet, A., Tirman, S., Cybulla, E., Meroni, A., Vindigni, A., 2021. To skip or not to skip: choosing repriming to tolerate DNA damage. Mol. Cell 81, 649–658. https://doi.org/10.1016/j.molcel.2021.01.012

Rajendran, P., Nandakumar, N., Rengarajan, T., Palaniswami, R., Gnanadhas, E.N., Lakshminarasaiah, U., Gopas, J., Nishigaki, I., 2014. Antioxidants and human diseases. Clin. Chim. Acta. 436, 332–47. https://doi.org/10.1016/j.cca.2014.06.004

Reaban, M.E., Lebowitz, J., Griffin, J.A., 1994. Transcription induces the formation of a stable RNA.DNA hybrid in the immunoglobulin alpha switch region. J. Biol. Chem. 269, 21850–7.

Rhee, D.B., Ghosh, A., Lu, J., Bohr, V.A., Liu, Y., 2011. Factors that influence telomeric oxidative base damage and repair by DNA glycosylase OGG1. DNA Repair (Amst). 10, 34–44. https://doi.org/10.1016/j.dnarep.2010.09.008

Rickman, K.A., Noonan, R.J., Lach, F.P., Sridhar, S., Wang, A.T., Abhyankar, A., Huang, A., Kelly, M., Auerbach, A.D., Smogorzewska, A., 2020. Distinct roles of BRCA2 in replication fork protection in response to hydroxyurea and DNA interstrand cross-links. Genes Dev. 34, 832–846. https://doi.org/10.1101/gad.336446.120

Ristow, M., Zarse, K., 2010. How increased oxidative stress promotes longevity and metabolic health: The concept of mitochondrial hormesis (mitohormesis). Exp. Gerontol. 45, 410–8. https://doi.org/10.1016/j.exger.2010.03.014

Rogakou, E.P., Pilch, D.R., Orr, A.H., Ivanova, V.S., Bonner, W.M., 1998. DNA double-stranded breaks induce histone H2AX phosphorylation on serine 139. J. Biol. Chem. 273, 5858–5868. https://doi.org/10.1074/jbc.273.10.5858

Rosenquist, T.A., Zharkov, D.O., Grollman, A.P., 1997. Cloning and characterization of a mammalian 8-oxoguanine DNA glycosylase. Proc. Natl. Acad. Sci. U. S. A. 94, 7429–34. https://doi.org/10.1073/pnas.94.14.7429

Rougvie, A.E., Lis, J.T., 1988. The RNA polymerase II molecule at the 5' end of the uninduced hsp70 gene of D. melanogaster is transcriptionally engaged. Cell 54, 795–804. https://doi.org/10.1016/s0092-8674(88)91087-2

Ruff, P., Donnianni, R.A., Glancy, E., Oh, J., Symington, L.S., 2016. RPA Stabilization of Single-Stranded DNA Is Critical for Break-Induced Replication. Cell Rep. 17, 3359–3368. https://doi.org/10.1016/j.celrep.2016.12.003

Russo, M.T., De Luca, G., Degan, P., Parlanti, E., Dogliotti, E., Barnes, D.E., Lindahl, T., Yang, H., Miller, J.H., Bignami, M., 2004. Accumulation of the oxidative base lesion 8-hydroxyguanine in DNA of tumor-prone mice defective in both the Myh and Ogg1 DNA glycosylases. Cancer Res. 64, 4411–4. https://doi.org/10.1158/0008-5472.CAN-04-0355

Rybin, M.J., Ramic, M., Ricciardi, N.R., Kapranov, P., Wahlestedt, C., Zeier, Z., 2021. Emerging Technologies for Genome-Wide Profiling of DNA Breakage. Front. Genet. 11. https://doi.org/10.3389/fgene.2020.610386

Ryu, S., Tjian, R., 1999. Purification of transcription cofactor complex CRSP. Proc. Natl. Acad. Sci. U. S. A. 96, 7137–42. https://doi.org/10.1073/pnas.96.13.7137

Saini, N., Gordenin, D.A., 2020. Hypermutation in single-stranded DNA. DNA Repair (Amst). 91–92. https://doi.org/10.1016/j.dnarep.2020.102868

Saini, N., Ramakrishnan, S., Elango, R., Ayyar, S., Zhang, Y., Deem, A., Ira, G., Haber, J.E., Lobachev, K.S., Malkova, A., 2013. Migrating bubble during break-induced replication drives conservative DNA synthesis. Nature 502, 389–392. https://doi.org/10.1038/nature12584

Sanchez, A., de Vivo, A., Tonzi, P., Kim, J., Huang, T.T., Kee, Y., 2020. Transcription-replication conflicts as a source of common fragile site instability caused by BMI1-RNF2 deficiency. PLoS Genet. 16. https://doi.org/10.1371/journal.pgen.1008524

Saponaro, M., Kantidakis, T., Mitter, R., Kelly, G.P., Heron, M., Williams, H., Söding, J., Stewart, A., Svejstrup, J.Q., 2014. RECQL5 Controls Transcript Elongation and Suppresses Genome Instability Associated with Transcription Stress. Cell 157, 1037–1049. https://doi.org/10.1016/j.cell.2014.03.048

Sarbajna, S., West, S.C., 2014. Holliday junction processing enzymes as guardians of genome stability. Trends Biochem. Sci. 39, 409–19. https://doi.org/10.1016/j.tibs.2014.07.003

Sartori, A.A., Lukas, C., Coates, J., Mistrik, M., Fu, S., Bartek, J., Baer, R., Lukas, J., Jackson, S.P., 2007. Human CtIP promotes DNA end resection. Nature 450, 509–514. https://doi.org/10.1038/nature06337

Sassa, A., Beard, W.A., Prasad, R., Wilson, S.H., 2012. DNA sequence context effects on the glycosylase activity of human 8-oxoguanine DNA glycosylase. J. Biol. Chem. 287, 36702–36710. https://doi.org/10.1074/jbc.M112.397786

Schlacher, K., Wu, H., Jasin, M., 2012. A Distinct Replication Fork Protection Pathway Connects Fanconi Anemia Tumor Suppressors to RAD51-BRCA1/2. Cancer Cell 22, 106–116. https://doi.org/10.1016/j.ccr.2012.05.015

Sengupta, S., Van Deursen, F., De Piccoli, G., Labib, K., 2013. Dpb2 Integrates the Leading-Strand DNA Polymerase into the Eukaryotic Replisome. Curr. Biol. 23, 543–552. https://doi.org/10.1016/j.cub.2013.02.011

Sharma, V., Collins, L.B., Chen, T.-H., Herr, N., Takeda, S., Sun, W., Swenberg, J.A., Nakamura, J., 2016. Oxidative stress at low levels can induce clustered DNA lesions leading to NHEJ mediated mutations. Oncotarget 7, 25377–90. https://doi.org/10.18632/oncotarget.8298

Shechter, D., Costanzo, V., Gautier, J., 2004. Regulation of DNA replication by ATR: signaling in response to DNA intermediates. DNA Repair (Amst). 3, 901–8. https://doi.org/10.1016/j.dnarep.2004.03.020

Shibutani, S., Takeshita, M., Grollman, A.P., 1991. Insertion of specific bases during DNA synthesis past the oxidation-damaged base 8-oxodG. Nature 349, 431–4. https://doi.org/10.1038/349431a0

Sieber, O.M., Lipton, L., Crabtree, M., Heinimann, K., Fidalgo, P., Phillips, R.K.S., Bisgaard, M.-L., Orntoft, T.F., Aaltonen, L.A., Hodgson, S. V., Thomas, H.J.W., et al., 2003. Multiple colorectal adenomas, classic adenomatous polyposis, and germ-line mutations in MYH. N. Engl. J. Med. 348, 791–9. https://doi.org/10.1056/NEJMoa025283

Simon, A.C., Zhou, J.C., Perera, R.L., Van Deursen, F., Evrin, C., Ivanova, M.E., Kilkenny, M.L., Renault, L., Kjaer, S., Matak-Vinkovi, D., Labib, K., Costa, A., Pellegrini, L., 2014. A Ctf4 trimer couples the CMG helicase to DNA polymerase Î± in the eukaryotic replisome. Nature 510, 293–297. https://doi.org/10.1038/nature13234

Singh, J., Padgett, R.A., 2009. Rates of in situ transcription and splicing in large human genes. Nat. Struct. Mol. Biol. 16, 1128–1133. https://doi.org/10.1038/nsmb.1666

Singh, Y.P., Patel, R.N., Singh, Y., Butcher, R.J., Vishakarma, P.K., Singh, R.K.B., 2017. Structure and antioxidant superoxide dismutase activity of copper(II) hydrazone complexes. Polyhedron 122, 1–15. https://doi.org/10.1016/j.poly.2016.11.013

Skourti-Stathaki, K., Proudfoot, N.J., Gromak, N., 2011. Human Senataxin Resolves RNA/DNA Hybrids Formed at Transcriptional Pause Sites to Promote Xrn2-Dependent Termination. Mol. Cell 42, 794–805. https://doi.org/10.1016/j.molcel.2011.04.026

Smith, C.E., Llorente, B., Symington, L.S., 2007. Template switching during break-induced replication. Nature 447, 102–105. https://doi.org/10.1038/nature05723

Sneeden, J.L., Grossi, S.M., Tappin, I., Hurwitz, J., Heyer, W.D., 2013. Reconstitution of recombination-associated DNA synthesis with human proteins. Nucleic Acids Res. 41, 4913–4925. https://doi.org/10.1093/nar/gkt192

Sommers, J.A., Rawtani, N., Gupta, R., Bugreev, D. V., Mazin, A. V., Cantor, S.B., Brosh, R.M., 2009. FANCJ uses its motor ATPase to destabilize protein-DNA complexes, unwind triplexes, and inhibit RAD51 strand exchange. J. Biol. Chem. 284, 7505–7517. https://doi.org/10.1074/jbc.M809019200

Sotiriou, S.K., Kamileri, I., Lugli, N., Evangelou, K., Da-Ré, C., Huber, F., Padayachy, L., Tardy, S., Nicati, N.L., Barriot, S., Ochs, F., Lukas, C., Lukas, J., et al., 2016. Mammalian RAD52 Functions in Break-Induced Replication Repair of Collapsed DNA Replication Forks. Mol. Cell 64, 1127–1134. https://doi.org/10.1016/j.molcel.2016.10.038

Spiegel, J., Adhikari, S., Balasubramanian, S., 2020. The Structure and Function of DNA G-Quadruplexes. Trends Chem. 2, 123–136. https://doi.org/10.1016/j.trechm.2019.07.002

Spies, J., Waizenegger, A., Barton, O., Sürder, M., Wright, W.D., Heyer, W.D., Löbrich, M., 2016. Nek1 Regulates Rad54 to Orchestrate Homologous Recombination and Replication Fork Stability. Mol. Cell 62, 903–917. https://doi.org/10.1016/j.molcel.2016.04.032

Srivatsan, A., Tehranchi, A., MacAlpine, D.M., Wang, J.D., 2010. Co-orientation of replication and transcription preserves genome integrity. PLoS Genet. 6. https://doi.org/10.1371/journal.pgen.1000810

Strumberg, D., Pilon, A.A., Smith, M., Hickey, R., Malkas, L., Pommier, Y., 2000. Conversion of Topoisomerase I Cleavage Complexes on the Leading Strand of Ribosomal DNA into 5′-Phosphorylated DNA Double-Strand Breaks by Replication Runoff. Mol. Cell. Biol. 20, 3977–3987. https://doi.org/10.1128/mcb.20.11.3977-3987.2000

Symington, L.S., 2014. End resection at double-strand breaks: Mechanism and regulation. Cold Spring Harb. Perspect. Biol. 6. https://doi.org/10.1101/cshperspect.a016436

Tanaka, S., Araki, H., 2013. Helicase activation and establishment of replication forks at chromosomal origins of replication. Cold Spring Harb. Perspect. Biol. 5. https://doi.org/10.1101/cshperspect.a010371

Ticau, S., Friedman, L.J., Ivica, N.A., Gelles, J., Bell, S.P., 2015. Single-molecule studies of origin licensing reveal mechanisms ensuring bidirectional helicase loading. Cell 161, 513–525. https://doi.org/10.1016/j.cell.2015.03.012

Trautinger, B.W., Jaktaji, R.P., Rusakova, E., Lloyd, R.G., 2005. RNA polymerase modulators and DNA repair activities resolve conflicts between DNA replication and transcription. Mol. Cell 19, 247–258. https://doi.org/10.1016/j.molcel.2005.06.004

Tsai, C.J., Kim, S.A., Chu, G., 2007. Cernunnos/XLF promotes the ligation of mismatched and noncohesive DNA ends. Proc. Natl. Acad. Sci. U. S. A. 104, 7851–6. https://doi.org/10.1073/pnas.0702620104

Tsuzuki, T., Egashira, A., Yamauchi, K., Yoshiyama, K., Maki, H., 2002. Spontaneous tumorigenesis and mutagenesis in mice defective in the MTH1 gene encoding 8-oxo-dGTPase. Int. Congr. Ser. 1236, 111–114. https://doi.org/10.1016/S0531-5131(01)00760-9

Tubbs, A., Nussenzweig, A., 2017. Endogenous DNA Damage as a Source of Genomic Instability in Cancer. Cell 168, 644–656. https://doi.org/10.1016/j.cell.2017.01.002

Tuduri, S., Crabbé, L., Conti, C., Tourrière, H., Holtgreve-Grez, H., Jauch, A., Pantesco, V., De Vos, J., Thomas, A., Theillet, C., Pommier, Y., Tazi, J., Coquelle, A., Pasero, P., 2009. Topoisomerase I suppresses genomic instability by preventing interference between replication and transcription. Nat. Cell Biol. 11, 1315–1324. https://doi.org/10.1038/ncb1984

Tye, S., Ronson, G.E., Morris, J.R., 2021. A fork in the road: Where homologous recombination and stalled replication fork protection part ways. Semin. Cell Dev. Biol. 113, 14–26. https://doi.org/10.1016/j.semcdb.2020.07.004

van Attikum, H., Gasser, S.M., 2009. Crosstalk between histone modifications during the DNA damage response. Trends Cell Biol. 19, 207–17. https://doi.org/10.1016/j.tcb.2009.03.001

van den Boogaard, M.L., Oka, R., Hakkert, A., Schild, L., Ebus, M.E., van Gerven, M.R., Zwijnenburg, D.A., Molenaar, P., Hoyng, L.L., Dolman, M.E.M., et al., 2021. Defects in 8-oxo-guanine repair pathway cause high frequency of C > A substitutions in neuroblastoma. Proc. Natl. Acad. Sci. 118, e2007898118. https://doi.org/10.1073/pnas.2007898118

van Gent, D.C., Hoeijmakers, J.H., Kanaar, R., 2001. Chromosomal stability and the DNA double-stranded break connection. Nat. Rev. Genet. 2, 196–206. https://doi.org/10.1038/35056049

Vazquez-Torres, A., Jones-Carson, J., Mastroeni, P., Ischiropoulos, H., Fang, F.C., 2000. Antimicrobial actions of the NADPH phagocyte oxidase and inducible nitric oxide synthase in experimental salmonellosis. I. Effects on microbial killing by activated peritoneal macrophages in vitro. J. Exp. Med. 192, 227–36. https://doi.org/10.1084/jem.192.2.227

Walker, J.R., Corpina, R.A., Goldberg, J., 2001. Structure of the Ku heterodimer bound to DNA and its implications for double-strand break repair. Nature 412, 607–14. https://doi.org/10.1038/35088000

Wang, R., Li, C., Qiao, P., Xue, Y., Zheng, X., Chen, H., Zeng, X., Liu, W., Boldogh, I., Ba, X., 2018. OGG1-initiated base excision repair exacerbates oxidative stress-induced parthanatos. Cell Death Dis. 9. https://doi.org/10.1038/s41419-018-0680-0

Ward, I.M., Chen, J., 2001. Histone H2AX Is Phosphorylated in an ATR-dependent Manner in Response to Replicational Stress. J. Biol. Chem. 276, 47759–47762. https://doi.org/10.1074/jbc.C100569200

Wei, P.-C., Chang, A.N., Kao, J., Du, Z., Meyers, R.M., Alt, F.W., Schwer, B., 2016. Long Neural Genes Harbor Recurrent DNA Break Clusters in Neural Stem/Progenitor Cells. Cell 164, 644–655. https://doi.org/10.1016/j.cell.2015.12.039

West, S., Gromak, N., Proudfoot, N.J., 2004. Human 5′ → 3′ exonuclease Xm2 promotes transcription termination at co-transcriptional cleavage sites. Nature 432, 522–525. https://doi.org/10.1038/nature03035

Weyand, C.M., Shen, Y., Goronzy, J.J., 2018. Redox-sensitive signaling in inflammatory T cells and in autoimmune disease. Free Radic. Biol. Med. 125, 36–43. https://doi.org/10.1016/j.freeradbiomed.2018.03.004

White, E.J., Emanuelsson, O., Scalzo, D., Royce, T., Kosak, S., Oakeley, E.J., Weissman, S., Gerstein, M., Groudine, M., Snyder, M., Schübeler, D., 2004. DNA replication-timing analysis of human chromosome 22 at high resolution and different developmental states. Proc. Natl. Acad. Sci. U. S. A. 101, 17771–6. https://doi.org/10.1073/pnas.0408170101

Williams, S.D., David, S.S., 1998. Evidence that MutY is a monofunctional glycosylase capable of forming a covalent Schiff base intermediate with substrate DNA. Nucleic Acids Res. 26, 5123–33. https://doi.org/10.1093/nar/26.22.5123

Wilson, M.A., Kwon, Y., Xu, Y., Chung, W.H., Chi, P., Niu, H., Mayle, R., Chen, X., Malkova, A., Sung, P., Ira, G., 2013. Pif1 helicase and Polδ promote recombination-coupled DNA synthesis via bubble migration. Nature 502, 393–396. https://doi.org/10.1038/nature12585

Wobbe, C.R., Weissbach, L., Borowiec, J.A., Dean, F.B., Murakami, Y., Bullock, P., Hurwitz, J., 1987. Replication of simian virus 40 origin-containing DNA in vitro with purified proteins. Proc. Natl. Acad. Sci. U. S. A. 84, 1834–8. https://doi.org/10.1073/pnas.84.7.1834

Woodfine, K., Fiegler, H., Beare, D.M., Collins, J.E., McCann, O.T., Young, B.D., Debernardi, S., Mott, R., Dunham, I., Carter, N.P., 2004. Replication timing of the human genome. Hum. Mol. Genet. 13, 191–202. https://doi.org/10.1093/hmg/ddh016

Wright, W.D., Shah, S.S., Heyer, W.-D., 2018. Homologous recombination and the repair of DNA double-strand breaks. J. Biol. Chem. 293, 10524–10535. https://doi.org/10.1074/jbc.TM118.000372

Wyman, C., Ristic, D., Kanaar, R., 2004. Homologous recombination-mediated double-strand break repair. DNA Repair (Amst). 3, 827–33. https://doi.org/10.1016/j.dnarep.2004.03.037

Xie, A., Hartlerode, A., Stucki, M., Odate, S., Puget, N., Kwok, A., Nagaraju, G., Yan, C., Alt, F.W., Chen, J., Jackson, S.P., Scully, R., 2007. Distinct Roles of Chromatin-Associated Proteins MDC1 and 53BP1 in Mammalian Double-Strand Break Repair. Mol. Cell 28, 1045–1057. https://doi.org/10.1016/j.molcel.2007.12.005

Xie, Y., Yang, H., Cunanan, C., Okamoto, K., Shibata, D., Pan, J., Barnes, D.E., Lindahl, T., McIlhatton, M., Fishel, R., Miller, J.H., 2004. Deficiencies in mouse Myh and Ogg1 result in tumor predisposition and G to T mutations in codon 12 of the K-ras oncogene in lung tumors. Cancer Res. 64, 3096–102. https://doi.org/10.1158/0008-5472.can-03-3834

Yamaguchi, Y., Wada, T., Watanabe, D., Takagi, T., Hasegawa, J., Handa, H., 1999. Structure and function of the human transcription elongation factor DSIF. J. Biol. Chem. 274, 8085–8092. https://doi.org/10.1074/jbc.274.12.8085

Ye, B., Hou, N., Xiao, L., Xu, Y., Xu, H., Li, F., 2016. Dynamic monitoring of oxidative DNA double-strand break and repair in cardiomyocytes. Cardiovasc. Pathol. 25, 93–100. https://doi.org/10.1016/j.carpath.2015.10.010

Yekezare, M., Gómez-González, B., Diffley, J.F.X., 2013. Controlling DNA replication origins in response to DNA damage - inhibit globally, activate locally. J. Cell Sci. 126, 1297–306. https://doi.org/10.1242/jcs.096701

Zellweger, R., Dalcher, D., Mutreja, K., Berti, M., Schmid, J.A., Herrador, R., Vindigni, A., Lopes, M., 2015. Rad51-mediated replication fork reversal is a global response to genotoxic treatments in human cells. J. Cell Biol. 208, 563–579. https://doi.org/10.1083/jcb.201406099

Zeman, M.K., Cimprich, K.A., 2014. Causes and consequences of replication stress. Nat. Cell Biol. 16, 2–9. https://doi.org/10.1038/ncb2897

Zhang, L., Misiara, L., Samaranayake, G.J., Sharma, N., Nguyen, D.M., Tahara, Y.K., Kool, E.T., Rai, P., 2021. OGG1 co-inhibition antagonizes the tumor-inhibitory effects of targeting MTH1. Redox Biol. 40. https://doi.org/10.1016/j.redox.2020.101848

Zhou, W., Ma, L., Yang, J., Qiao, H., Li, L., Guo, Q., Ma, J., Zhao, L., Wang, J., Jiang, G., Wan, X., Adam Goscinski, M., Ding, L., Zheng, Y., Li, W., Liu, H., Suo, Z., Zhao, W., 2019. Potent and specific MTH1 inhibitors targeting gastric cancer. Cell Death Dis. 10. https://doi.org/10.1038/s41419-019-1665-3

Acknowledgments

First of all, I would like to thank Prof. Dr. Markus Löbrich for the opportunity to work in his group and for supervising my PhD thesis. Also for the interesting and stimulating discussions and the great ideas that made this thesis possible. Further thanks go to Prof. Dr. M. Cristina Cardoso for being my second supervisor and to Prof. Dr. Alexander Löwer and Prof. Dr. Markus Christmann for kindly accepting my request to be my examiner.

Many thanks to Michael Ensminger for his help in the day-to-day laboratory work, for the many interesting scientific and non-scientific discussions, and for correcting my thesis. I could not have had a more dedicated and helpful supervisor. I would also like to thank Marta Llorens Agost for correcting my thesis and for her supportive comments and Ilaria Ghiro for bioinformatics support and patience in discussing with computer laymen.

Furthermore, I would also like to thank our technical staff Ratna Weimer, Christel Braun, Bettina Basso and Cornelia Schmidt, who were always there when needed and made the work in the lab so much easier. To all former and current members of the group, I would like to say a huge thank you. You were not only a great help (occasionally also a nightmare) in the lab, but also a really great company in our free time. Amir, Amira, Andres, Anugrah, Holly, I will miss all the great moments we had over the last years.

A very special thanks goes to Emina Merdan for her constant support, encouraging words, for listening to all the problems and worries and of course for always being there for me. Last but not least, I would like to thank my family and friends who have always supported me in god and in bad times. Especially my parents, André, Michaela, Eliza and Leonas, thank you. It is only because of you that I am able to be the person I am today.